

EUROPEAN ORGANISATION FOR NUCLEAR RESEARCH (CERN)



Submitted to: JHEP



CERN-EP-2024-322
19th December 2024

Differential cross-section measurements of D^\pm and D_s^\pm meson production in proton–proton collisions at $\sqrt{s} = 13$ TeV with the ATLAS detector

The ATLAS Collaboration

The production of D^\pm and D_s^\pm charmed mesons is measured using the $D^\pm/D_s^\pm \rightarrow \phi(\mu\mu)\pi^\pm$ decay channel with 137 fb^{-1} of $\sqrt{s} = 13$ TeV proton–proton collision data collected with the ATLAS detector at the Large Hadron Collider during the years 2016–2018. The charmed mesons are reconstructed in the range of transverse momentum $12 < p_T < 100$ GeV and pseudorapidity $|\eta| < 2.5$. The differential cross-sections are measured as a function of transverse momentum and pseudorapidity, and compared with next-to-leading-order QCD predictions. The predictions are found to be consistent with the measurements in the visible kinematic region within the large theoretical uncertainties.

Contents

1	Introduction	3
2	ATLAS detector	4
3	Data sample, event simulation and theoretical predictions	5
4	Event reconstruction and selection	6
5	Signal extraction and cross-section measurement	7
	5.1 Invariant mass fit model	8
	5.2 Lifetime fit model	9
	5.3 Cross-section measurement	12
6	Systematic uncertainties	14
7	Results	16
8	Conclusions	21

1 Introduction

The production of heavy hadrons in proton–proton collisions is a fundamental process that provides a crucial test of perturbative quantum chromodynamics (QCD) calculations. However, large uncertainties persist in current theoretical predictions due to the fact that the masses of heavy quarks are comparable to the typical energy scales of the hard scattering processes [1, 2]. Moreover, heavy hadrons can be produced promptly via the hadronisation of charm quarks from the initial hard scattering process, or non-promptly in decays of b -hadrons; precise predictions of such processes are challenging, due to difficulties in modelling non-perturbative effects such as hadronisation, as well as uncertainties in the fragmentation functions and decay dynamics of heavy-flavour hadrons. Given the sizeable theoretical uncertainties, experimental constraints on heavy hadron production cross-sections are important to improve calculation techniques, as well as in searches for new physics phenomena, where heavy hadron production is often either a signal process or a significant background process. For instance, several charmed and bottom mesons have significant decay branching ratios to τ -lepton final states [3]; precise cross-section measurements are necessary for using such decays to search for lepton-flavour-violating τ -lepton decays [4] at the Large Hadron Collider (LHC) [5].

At the LHC, prompt and non-prompt D meson¹ production in proton–proton (pp) collisions has been measured by different experiments. The ALICE Collaboration reported the differential production cross-sections of prompt D^0 , D^\pm , $D^{*\pm}$, and D_s^\pm mesons at a centre-of-mass energy of $\sqrt{s} = 13$ TeV, in the mid-rapidity region and in different ranges of transverse momentum, p_T ; in particular, the D^\pm meson cross-section was measured up to p_T of 50 GeV and the D_s^\pm meson cross-section was measured up to p_T of 36 GeV [6]. Recently, the ALICE Collaboration also published differential production cross-sections of non-prompt D^0 , D^\pm and D_s^\pm mesons in the range of $p_T < 24$ GeV; the results are compared to the prompt measurements to evaluate the non-prompt production fraction [7]. The ATLAS Collaboration has measured $D^{*\pm}$, D^\pm , and D_s^\pm meson production at $\sqrt{s} = 7$ TeV [8], but no such measurement has been performed at $\sqrt{s} = 13$ TeV, nor has the production cross-section of the D_s^\pm meson been measured differentially. A study conducted by the CMS Collaboration reported the differential cross-sections of $D^{*\pm}$, D^0 , and D^\pm with p_T up to 100 GeV based on a partial data sample at $\sqrt{s} = 13$ TeV collected in 2016 [9]. The LHCb Collaboration has published the measurements of the production cross-sections of prompt D^0 , D^\pm , $D^{*\pm}$, and D_s^\pm mesons in the range of $p_T < 15$ GeV in the forward region using $\sqrt{s} = 13$ TeV data [10].

This paper presents a measurement of D^\pm and D_s^\pm meson differential production cross-sections performed with the ATLAS detector using the pp collision data at $\sqrt{s} = 13$ TeV collected during the years 2016–2018. To measure the D^\pm and D_s^\pm mesons produced at the LHC, this study makes use of the semileptonic decay channels $D^\pm/D_s^\pm \rightarrow \phi(\mu\mu)\pi^\pm$. In comparison to reconstructing the fully hadronic decays of the D mesons, the selected decay channels make use of the precise muon reconstruction and identification in the ATLAS detector, allowing a much cleaner signature with a lower background level. The final state of two muons and one pion ($\mu\mu\pi$) is fully reconstructed and identified, to construct the D meson decay vertex. The yields of the D^\pm and D_s^\pm meson signals are then extracted simultaneously by fitting the invariant mass distributions of the $\mu\mu\pi$ system.

To calculate the production cross-sections, simulated events are used to evaluate the reconstruction efficiencies and acceptance. Because of the difficulties in separating the D mesons produced by an initial charm quark (prompt) and those produced by an initial bottom quark (non-prompt), this study does not

¹ In this paper, the \pm symbol is used to represent both charge conjugates inclusively for different D mesons; the D^0 symbol is used to represent D^0 and \bar{D}^0 mesons inclusively.

attempt to extract the prompt and non-prompt signal yields separately; however, their relative contributions in simulated events are constrained to match the data by fitting the pseudo-proper lifetime distribution. The yields and the cross-sections presented are inclusive of both prompt and non-prompt D mesons, unless otherwise specified.

The inclusive and differential cross-sections of the D^\pm and D_s^\pm mesons are reported in the range of $|\eta| < 2.5$ and $12 < p_T < 100$ GeV and compared with state-of-the-art next-to-leading-order (NLO) calculations. This is the first differential measurement of the D_s^\pm meson production reported by the ATLAS Collaboration, and the first time such a measurement has been performed up to transverse momenta of 100 GeV at the LHC.

2 ATLAS detector

The ATLAS detector [11] at the LHC covers nearly the entire solid angle around the collision point.² It consists of an inner tracking detector surrounded by a thin superconducting solenoid, electromagnetic and hadronic calorimeters, and a muon spectrometer incorporating three large superconducting air-core toroidal magnets.

The inner-detector system (ID) is immersed in a 2 T axial magnetic field and provides charged-particle tracking in the range $|\eta| < 2.5$. The high-granularity silicon pixel detector covers the vertex region and typically provides four measurements per track, the first hit generally being in the insertable B-layer (IBL) installed before Run 2 [12, 13]. It is followed by the SemiConductor Tracker (SCT), which usually provides eight measurements per track. These silicon detectors are complemented by the transition radiation tracker (TRT), which enables radially extended track reconstruction up to $|\eta| = 2.0$. The TRT also provides electron identification information based on the fraction of hits (typically 30 in total) above a higher energy-deposit threshold corresponding to transition radiation.

The calorimeter system covers the pseudorapidity range $|\eta| < 4.9$. Within the region $|\eta| < 3.2$, electromagnetic calorimetry is provided by barrel and endcap high-granularity lead/liquid-argon (LAr) calorimeters, with an additional thin LAr presampler covering $|\eta| < 1.8$ to correct for energy loss in material upstream of the calorimeters. Hadronic calorimetry is provided by the steel/scintillator-tile calorimeter, segmented into three barrel structures within $|\eta| < 1.7$, and two copper/LAr hadronic endcap calorimeters. The solid angle coverage is completed with forward copper/LAr and tungsten/LAr calorimeter modules optimised for electromagnetic and hadronic energy measurements respectively.

The muon spectrometer (MS) comprises separate trigger and high-precision tracking chambers measuring the deflection of muons in a magnetic field generated by the superconducting air-core toroidal magnets. The field integral of the toroids ranges between 2.0 and 6.0 T m across most of the detector. Three layers of precision chambers, each consisting of layers of monitored drift tubes, cover the region $|\eta| < 2.7$, complemented by cathode-strip chambers in the forward region, where the background is highest. The muon trigger system covers the range $|\eta| < 2.4$ with resistive-plate chambers in the barrel, and thin-gap chambers in the endcap regions.

² ATLAS uses a right-handed coordinate system with its origin at the nominal interaction point (IP) in the centre of the detector and the z -axis along the beam pipe. The x -axis points from the IP to the centre of the LHC ring, and the y -axis points upwards. Polar coordinates (r, ϕ) are used in the transverse plane, ϕ being the azimuthal angle around the z -axis. The pseudorapidity is defined in terms of the polar angle θ as $\eta = -\ln \tan(\theta/2)$ and is equal to the rapidity $y = \frac{1}{2} \ln \left(\frac{E+p_z}{E-p_z} \right)$ in the relativistic limit. Angular distance is measured in units of $\Delta R \equiv \sqrt{(\Delta y)^2 + (\Delta \phi)^2}$.

The luminosity is measured mainly by the LUCID-2 [14] detector that records Cherenkov light produced in the quartz windows of photomultipliers located close to the beam pipe.

Events are selected by the first-level trigger system implemented in custom hardware, followed by selections made by algorithms implemented in software in the high-level trigger [15]. The first-level trigger accepts events from the 40 MHz bunch crossings at a rate below 100 kHz, which the high-level trigger further reduces in order to record complete events to disk at about 1 kHz.

A software suite [16] is used in data simulation, in the reconstruction and analysis of real and simulated data, in detector operations, and in the trigger and data acquisition systems of the experiment.

3 Data sample, event simulation and theoretical predictions

The data used in this analysis were collected in 2016–2018 with the ATLAS detector in pp collisions at $\sqrt{s} = 13$ TeV at the LHC. Data collected during 2015 were not used for this study, because of the unavailability of low- p_T di-muon triggers in the di-muon invariant mass range of interest. The data are selected after requiring each detector component to be fully operational [17]. The analysed data sample corresponds to an integrated luminosity of 137 fb^{-1} [18].

To model inelastic events produced in pp collisions, a large sample of Monte Carlo (MC) simulated events was prepared using the PYTHIA 8.212 [19] event generator. The simulation was performed using leading-order (LO) matrix elements for all $2 \rightarrow 2$ QCD processes. Initial-state and final-state parton showering were used to simulate the effect of higher-order processes. The NNPDF2.3_{LO} [20] parameterisation provided the parton distribution functions (PDF) of the proton. The charm quark and bottom quark masses were set to 1.5 GeV and 4.8 GeV, respectively. The event sample was simulated using the ATLAS A14 set of tuned parameters [21]. Separate samples were generated for $pp \rightarrow c\bar{c}$ and $pp \rightarrow b\bar{b}$ processes, corresponding to prompt and non-prompt production of D mesons, respectively. The generated D^\pm and D_s^\pm mesons were decayed into $\phi(\mu\mu)\pi^\pm$. The generated events were passed through a full ATLAS detector simulation [22] based on GEANT4 [23] and processed with the same reconstruction algorithms as used for the data. The generation of the simulated event samples includes the effect of multiple pp interactions per bunch crossing (pile-up), as well as the effect on the detector response due to interactions from bunch crossings before or after the one containing the hard interaction. The effect of pile-up was modelled by overlaying the simulated hard-scattering event with inelastic pp collisions generated with PYTHIA 8.186 [24] using the NNPDF2.3_{LO} PDF set and the A3 set of tuned parameters [25]. The simulated events were processed through the same reconstruction algorithms as used for the data.

The measured cross-sections are compared with the general-mass variable-flavour-number scheme (GM-VFNS) [1, 26–29] and the fixed-order next-to-leading-logarithm (FONLL) [30, 31] predictions. These calculations provide more reliable predictions than the traditional NLO massive and massless calculations in the intermediate and high transverse momentum range, where the heavy quark mass, m_Q , is not negligible compared to the transverse momentum of the quark, p_{TQ} . Most of the setup for GM-VFNS and FONLL is unchanged as described in the previous ATLAS measurements [8]; the only updates are the PDF set and the fragmentation fractions used in the FONLL predictions.

The GM-VFNS prediction aims to combine the massless scheme with the massive scheme. In the calculation, the charm quark PDF evolves with massless evolution, while the heavy quark mass is retained in the hard-scattering calculation. With such an approach, the calculation agrees with the massless scheme at $p_{TQ} \gg m_Q$, and with the massive scheme at $p_{TQ} \approx m_Q$. The GM-VFNS calculation uses

the CT14_{NLO} [32] PDF set and the fragmentation functions are taken from the KKKS08 set [33]. The prediction is available for both D^\pm and D_s^\pm mesons; the values are provided by the authors themselves. The uncertainties in the GM-VFNS predictions are dominated by QCD scale uncertainties, namely those of the renormalisation and factorisation scales for initial-state singularities and of the factorisation scale for final-state singularities.

The FONLL calculation consists of three components: the heavy quark production cross-section calculated in perturbative QCD, the non-perturbative heavy-flavour fragmentation, and the decay function describing the heavy hadron decay into leptons. The principle of FONLL is to expand the massless scheme computation in powers of the strong coupling α_s , and replace a finite number of terms with their massive scheme counterparts. For instance, the massive and massless scheme predictions are matched exactly up to $O(\alpha_s^3)$, giving predictions that are reliable for both $p_{TQ} \approx m_Q$ and $p_{TQ} \gg m_Q$ regions. Currently, the FONLL calculation is available for the D^\pm meson, but not for the D_s^\pm meson [30, 31, 34, 35]. The calculation uses the NNPDF3.0_{NLO} [36] PDF set, and the fragmentation fractions $f(b/c \rightarrow D)$ are taken from averaging the LEP measurements [37]. The fragmentation fractions, updated by the author of Ref. [37] using the newest values of charmed hadron decay branching ratios in Ref. [3], are $f(b \rightarrow D^\pm) = 0.217 \pm 0.011$ and $f(c \rightarrow D^\pm) = 0.219 \pm 0.010$.³ The theoretical uncertainties considered include the renormalisation and factorisation scale uncertainties, the pole-mass uncertainties of charm and bottom quarks, the PDF uncertainty, and the fragmentation-fraction uncertainty.

For both GM-VFNS and FONLL, the inclusive cross-sections at $\sqrt{s} = 13$ TeV are also compared with the corresponding values at $\sqrt{s} = 7$ TeV in the same fiducial volume. In such comparisons, the scale uncertainties at different centre-of-mass energies are assumed to be fully correlated, in order to evaluate the ratios between cross-sections at different centre-of-mass energies.

4 Event reconstruction and selection

To identify and select the decay $D^\pm/D_s^\pm \rightarrow \phi(\mu\mu)\pi^\pm$, a series of selection criteria are defined to enhance the signal-to-background ratio; the selections are summarised in Table 1. The events are first required to have been accepted by two-muon triggers, which pre-selected muons with certain p_T thresholds and a loose di-muon invariant mass requirement. At least one of the two muons was required to satisfy a p_T threshold of 6 GeV; the threshold for the other muon was either 6 GeV or 11 GeV, depending on the year of data-taking [38]. Reconstructed muons are required to have a transverse momentum greater than 6 GeV, to be within the pseudorapidity range of $|\eta| < 2.5$, and to satisfy the *Loose* identification working point requirements [39]. Combined ID+MS measurements of track parameters are used for muons. Di-muon candidates are also required to contain two selected muons with opposite electric charges Q_μ . The di-muon invariant mass is required to agree with the ϕ meson mass of 1 019.5 MeV [3] within a window $\delta m(|\eta|)$ that scales linearly as a function of absolute pseudorapidity $|\eta|$, from 24 MeV at $|\eta| = 0$ to 48 MeV at $|\eta| = 2.5$. This requirement retains approximately 90% of di-muon signal events in MC simulated events. In addition, one track satisfying the *Loose* identification working point requirements [40], with p_T of at least 1 GeV and within the pseudorapidity range of $|\eta| < 2.5$, is required to be reconstructed in the ID.

³ In this paper, the fragmentation fractions obtained by averaging the LEP measurements are used, because the p_T range of interest is relatively high compared to the D^\pm and D_s^\pm meson masses. It is also noted that the ALICE Collaboration has measured the fragmentation fractions in the low- p_T range, where the p_T of the quarks is comparable to the mass of the hadrons ($p_{TQ} \approx m_Q$). If the fragmentation values obtained by the ALICE Collaboration were used, the FONLL prediction would be lowered by approximately 10%.

Table 1: Summary of selection requirements, with items defined in the text.

	Selection
Muon objects	Two muons satisfying the <i>Loose</i> [39] working point
Track object	One track satisfying the <i>Loose</i> [40] working point
Transverse momentum	$p_T^\mu > 6 \text{ GeV}, p_T^\pi > 1 \text{ GeV}$
Total charge	$ Q_{\text{triplet}} = 1$
Opposite charge muons	$Q_{\mu_1} \times Q_{\mu_2} = -1$
Di-muon invariant mass	$ m_{\mu\mu} - m_\phi < \delta m(\eta)$
L_{xy} significance	$\text{Sig}(L_{xy}) > 3$
a_{xy}^0 significance	$ \text{Sig}(a_{xy}^0) < 4$
Vertex p -value	$\log(p_0^{\text{vertex}}) > -0.8$
Highest vertex p -value	The vertex with $\text{Max}(p_0^{\text{vertex}})$ in the event

All possible di-muon-plus-track ($\mu\mu\pi$) combinations are used as inputs to D meson candidate secondary vertex (SV) fits, to maximize the number of vertex candidates. For each candidate, a primary vertex (PV) refit [41] is performed after removing the three tracks associated to the candidate, providing an updated PV position. Due to the D^\pm and D_s^\pm lifetime, the three-particle SV is often separated from the primary vertex. The characteristics of the separation between the SV and the PV are therefore used to reject background. Two projections of the SV displacement relative to the PV in the transverse plane are used: $L_{xy} = |\vec{L}_T| \cos \theta_{xy}$ and $a_{xy}^0 = |\vec{L}_T| \sin \theta_{xy}$, where \vec{L}_T is the vector connecting the PV and the SV in the transverse plane, and θ_{xy} is the angle between \vec{L}_T and the transverse momentum \vec{p}_T of the $\mu\mu\pi$ candidate. Since a large separation in L_{xy} distributions is observed between signal and background events, a stringent cut is placed on this variable. For a_{xy}^0 , the background distribution has a tail similar to the non-prompt signal. To account for detector resolution, the significance of L_{xy} and a_{xy}^0 , $\text{Sig}(L_{xy})$ and $\text{Sig}(a_{xy}^0)$, are defined as $L_{xy}/\sigma_{L_{xy}}$ and $a_{xy}^0/\sigma_{a_{xy}^0}$, where $\sigma_{L_{xy}}$ and $\sigma_{a_{xy}^0}$ are the uncertainties in L_{xy} and a_{xy}^0 , respectively. The selections placed on these two variables are $\text{Sig}(L_{xy}) > 3$ and $|\text{Sig}(a_{xy}^0)| < 4$.

Given the large number of low- p_T tracks originating from hadronic activity, many tracks that are not produced by D meson decays are mistakenly included as candidates. To suppress these combinatorial backgrounds, which are often poorly reconstructed, requirements are placed on the goodness of fits for the SV. The SV p -value p_0^{vertex} is defined as the probability of obtaining a χ^2 value larger than that of the reconstructed SV; only SVs with $\log(p_0^{\text{vertex}}) > -0.8$ (i.e. $p_0^{\text{vertex}} > 0.158$) are selected. Because of the detector coverage and the trigger thresholds, the final candidate is required to have a transverse momentum above 12 GeV and to be within the pseudorapidity range of $|\eta| < 2.5$. In the following sections, p_T and η will refer to the transverse momentum and pseudorapidity of the $\mu\mu\pi$ system unless otherwise specified. At the end of the selection chain, only the $\mu\mu\pi$ candidate with the highest vertex fit probability p -value p_0^{vertex} is selected per event.

5 Signal extraction and cross-section measurement

To extract the signal, the invariant mass of the di-muon-plus-track candidates $m_{\mu\mu\pi}$ is constructed. The yields of the D mesons are then extracted by performing fits to the distributions of $m_{\mu\mu\pi}$ in bins of p_T and $|\eta|$; the model for this fit is described in Section 5.1. Since evaluating the differential cross-section

requires reconstruction efficiencies in multiple bins, such values are derived from MC simulated events. The reconstruction efficiencies are different for D mesons produced promptly and non-promptly, of which the relative contributions can be poorly modelled in MC simulation; therefore, an additional study is performed to constrain the fraction of non-prompt production from data. This involves extracting the signal yields in bins of pseudo-proper lifetimes and fitting the resulting distributions with templates from MC simulated events corresponding to prompt and non-prompt production; this procedure is described in Section 5.2. Finally, the cross-section calculation is described in Section 5.3.

5.1 Invariant mass fit model

Since a fit to the invariant mass $m_{\mu\mu\pi}$ is used to extract the signal yield in bins of p_T , η , and lifetime, the fit model must be flexible and stable enough to extract yields in subsets of data with different sample sizes and signal-to-background ratios. For the D^\pm and D_s^\pm signals, the fit models P_{D^\pm} and $P_{D_s^\pm}$ are chosen to be non-relativistic Voigtian distributions (Voigt), because of the small number of floating shape parameters (three) and their good performance based on tests in simulated samples. A Voigtian distribution is the convolution of a Breit–Wigner distribution with a Gaussian (Gauss) distribution [42]. Since the D^\pm and D_s^\pm mesons have negligible natural widths, the detector resolution is absorbed by the shape parameters of both the Breit–Wigner distribution and the Gaussian distribution. The background contribution P_{Bkg} , originating mainly from combinatorics, is extracted using a normalised quadratic exponential distribution. Using RooFit [43], the extended unbinned maximum likelihood $\mathcal{L}(m)$ of the combined fit function is implemented as the following:

$$\begin{aligned}\mathcal{L}(m) &= \frac{e^{-(S_{D^\pm} + S_{D_s^\pm} + B)}}{n!} \prod [S_{D^\pm} P_{D^\pm}(m) + S_{D_s^\pm} P_{D_s^\pm}(m) + B P_{\text{Bkg}}(m)] \times \mathcal{G}(\Delta), \\ P_{D^\pm}(m) &= \text{Voigt}(m; m_{D^\pm}, \gamma_{D^\pm}, \sigma_{D^\pm}), \\ P_{D_s^\pm}(m) &= \text{Voigt}(m; m_{D_s^\pm}, \gamma_{D_s^\pm}, \sigma_{D_s^\pm}), \\ P_{\text{Bkg}}(m) &= A_{\text{norm}} \cdot e^{(c_1 m + c_2 m^2)}, \\ \mathcal{G}(\Delta) &= \text{Gauss}(\Delta; \mu_\Delta, \sigma_\Delta),\end{aligned}\tag{1}$$

where A_{norm} is the normalisation factor of the quadratic exponential distribution, and S_{D^\pm} , $S_{D_s^\pm}$ and B are the yields of D^\pm mesons, D_s^\pm mesons and background, respectively. The Voigtian distributions of the D^\pm and D_s^\pm mesons are parameterised by the mean parameters m_{D^\pm} and $m_{D_s^\pm}$, while γ_{D^\pm} and $\gamma_{D_s^\pm}$ are the widths of the Breit–Wigner distributions and the widths of the Gaussian distributions are σ_{D^\pm} and $\sigma_{D_s^\pm}$. The parameter c_1 is the linear rate parameter as in a simple exponential distribution, while the parameter c_2 is the quadratic part that is multiplied by m^2 . The mass difference Δ is defined as $m_{D_s^\pm} - m_{D^\pm}$, which is constrained to be close to the world average mass difference μ_Δ [3] of the two D mesons by using an additional Gaussian constraint $\mathcal{G}(\Delta)$ with mean μ_Δ and width σ_Δ .

In the model, the parameters of interest are the yields S_{D^\pm} and $S_{D_s^\pm}$, while the other parameters that determine the background model and the signal shape are regarded as nuisance parameters. To improve the stability of the fit model, particularly in bins with low numbers of candidates, fits are performed to the MC simulated events to fix some of the nuisance parameters, including γ_{D^\pm} and $\gamma_{D_s^\pm}$. The unbinned maximum-likelihood fit to the mass spectrum is presented in Figure 1; for each data point, the pull is defined as the difference between the data and the fitted model divided by the statistical uncertainty in the data point. It can be observed in the figure and in the fits to different kinematic regions in Section 5.3 that this approach achieves compatibility with the observed data while reducing the number of fit parameters.

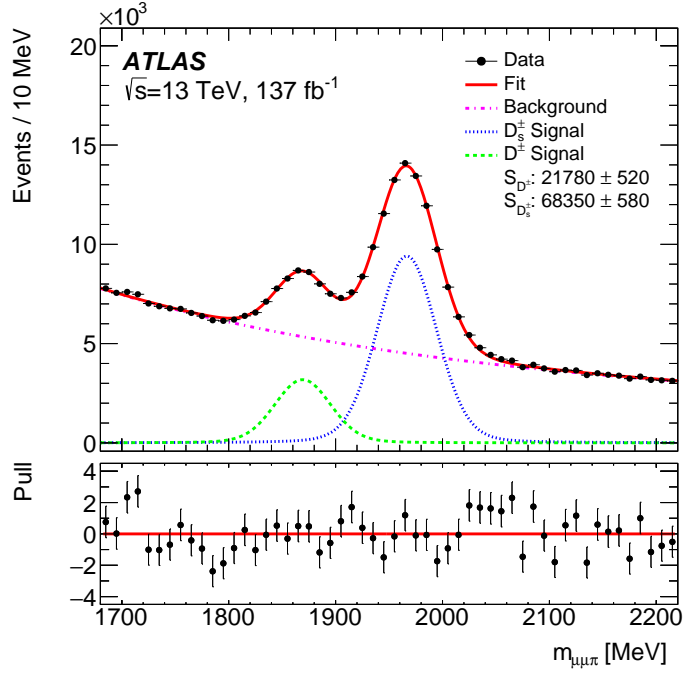


Figure 1: Invariant mass distribution of the di-muon-plus-track candidates. The unbinned fit according to Eq. (1) is shown as a solid line, with the signal components for the D^\pm and D_s^\pm resonance fit presented as dashed and dotted lines, respectively; the background-only contribution is shown as a dash-dotted line. The signal yields extracted are also shown with corresponding statistical uncertainties. The lower panel shows the pull distribution.

5.2 Lifetime fit model

This section describes the extraction of prompt and non-prompt lifetime templates from the MC simulation, together with a template fit to the data to estimate the contribution from non-prompt processes. To quantify the proportion of non-prompt processes, the non-prompt fraction f_{NP} is defined as the yield of non-prompt signal yield divided by the total signal yield. The two production mechanisms mainly differ in terms of the average decay distance from the PV. From the reconstructed vertex position, the pseudo-proper-lifetime (hereinafter referred to as lifetime) τ of the $\mu\mu\pi$ candidates is calculated as:

$$\tau = \frac{m_{\mu\mu\pi} L_{xy}}{p_T}. \quad (2)$$

Because of the relatively long lifetime of D^\pm (D_s^\pm) mesons, they can travel for approximately 1 ps (0.5 ps) before they decay into a ϕ meson and a pion. The prompt contribution therefore includes an exponential distribution (Exp) to describe the physical exponential decay of the particle, which is convolved with a Gaussian distribution (Gauss) and an error function (Erf) to account for the detector resolution and the turn-on effect at low lifetime. The turn-on effect describes the transition in efficiency from zero to a constant at low lifetime, which is mainly due to the requirement on the significance of L_{xy} .

For the non-prompt production mode, the B meson, which has a typical lifetime of 1.5 ps, can travel a few millimeters before it decays into a D^\pm/D_s^\pm meson. The non-prompt contribution therefore includes one exponential distribution to account for the cascade decay of the B meson, and another exponential

distribution to account for the lifetime of the D^\pm/D_s^\pm mesons. As for the prompt contribution, the distribution is also convolved with a Gaussian distribution and an error function to account for detector effects.

The templates for the non-prompt contribution $P_{bb}(\tau)$ and the template for the prompt contribution $P_{cc}(\tau)$ are defined as follows:

$$\begin{aligned} P_{bb}(\tau) &= \text{Exp}(\tau; \tau_D^{bb}) * \text{Exp}(\tau; \tau_B^{bb}) * \text{Gauss}(\tau; \mu^{bb}, \sigma_{\text{res}}^{bb}) * \text{Erf}(\tau; \tau_{\text{turn-on}}^{bb}, \beta^{bb}), \\ P_{cc}(\tau) &= \text{Exp}(\tau; \tau_D^{cc}) * \text{Gauss}(\tau; \mu^{cc}, \sigma_{\text{res}}^{cc}) * \text{Erf}(\tau; \tau_{\text{turn-on}}^{cc}, \beta^{cc}). \end{aligned} \quad (3)$$

Here the asterisk sign $*$ indicates the linear convolution between the functions, τ is the lifetime of the secondary vertex, τ_D^{bb} and τ_D^{cc} are the lifetime components of the D^\pm/D_s^\pm meson, τ_B^{bb} is the lifetime component of the B meson for the non-prompt decay, μ^{bb} and μ^{cc} represent a constant shift in lifetime due to detector bias, σ_{res}^{bb} and σ_{res}^{cc} describe the smearing due to detector resolution, $\tau_{\text{turn-on}}^{bb}$ and $\tau_{\text{turn-on}}^{cc}$ represent a constant shift in lifetime due to the turn-on effect, and β^{bb} and β^{cc} are multiplicative factors applied to the lifetime that determine the sharpness of the turn-on effect. These functions are fitted to the prompt and non-prompt MC simulated events separately to extract the templates, and the parameters are fixed before extracting the non-prompt fraction from data.

Before performing a lifetime fit to the data using the MC templates, the signal distribution must be extracted from data by removing the background contribution. Invariant mass fits (as described in Section 5.1) are performed in bins of the lifetime, τ , allowing the signal yield N_i and its uncertainty σ_i to be extracted in each lifetime interval i for the data. A minimum χ^2 fit is performed on the extracted signal distribution using the prompt and non-prompt lifetime templates. Since the parameters of the individual MC templates are fixed, the only fit parameter is the non-prompt fraction f_{NP} . With such an approach, the fits can extract yields up to lifetimes of 5.0 ps for the D_s^\pm meson and 8.0 ps for the D^\pm meson; beyond this, there are insufficient data to perform the fits. Because the signal yields are extracted in finite bins of lifetime, the sharply rising slope at low lifetime cannot be reliably extracted; therefore, the region with low lifetime is excluded from the fit. For the D^\pm meson, the region with lifetime less than 1.0 ps is excluded; for the D_s^\pm meson, the region with lifetime less than 0.5 ps is excluded.

The procedure is applied separately for D^\pm and D_s^\pm mesons across three bins of p_T ; in each bin of p_T , the individual templates and the combined models are all fitted separately. The bins are defined to capture the falling shape of f_{NP} , while ensuring enough data are present in each bin. The bin boundaries in p_T are [12, 20, 30, 100] GeV. Figure 2 shows the extracted signal from data and the fits with the combined model for the first p_T region. The χ^2 divided by the number of degrees of freedom of the fits ranges from 0.6 to 1.5, showing a good agreement between the model and the data.

Figure 3 shows the extracted non-prompt fraction and the corresponding statistical uncertainties for both D^\pm and D_s^\pm in bins of p_T . The statistical uncertainties for D^\pm mesons are larger than for D_s^\pm mesons. This is due to the lower yield and the longer lifetime of the D^\pm meson, which causes the discriminating power of the fit to decrease due to the similarity of the prompt and non-prompt shapes.

The non-prompt fraction is then used to construct the weights for the MC simulated events, such that the non-prompt contribution in data is matched in the MC simulated events. The uncertainties in the non-prompt fractions are relatively large; therefore, no interpretation or comparison is made with theoretical predictions. However, the extracted uncertainties in the non-prompt fractions allow the systematic uncertainties for the two production mechanisms to be evaluated.

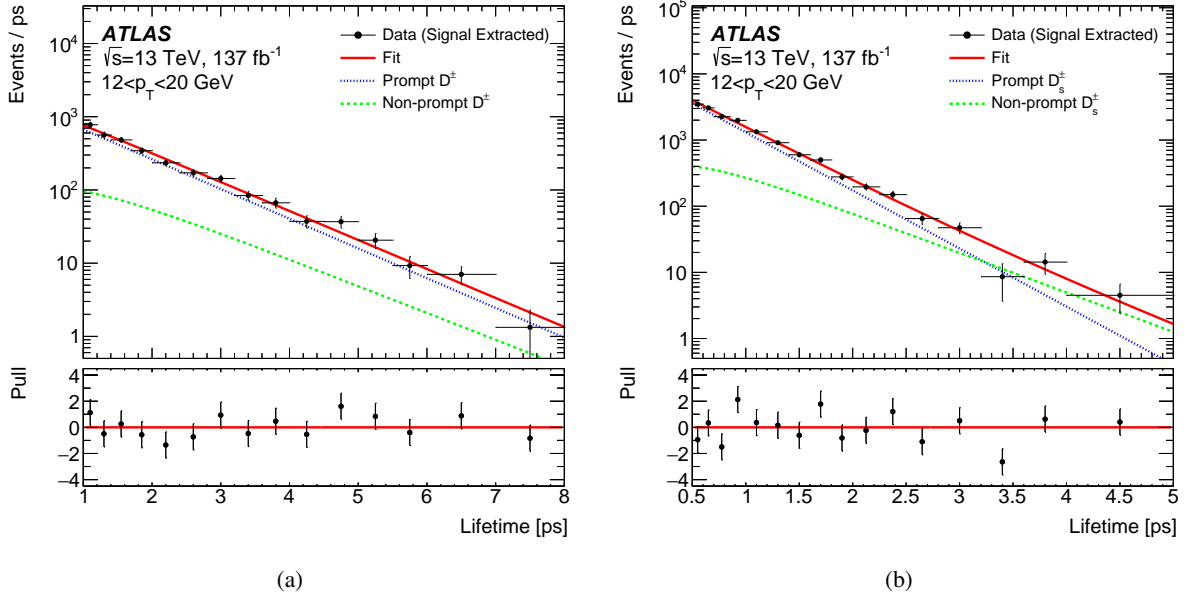


Figure 2: Template fits to the lifetime distribution extracted from data for (a) D^\pm and (b) D_s^\pm mesons in the range of $12 < p_T < 20$ GeV. The prompt and non-prompt contributions are presented as dotted and dashed lines, respectively; the combined fits are shown as solid lines. The bin sizes are variable, and the data points are drawn at the bin centres. The lower panels show the pull distributions.

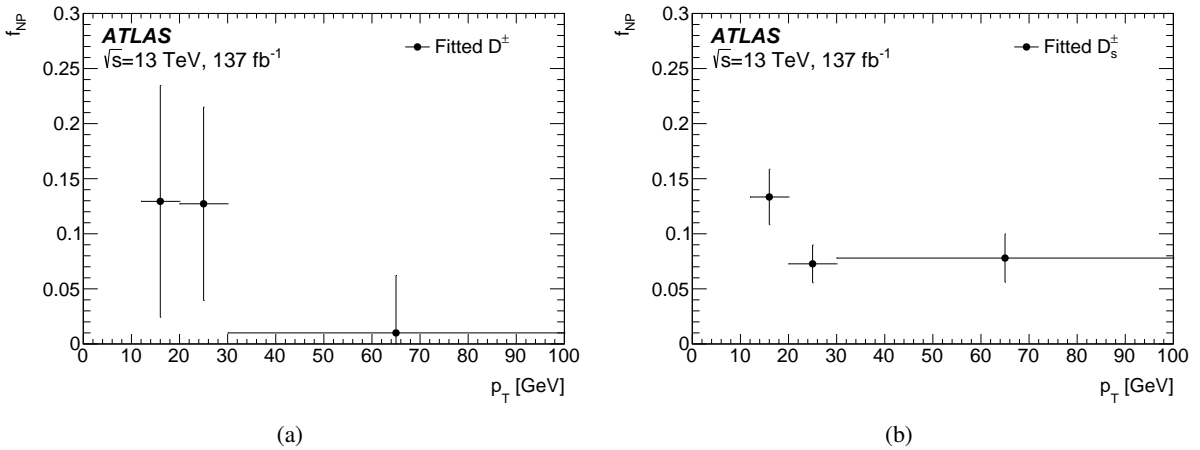


Figure 3: Estimated non-prompt fraction of (a) D^\pm and (b) D_s^\pm mesons production as a function of p_T , in the fiducial volume defined by $12 < p_T < 100$ GeV and $|\eta| < 2.5$. Only the statistical uncertainties are shown.

5.3 Cross-section measurement

The differential cross-section is measured in the fiducial volume defined by $12 < p_T < 100$ GeV and $|\eta| < 2.5$ for D^\pm and D_s^\pm mesons, in nine bins of p_T and five bins in $|\eta|$. To obtain the differential cross-section in a given bin, the yields of D^\pm and D_s^\pm mesons in the bin are obtained from a fit to the triplet mass $m_{\mu\mu\pi}$, as described in Section 5.1. Figures 4 and 5 show the examples of the invariant mass fits in two bins of p_T and $|\eta|$ to extract the signal.

For each bin in p_T (denoted by i) and each bin in $|\eta|$ (denoted by j), the yield obtained is then divided by the overall efficiency, bin width, branching ratio \mathcal{B} , and the integrated luminosity to evaluate the differential production cross-section. The differential cross-sections in p_T and $|\eta|$ are given by the following equations:

$$\left. \frac{d\sigma}{dp_T} \right|_i = \frac{S_{D^\pm/D_s^\pm}^i}{\int \mathcal{L} dt \times C^i \times \mathcal{B}(D^\pm/D_s^\pm \rightarrow \phi(\mu\mu)\pi^\pm) \times \Delta^i p_T},$$

$$\left. \frac{d\sigma}{d|\eta|} \right|_j = \frac{S_{D^\pm/D_s^\pm}^j}{\int \mathcal{L} dt \times C^j \times \mathcal{B}(D^\pm/D_s^\pm \rightarrow \phi(\mu\mu)\pi^\pm) \times \Delta^j |\eta|},$$
(4)

where $S_{D^\pm/D_s^\pm}^i$ and $S_{D^\pm/D_s^\pm}^j$ are the yields of D^\pm and D_s^\pm signals extracted in bins of p_T and $|\eta|$, $\Delta^i p_T$ is the bin width in p_T , and $\Delta^j |\eta|$ is the bin width in $|\eta|$. The integrated luminosity, $\int \mathcal{L} dt$, is 137 fb^{-1} [18]. The correction factors C^i and C^j account for the reconstruction and selection efficiency and acceptance, which are derived bin-by-bin in p_T and $|\eta|$, respectively, using MC simulated events.

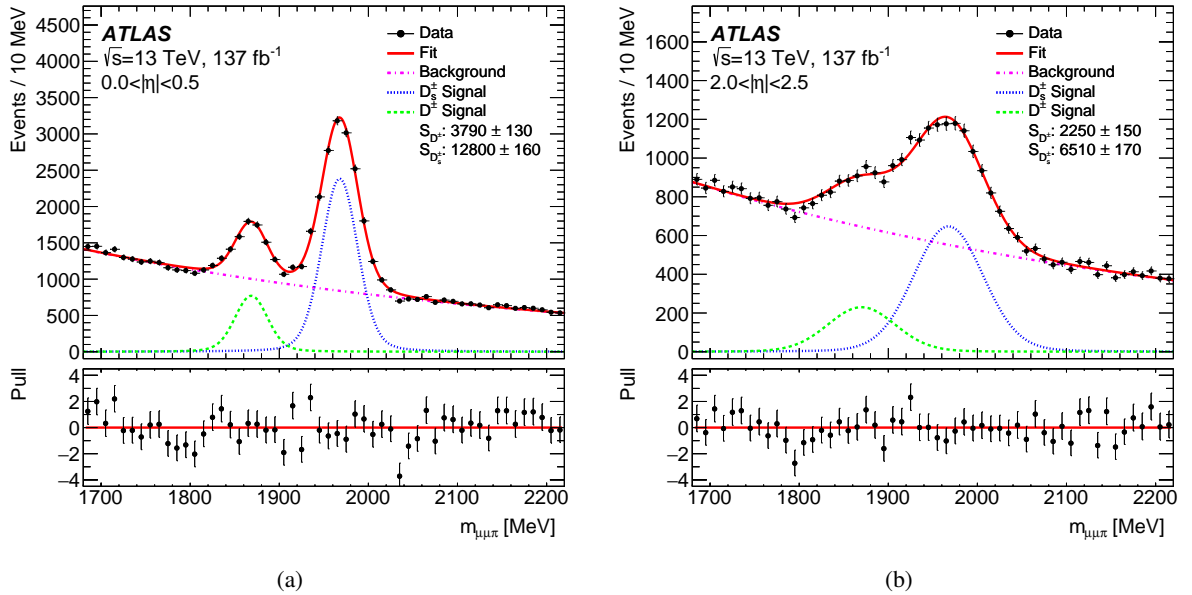


Figure 4: Examples of fits to the distribution of invariant mass $m_{\mu\mu\pi}$ in regions of (a) $0.0 < |\eta| < 0.5$ and (b) $2.0 < |\eta| < 2.5$. The unbinned fits according to Eq. (1) are shown as solid lines, with the signal components for the D^\pm and D_s^\pm resonance fit presented as dashed and dotted lines, respectively; the background-only contributions are shown as dash-dotted lines. The signal yields extracted are also shown with corresponding statistical uncertainties. The lower panels show the pull distributions.

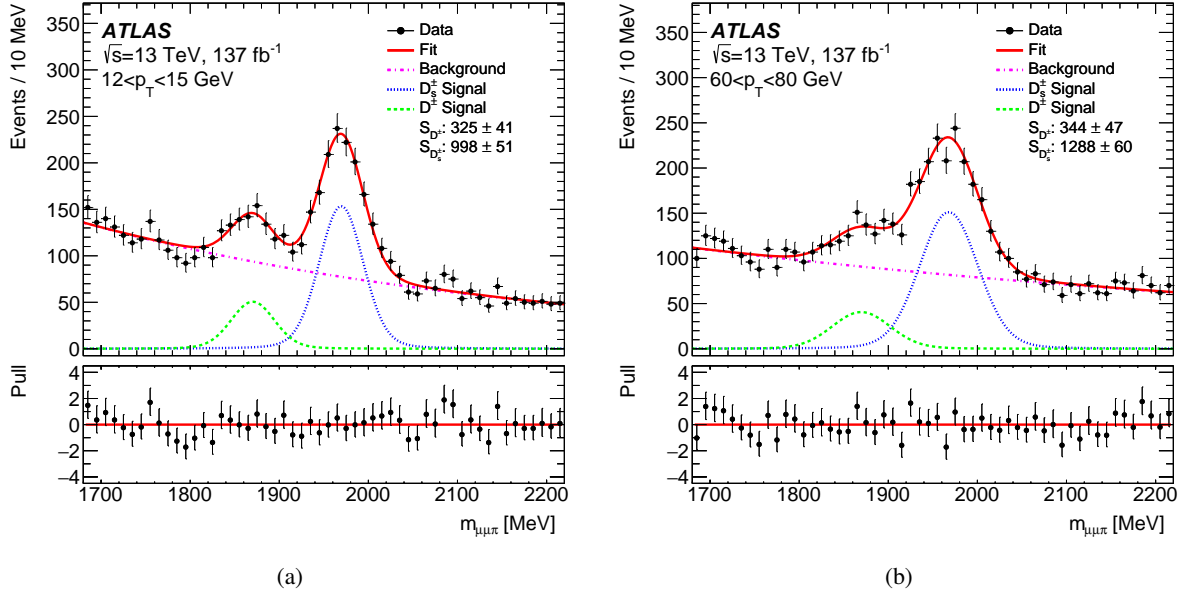


Figure 5: Examples of fits to the distribution of invariant mass $m_{\mu\mu\pi}$ in regions of (a) $12 < p_T < 15$ GeV and (b) $60 < p_T < 80$ GeV. The unbinned fits according to Eq. (1) are shown as solid lines, with the signal components for the D^\pm and D_s^\pm resonance fit presented as dashed and dotted lines, respectively; the background-only contributions are shown as dash-dotted lines. The signal yields extracted are also shown with corresponding statistical uncertainties. The lower panels show the pull distributions.

The branching ratio of the D_s^\pm decay chain is given by:

$$\mathcal{B}(D_s^\pm \rightarrow \phi(\mu\mu)\pi^\pm) = \frac{\mathcal{B}(D_s^\pm \rightarrow \phi(K^+K^-)\pi^\pm)}{\mathcal{B}(\phi \rightarrow K^+K^-)} \times \mathcal{B}(\phi \rightarrow \mu\mu), \quad (5)$$

as the uncertainties of the world average branching ratios of the $D_s^\pm \rightarrow \phi(K^+K^-)\pi^\pm$ and $\phi \rightarrow K^+K^-$ processes combined are better than the branching ratio of $D_s^\pm \rightarrow \phi\pi^\pm$ [3]. For the D^\pm meson, the branching ratio is taken as the product of the branching ratios of the $D^\pm \rightarrow \phi\pi^\pm$ and $\phi \rightarrow \mu\mu$ processes [3].

The cross-section in the fiducial volume is determined by summing over the bins i of the differential cross-section as a function of p_T , according to:

$$\sigma_{\text{fiducial}} = \sum_i \left. \frac{d\sigma}{dp_T} \right|_i \Delta^i p_T. \quad (6)$$

Summing over the differential cross-section in bins of $|\eta|$ is found to give a consistent result when compared to summing over p_T .

To facilitate the use of the result as a normalisation for other studies and as a comparison with previous measurements, different fiducial volumes are considered. The lower p_T boundary of 12 GeV corresponds to the lowest p_T reach; the p_T boundaries of 15 and 20 GeV are also considered. The p_T boundary of 15 GeV provides a p_T range that is above the trigger efficiency plateau to reduce the muon and trigger uncertainties; the p_T boundary of 20 GeV provides a p_T range compatible with the previous ATLAS measurements [8].

6 Systematic uncertainties

The uncertainties in the signal yields, acceptance correction factors, integrated luminosity, and the decay branching ratios are propagated linearly to the differential and thus to the integrated fiducial cross-sections according to Eq. (4). The systematic uncertainties can be categorised into detector effects, production modelling, branching ratio, MC simulated data sample size and signal extraction.

The systematic uncertainties due to detector effects are as follows:

Muon reconstruction: The muon reconstruction and identification efficiency uncertainties [39] affect the acceptance correction factors in Eq. (4), while those on muon momentum calibration [44] can also cause bin migrations in the differential measurements.

Track reconstruction: The uncertainty in the track reconstruction efficiency arises primarily from the limited knowledge of the ID material description used in MC simulation. Uncertainties in track momentum and impact parameter calibration are also accounted for in vertex fitting and selection [45].

Pile-up reweighting: Pile-up refers to the number of simultaneous pp collisions in the same event. Weights are applied to MC simulation to make the pile-up distribution match that in data and are varied according to its uncertainty.

Trigger: The trigger efficiencies are measured in data using $J/\psi \rightarrow \mu\mu$ events following the procedure described in Ref. [46]. The MC simulated samples are corrected to reproduce the measured efficiencies, and the uncertainty of the measurement is accounted for as a systematic uncertainty.

Luminosity: The uncertainty in the integrated luminosity of the combined data sample from 2016, 2017, and 2018 is 0.84%, using the same methodology as in Ref. [18], and obtained using the LUCID-2 detector [14] for the primary luminosity measurements, complemented by measurements using the ID and calorimeters.

The systematic uncertainties due to the modelling of D^\pm and D_s^\pm mesons production are as follows:

Non-prompt fraction: To correct for the MC modelling of the non-prompt D^\pm and D_s^\pm mesons production fraction, the procedure described in Section 5.2 is used and its uncertainty is propagated.

Production kinematics: The MC simulated p_T spectra of D^\pm and D_s^\pm mesons production are corrected to match the distribution extracted from data. The statistical uncertainties in the data spectra are propagated to the acceptance correction factors using this procedure. The uncertainties due to the $|\eta|$ spectra modelling are found to be negligible, while those of the p_T spectra have a small effect when propagated to the differential cross-section measurements in $|\eta|$.

The remaining systematic uncertainties are as follows:

Branching ratio: The uncertainties in the branching ratios are taken from Ref. [3]. For the D^\pm meson, the total uncertainty in the decay chain is 7.2%, while that of the D_s^\pm meson is 7.3%.

MC simulated sample size: The statistical uncertainty due to limited size of MC simulated signal samples is propagated to the measurement results via the acceptance correction factors.

Fit model: The fit model systematic uncertainties can be separated into contributions from the signal model and the background model. By varying the models, the difference in yield is taken as a systematic uncertainty. MC pseudo data are generated according to the distribution obtained from data, according to Poisson fluctuations; fits with alternative models are then applied to the pseudo data. For the signal model, the Bukin model [47] and triple Gaussian models are chosen as alternatives. For the background model, a simple exponential model is taken as the alternative. By repeatedly fitting the nominal models and the alternative models to the pseudo data, the distributions of the yield estimators are obtained. The mean yield differences between the nominal model and the alternative models are taken as the systematic uncertainties. The background model systematic uncertainty is also checked to cover the effects of possible contributions from partially reconstructed D meson decays, such as $D^\pm/D_s^\pm \rightarrow \phi\pi^\pm\pi^0$ decays.

The uncertainties above are evaluated in bins of p_T and $|\eta|$, except for the uncertainties in the luminosity and branching ratios. Figures 6 and 7 show the systematic uncertainty profiles of D^\pm and D_s^\pm mesons in bins of p_T and $|\eta|$.

For the D_s^\pm measurement, the largest systematic uncertainty contributions arise from the decay branching ratios, followed by the trigger uncertainty and background modelling uncertainty. For the D^\pm cross-section, the background modelling uncertainty dominates in most of the phase space. The combined systematic uncertainty is mainly in the range of 10%–14% for the D_s^\pm and 15%–20% for the D^\pm due to the latter being more sensitive to the choice of background model.

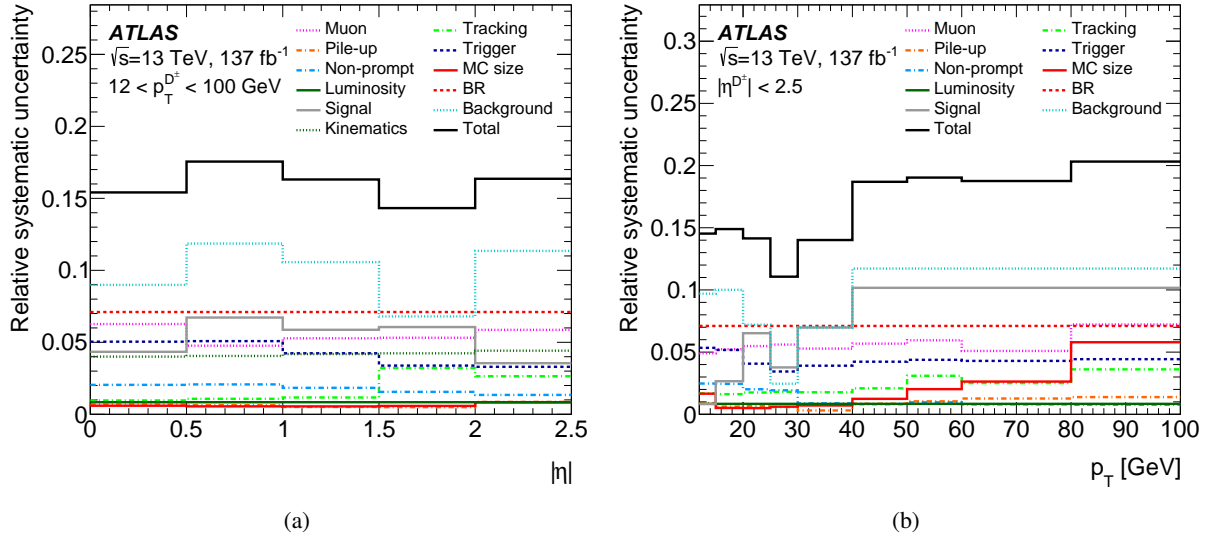


Figure 6: Relative systematic uncertainty profile of the differential cross-sections for D^\pm mesons, in bins of (a) $|\eta|$ and (b) p_T . The systematic uncertainties shown are also combined in quadrature (upper solid line).

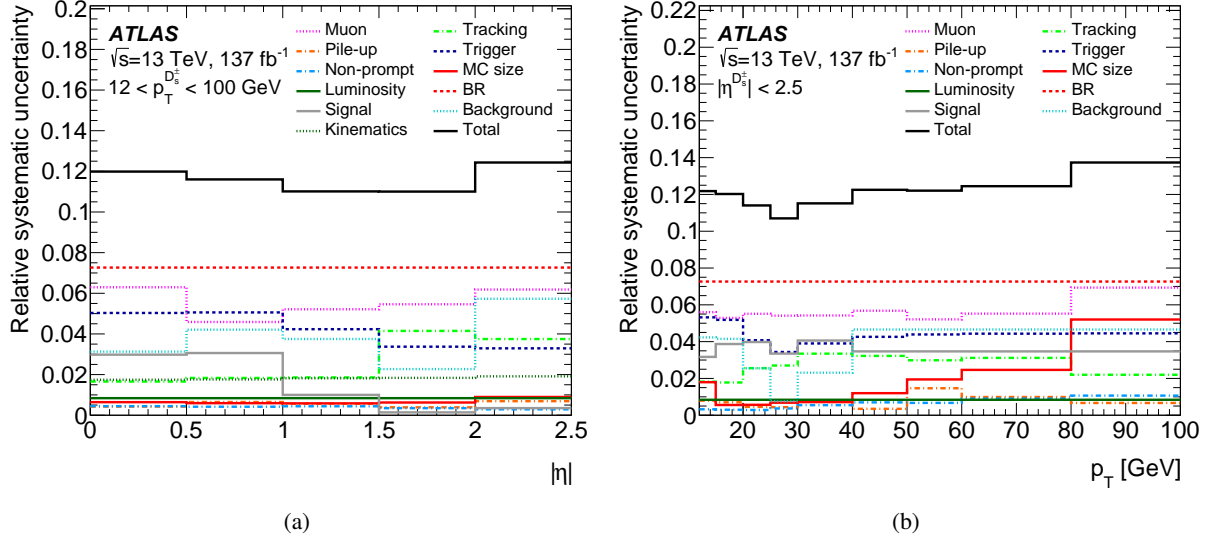


Figure 7: Relative systematic uncertainty profile of the differential cross-sections for D_s^\pm mesons, in bins of (a) $|\eta|$ and (b) p_T . The systematic uncertainties shown are also combined in quadrature (upper solid line).

7 Results

The values of the measured differential cross-sections and the theory predictions are shown in Tables 2 to 5 for D^\pm and D_s^\pm mesons; they are also shown in Figure 8. The fiducial cross-section is summarised in Table 6, including the theory predictions available.

Table 2: The measured differential cross-sections and the predictions from GM-VFNS and FONLL calculations for the D^\pm meson in bins of $|\eta|$ for $12 < p_T < 100$ GeV.

Range	Differential cross-section [μb]		
	Data	GM-VFNS	FONLL
	$\frac{d\sigma}{d \eta } \pm \delta_{\text{stat}} \pm \delta_{\text{syst}}$	$\frac{d\sigma}{d \eta } \pm \delta_{\text{theory}}$	$\frac{d\sigma}{d \eta } \pm \delta_{\text{theory}}$
$0.0 < \eta < 0.5$	$5.15 \pm 0.18 \pm 0.79$	$6.4^{+1.3}_{-1.1}$	$4.7^{+1.2}_{-0.9}$
$0.5 < \eta < 1.0$	$5.8 \pm 0.2 \pm 1.0$	$6.2^{+1.3}_{-1.0}$	$4.5^{+1.2}_{-0.9}$
$1.0 < \eta < 1.5$	$4.96 \pm 0.22 \pm 0.81$	$5.8^{+1.2}_{-1.0}$	$4.2^{+1.1}_{-0.8}$
$1.5 < \eta < 2.0$	$3.62 \pm 0.18 \pm 0.50$	$5.3^{+1.1}_{-0.9}$	$3.8^{+1.0}_{-0.7}$
$2.0 < \eta < 2.5$	$3.33 \pm 0.23 \pm 0.55$	$4.5^{+0.9}_{-0.8}$	$3.2^{+0.9}_{-0.6}$

Table 3: The measured differential cross-sections and the predictions from GM-VFNS and FONLL calculations for the D^\pm meson in bins of p_T for $|\eta| < 2.5$.

Range [GeV]	Differential cross-section [pb/GeV]		
	Data	GM-VFNS	FONLL
	$\frac{d\sigma}{dp_T} \pm \delta_{\text{stat}} \pm \delta_{\text{syst}}$	$\frac{d\sigma}{dp_T} \pm \delta_{\text{theory}}$	$\frac{d\sigma}{dp_T} \pm \delta_{\text{theory}}$
$12 < p_T < 15$	$(1.80 \pm 0.23 \pm 0.26) \times 10^6$	$2.45^{+0.58}_{-0.44} \times 10^6$	$1.82^{+0.54}_{-0.38} \times 10^6$
$15 < p_T < 20$	$(7.0 \pm 0.3 \pm 1.1) \times 10^5$	$8.5^{+1.7}_{-1.4} \times 10^5$	$6.1^{+1.5}_{-1.1} \times 10^5$
$20 < p_T < 25$	$(2.10 \pm 0.08 \pm 0.29) \times 10^5$	$2.76^{+0.44}_{-0.39} \times 10^5$	$1.90^{+0.39}_{-0.31} \times 10^5$
$25 < p_T < 30$	$(9.2 \pm 0.4 \pm 1.0) \times 10^4$	$1.10^{+0.15}_{-0.14} \times 10^5$	$7.3^{+1.3}_{-1.1} \times 10^4$
$30 < p_T < 40$	$(2.86 \pm 0.12 \pm 0.40) \times 10^4$	$3.75^{+0.43}_{-0.44} \times 10^4$	$2.44^{+0.38}_{-0.33} \times 10^4$
$40 < p_T < 50$	$(8.7 \pm 0.6 \pm 1.6) \times 10^3$	$1.08^{+0.10}_{-0.11} \times 10^4$	$6.8^{+0.9}_{-0.8} \times 10^3$
$50 < p_T < 60$	$(2.45 \pm 0.30 \pm 0.46) \times 10^3$	$3.89^{+0.30}_{-0.37} \times 10^3$	$2.41^{+0.29}_{-0.28} \times 10^3$
$60 < p_T < 80$	$(8.9 \pm 1.2 \pm 1.7) \times 10^2$	$1.21^{+0.08}_{-0.10} \times 10^3$	$7.3^{+0.8}_{-0.8} \times 10^2$
$80 < p_T < 100$	$(1.78 \pm 0.64 \pm 0.36) \times 10^2$	$3.08^{+0.16}_{-0.24} \times 10^2$	$1.81^{+0.19}_{-0.18} \times 10^2$

Table 4: The measured differential cross-sections and the predictions from the GM-VFNS calculation for the D_s^\pm meson in bins of $|\eta|$ for $12 < p_T < 100$ GeV.

Range	Differential cross-section [μb]	
	Data	GM-VFNS
	$\frac{d\sigma}{d \eta } \pm \delta_{\text{stat}} \pm \delta_{\text{syst}}$	$\frac{d\sigma}{d \eta } \pm \delta_{\text{theory}}$
$0.0 < \eta < 0.5$	$2.51 \pm 0.03 \pm 0.30$	$2.69^{+0.56}_{-0.45}$
$0.5 < \eta < 1.0$	$2.61 \pm 0.03 \pm 0.30$	$2.62^{+0.55}_{-0.44}$
$1.0 < \eta < 1.5$	$2.23 \pm 0.04 \pm 0.24$	$2.46^{+0.51}_{-0.41}$
$1.5 < \eta < 2.0$	$1.79 \pm 0.03 \pm 0.18$	$2.22^{+0.46}_{-0.37}$
$2.0 < \eta < 2.5$	$1.44 \pm 0.04 \pm 0.17$	$1.90^{+0.39}_{-0.32}$

Table 5: The measured differential cross-sections and the predictions from the GM-VFNS calculation for the D_s^\pm meson in bins of p_T for $|\eta| < 2.5$.

Range [GeV]	Differential cross-section [pb/GeV]	
	Data	GM-VFNS
	$\frac{d\sigma}{dp_T} \pm \delta_{\text{stat}} \pm \delta_{\text{syst}}$	$\frac{d\sigma}{dp_T} \pm \delta_{\text{theory}}$
$12 < p_T < 15$	$(8.6 \pm 0.4 \pm 1.0) \times 10^5$	$1.02^{+0.24}_{-0.19} \times 10^6$
$15 < p_T < 20$	$(3.04 \pm 0.06 \pm 0.36) \times 10^5$	$3.62^{+0.71}_{-0.59} \times 10^5$
$20 < p_T < 25$	$(1.01 \pm 0.01 \pm 0.11) \times 10^5$	$1.19^{+0.19}_{-0.17} \times 10^5$
$25 < p_T < 30$	$(4.20 \pm 0.06 \pm 0.43) \times 10^4$	$4.75^{+0.65}_{-0.62} \times 10^4$
$30 < p_T < 40$	$(1.45 \pm 0.02 \pm 0.16) \times 10^4$	$1.64^{+0.19}_{-0.19} \times 10^4$
$40 < p_T < 50$	$(3.82 \pm 0.09 \pm 0.45) \times 10^3$	$4.74^{+0.45}_{-0.50} \times 10^3$
$50 < p_T < 60$	$(1.38 \pm 0.05 \pm 0.16) \times 10^3$	$1.73^{+0.14}_{-0.17} \times 10^3$
$60 < p_T < 80$	$(4.55 \pm 0.21 \pm 0.55) \times 10^2$	$5.39^{+0.37}_{-0.47} \times 10^2$
$80 < p_T < 100$	$(8.1 \pm 0.9 \pm 1.1) \times 10^1$	$1.38^{+0.08}_{-0.11} \times 10^2$

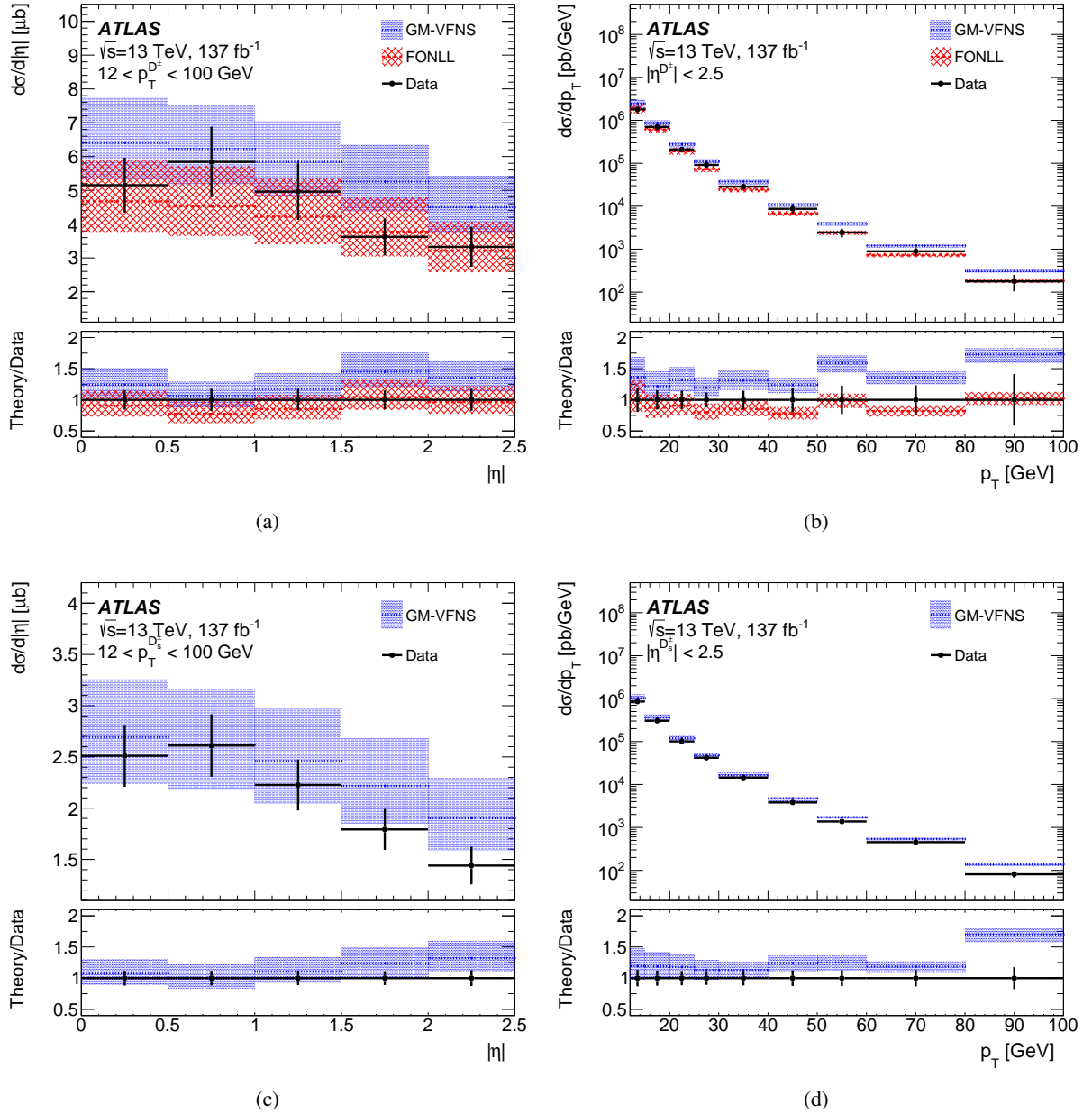


Figure 8: Differential cross-sections for D^\pm meson in bins of (a) $|\eta|$ and (b) p_T , and for D_s^\pm meson in bins of (c) $|\eta|$ and (d) p_T . The measured values with the statistical and systematic uncertainty are represented by the data points, while the theory predictions from GM-VFNS and FONLL are shown as dotted and dashed lines, respectively; the uncertainties on the theory predictions are represented by the hatched areas. The theory predictions are also divided by the measured values to obtain the ratios between the predictions and the measurements shown in the bottom panels.

Table 6: Inclusive D^\pm and D_s^\pm meson production cross-sections in different fiducial volumes defined by $|\eta| < 2.5$ and different p_T regions. For the ATLAS measurements, the statistical uncertainties and systematical uncertainties are shown independently; for the theoretical predictions the total theoretical uncertainties are shown.

D^\pm inclusive fiducial cross-section at $\sqrt{s} = 13$ TeV [nb]			
Fiducial volume	ATLAS	GM-VFNS	FONLL
	$\sigma \pm \delta_{\text{stat}} \pm \delta_{\text{syst}}$	$\sigma \pm \delta_{\text{theory}}$	$\sigma \pm \delta_{\text{theory}}$
$12 < p_T < 100$ GeV, $ \eta < 2.5$	$10\,800 \pm 900 \pm 1\,600$	$14\,100^{+2\,900}_{-2\,300}$	$10\,200^{+2\,300}_{-1\,700}$
$15 < p_T < 100$ GeV, $ \eta < 2.5$	$5\,430 \pm 550 \pm 780$	$6\,800^{+1\,200}_{-1\,000}$	$4\,730^{+900}_{-700}$
$20 < p_T < 100$ GeV, $ \eta < 2.5$	$1\,930 \pm 160 \pm 260$	$2\,480^{+350}_{-330}$	$1\,670^{+260}_{-220}$
D_s^\pm inclusive fiducial cross-section at $\sqrt{s} = 13$ TeV [nb]			
Fiducial volume	ATLAS	GM-VFNS	
	$\sigma \pm \delta_{\text{stat}} \pm \delta_{\text{syst}}$	$\sigma \pm \delta_{\text{theory}}$	
$12 < p_T < 100$ GeV, $ \eta < 2.5$	$5\,000 \pm 360 \pm 590$	$5\,900^{+1\,200}_{-1\,000}$	
$15 < p_T < 100$ GeV, $ \eta < 2.5$	$2\,440 \pm 190 \pm 280$	$2\,880^{+510}_{-440}$	
$20 < p_T < 100$ GeV, $ \eta < 2.5$	$920 \pm 60 \pm 100$	$1\,070^{+150}_{-140}$	

For the D^\pm meson, good agreement is observed at low p_T for both the GM-VFNS and FONLL predictions; the FONLL prediction is in general slightly lower than the measured differential cross-sections, while the GM-VFNS prediction is slightly higher. For higher p_T , the GM-VFNS prediction gives a larger value than the measured differential cross-section, while the FONLL prediction is still consistent with the measured values. When comparing in bins of $|\eta|$, good agreement is observed for both predictions, which is consistent with the observation in the low p_T bins.

For the D_s^\pm meson, only the GM-VFNS prediction is available for comparison. Similar behaviour is observed; the GM-VFNS prediction gives a larger value than the measured differential cross-section for both $|\eta|$ and p_T , with a trend towards a larger deviation at higher p_T .

The results are compared with those measured with the pp collision data collected at a centre-of-mass energy of $\sqrt{s} = 7$ TeV in 2010 [8]. Those measurements were performed using the $D^\pm \rightarrow K^\mp \pi^\pm \pi^\pm$ and $D_s^\pm \rightarrow \phi(K^+ K^-) \pi^\pm$ decays for $|\eta| < 2.1$. To perform a consistent comparison, the difference between the fiducial volumes, particularly in $|\eta|$, must be taken into account. Since the differential cross-section in bins of $|\eta|$ is rather flat and well modelled by MC simulation, the ratio of the fiducial volume of $|\eta| < 2.1$ to $|\eta| < 2.5$ is derived from MC simulation with a negligible systematic uncertainty. Table 7 shows the comparison between the fiducial cross-sections measured at $\sqrt{s} = 13$ TeV and $\sqrt{s} = 7$ TeV. For the D_s^\pm meson, the measurement has a 12% uncertainty, which is an improvement over the 20% uncertainty in the previous measurement. For the D^\pm meson, the measurement has a 14% uncertainty, which is larger than the previous uncertainty of 11%, mainly due to the background uncertainty driven by the low signal yield.

For both the ATLAS measurements, and the theory predictions, ratios between $\sqrt{s} = 7$ TeV and $\sqrt{s} = 13$ TeV are also computed. The statistical uncertainties in the two ATLAS measurements are independent because of the different data samples used; the systematic uncertainties are also assumed to be uncorrelated, because the two measurements used different decay channels with all main systematic uncertainty contributions being different. For FONLL and GM-VFNS, the uncertainties are assumed to be fully correlated between

Table 7: Inclusive D^\pm and D_s^\pm meson production cross-sections in a fiducial volume defined by $|\eta| < 2.1$ and $20 < p_T < 100$ GeV at $\sqrt{s} = 7$ TeV and $\sqrt{s} = 13$ TeV. The total uncertainties are shown for both the ATLAS measurements and the theoretical predictions. The ratio of $\sqrt{s} = 13$ TeV values over $\sqrt{s} = 7$ TeV values are also computed by assuming the uncertainties are independent for different centre-of-mass energies.

D^\pm inclusive fiducial cross-section [nb]			
	ATLAS	GM-VFNS	FONLL
	$\sigma \pm \delta_{\text{total}}$	$\sigma \pm \delta_{\text{theory}}$	$\sigma \pm \delta_{\text{theory}}$
$\sqrt{s} = 13$ TeV	$1\,690 \pm 270$	$2\,200^{+310}_{-290}$	$1\,480^{+230}_{-190}$
$\sqrt{s} = 7$ TeV	888 ± 97	980^{+120}_{-150}	620^{+100}_{-80}
Ratio (13 TeV/7 TeV)	1.9 ± 0.4	2.24 ± 0.04	2.38 ± 0.01
D_s^\pm inclusive fiducial cross-section [nb]			
	ATLAS	GM-VFNS	
	$\sigma \pm \delta_{\text{total}}$	$\sigma \pm \delta_{\text{theory}}$	
$\sqrt{s} = 13$ TeV	810 ± 100	950^{+140}_{-130}	
$\sqrt{s} = 7$ TeV	510 ± 100	470^{+56}_{-69}	
Ratio (13 TeV/7 TeV)	1.6 ± 0.4	2.02 ± 0.05	

$\sqrt{s} = 7$ TeV and $\sqrt{s} = 13$ TeV, as they are evaluated mainly from the variations of QCD scale uncertainties in a coherent way. In Table 7, it can be seen that the ratios obtained by GM-VFNS and FONLL are both consistent with the data within the uncertainties. There is, however, a significant difference between the ratios predicted by GM-VFNS and FONLL.

8 Conclusions

The production of D^\pm and D_s^\pm charmed mesons is measured in the kinematic region $12 < p_T < 100$ GeV and $|\eta| < 2.5$ with the ATLAS detector at the LHC using 137 fb^{-1} of $\sqrt{s} = 13$ TeV pp collision data. The differential cross-sections in bins of p_T and $|\eta|$ for D^\pm and D_s^\pm meson production are determined and compared with the available NLO QCD predictions. The fiducial cross-sections for D^\pm and D_s^\pm meson production are also presented; the values are compared with the predictions and with the measurement at $\sqrt{s} = 7$ TeV. For the D_s^\pm meson, this is the first measurement of the differential cross-section reported by the ATLAS Collaboration, and the first time such a measurement has been reported up to transverse momenta of 100 GeV, providing a benchmark for theoretical calculations in a previously unexplored kinematic space. The obtained cross-sections are compared with the predictions from the GM-VFNS and FONLL calculations, and the results are mostly consistent within the uncertainties, with slight deviation towards high- p_T regions.

Acknowledgements

We thank CERN for the very successful operation of the LHC and its injectors, as well as the support staff at CERN and at our institutions worldwide without whom ATLAS could not be operated efficiently.

The crucial computing support from all WLCG partners is acknowledged gratefully, in particular from CERN, the ATLAS Tier-1 facilities at TRIUMF/SFU (Canada), NDGF (Denmark, Norway, Sweden), CC-IN2P3 (France), KIT/GridKA (Germany), INFN-CNAF (Italy), NL-T1 (Netherlands), PIC (Spain), RAL (UK) and BNL (USA), the Tier-2 facilities worldwide and large non-WLCG resource providers. Major contributors of computing resources are listed in Ref. [48].

We gratefully acknowledge the support of ANPCyT, Argentina; YerPhI, Armenia; ARC, Australia; BMWFW and FWF, Austria; ANAS, Azerbaijan; CNPq and FAPESP, Brazil; NSERC, NRC and CFI, Canada; CERN; ANID, Chile; CAS, MOST and NSFC, China; Minciencias, Colombia; MEYS CR, Czech Republic; DNRF and DNSRC, Denmark; IN2P3-CNRS and CEA-DRF/IRFU, France; SRNSFG, Georgia; BMBF, HGF and MPG, Germany; GSRI, Greece; RGC and Hong Kong SAR, China; ISF and Benozio Center, Israel; INFN, Italy; MEXT and JSPS, Japan; CNRST, Morocco; NWO, Netherlands; RCN, Norway; MNiSW, Poland; FCT, Portugal; MNE/IFA, Romania; MSTDI, Serbia; MSSR, Slovakia; ARIS and MVZI, Slovenia; DSI/NRF, South Africa; MICIU/AEI, Spain; SRC and Wallenberg Foundation, Sweden; SERI, SNSF and Cantons of Bern and Geneva, Switzerland; NSTC, Taipei; TENMAK, Türkiye; STFC/UKRI, United Kingdom; DOE and NSF, United States of America.

Individual groups and members have received support from BCKDF, CANARIE, CRC and DRAC, Canada; CERN-CZ, FORTE and PRIMUS, Czech Republic; COST, ERC, ERDF, Horizon 2020, ICSC-NextGenerationEU and Marie Skłodowska-Curie Actions, European Union; Investissements d'Avenir Labex, Investissements d'Avenir Idex and ANR, France; DFG and AvH Foundation, Germany; Herakleitos, Thales and Aristeia programmes co-financed by EU-ESF and the Greek NSRF, Greece; BSF-NSF and MINERVA, Israel; NCN and NAWA, Poland; La Caixa Banking Foundation, CERCA Programme Generalitat de Catalunya and PROMETEO and GenT Programmes Generalitat Valenciana, Spain; Göran Gustafssons Stiftelse, Sweden; The Royal Society and Leverhulme Trust, United Kingdom.

In addition, individual members wish to acknowledge support from Armenia: Yerevan Physics Institute (FAPERJ); CERN: European Organization for Nuclear Research (CERN PJAS); Chile: Agencia Nacional de Investigación y Desarrollo (FONDECYT 1230812, FONDECYT 1230987, FONDECYT 1240864); China: Chinese Ministry of Science and Technology (MOST-2023YFA1605700, MOST-2023YFA1609300), National Natural Science Foundation of China (NSFC - 12175119, NSFC 12275265, NSFC-12075060); Czech Republic: Czech Science Foundation (GACR - 24-11373S), Ministry of Education Youth and Sports (FORTE CZ.02.01.01/00/22_008/0004632), PRIMUS Research Programme (PRIMUS/21/SCI/017); EU: H2020 European Research Council (ERC - 101002463); European Union: European Research Council (ERC - 948254, ERC 101089007), Horizon 2020 Framework Programme (MUCCA - CHIST-ERA-19-XAI-00), European Union, Future Artificial Intelligence Research (FAIR-NextGenerationEU PE00000013), Italian Center for High Performance Computing, Big Data and Quantum Computing (ICSC, NextGenerationEU); France: Agence Nationale de la Recherche (ANR-20-CE31-0013, ANR-21-CE31-0013, ANR-21-CE31-0022, ANR-22-EDIR-0002), Investissements d'Avenir Labex (ANR-11-LABX-0012); Germany: Baden-Württemberg Stiftung (BW Stiftung-Postdoc Eliteprogramme), Deutsche Forschungsgemeinschaft (DFG - 469666862, DFG - CR 312/5-2); Italy: Istituto Nazionale di Fisica Nucleare (ICSC, NextGenerationEU), Ministero dell'Università e della Ricerca (PRIN - 20223N7F8K - PNRR M4.C2.1.1); Japan: Japan Society for the Promotion of Science (JSPS KAKENHI JP22H01227, JSPS KAKENHI JP22H04944, JSPS

KAKENHI JP22KK0227, JSPS KAKENHI JP23KK0245); Netherlands: Netherlands Organisation for Scientific Research (NWO Veni 2020 - VI.Veni.202.179); Norway: Research Council of Norway (RCN-314472); Poland: Ministry of Science and Higher Education (IDUB AGH, POB8, D4 no 9722), Polish National Agency for Academic Exchange (PPN/PPO/2020/1/00002/U/00001), Polish National Science Centre (NCN 2021/42/E/ST2/00350, NCN OPUS nr 2022/47/B/ST2/03059, NCN UMO-2019/34/E/ST2/00393, NCN & H2020 MSCA 945339, UMO-2020/37/B/ST2/01043, UMO-2021/40/C/ST2/00187, UMO-2022/47/O/ST2/00148, UMO-2023/49/B/ST2/04085, UMO-2023/51/B/ST2/00920); Slovenia: Slovenian Research Agency (ARIS grant J1-3010); Spain: Generalitat Valenciana (Artemisa, FEDER, IDIFEDER/2018/048), Ministry of Science and Innovation (MCIN & NextGenEU PCI2022-135018-2, MICIN & FEDER PID2021-125273NB, RYC2019-028510-I, RYC2020-030254-I, RYC2021-031273-I, RYC2022-038164-I), PROMETEO and GenT Programmes Generalitat Valenciana (CIDEAGENT/2019/027); Sweden: Carl Trygger Foundation (Carl Trygger Foundation CTS 22:2312), Swedish Research Council (Swedish Research Council 2023-04654, VR 2018-00482, VR 2022-03845, VR 2022-04683, VR 2023-03403, VR grant 2021-03651), Knut and Alice Wallenberg Foundation (KAW 2018.0157, KAW 2018.0458, KAW 2019.0447, KAW 2022.0358); Switzerland: Swiss National Science Foundation (SNSF - PCEFP2_194658); United Kingdom: Leverhulme Trust (Leverhulme Trust RPG-2020-004), Royal Society (NIF-R1-231091); United States of America: U.S. Department of Energy (ECA DE-AC02-76SF00515), Neubauer Family Foundation.

References

- [1] B. A. Kniehl, G. Kramer, I. Schienbein and H. Spiesberger, *Reconciling open charm production at the Fermilab Tevatron with QCD*, *Phys. Rev. Lett.* **96** (2006) 012001, arXiv: [hep-ph/0508129](https://arxiv.org/abs/hep-ph/0508129).
- [2] B. A. Kniehl, G. Kramer, I. Schienbein and H. Spiesberger, *Inclusive charmed-meson production at the CERN LHC*, *Eur. Phys. J. C* **72** (2012) 2082, arXiv: [1202.0439](https://arxiv.org/abs/1202.0439) [[hep-ph](#)].
- [3] S. Navas et al., *Review of particle physics*, *Phys. Rev. D* **110** (2024) 030001.
- [4] ATLAS Collaboration, *Prospects for lepton flavour violation measurements in $\tau \rightarrow 3\mu$ decays with the ATLAS detector at the HL-LHC*, ATL-PHYS-PUB-2018-032, 2018, URL: <https://cds.cern.ch/record/2647956>.
- [5] L. Evans and P. Bryant, *LHC Machine*, *JINST* **3** (2008) S08001.
- [6] ALICE Collaboration, *Charm production and fragmentation fractions at midrapidity in pp collisions at $\sqrt{s} = 13$ TeV*, *JHEP* **12** (2023) 086, arXiv: [2308.04877](https://arxiv.org/abs/2308.04877) [[hep-ex](#)].
- [7] ALICE Collaboration, *Measurement of beauty-quark production in pp collisions at $\sqrt{s} = 13$ TeV via non-prompt D mesons*, *JHEP* **10** (2024) 110, arXiv: [2402.16417](https://arxiv.org/abs/2402.16417) [[hep-ex](#)].
- [8] ATLAS Collaboration, *Measurement of $D^{*\pm}$, D^\pm and D_s^\pm meson production cross sections in pp collisions at $\sqrt{s} = 7$ TeV with the ATLAS detector*, *Nucl. Phys. B* **907** (2016) 717, arXiv: [1512.02913](https://arxiv.org/abs/1512.02913) [[hep-ex](#)].
- [9] CMS Collaboration, *Measurement of prompt open-charm production cross sections in proton-proton collisions at $\sqrt{s} = 13$ TeV*, *JHEP* **11** (2021) 225, arXiv: [2107.01476](https://arxiv.org/abs/2107.01476) [[hep-ex](#)].

- [10] LHCb Collaboration, *Measurements of prompt charm production cross-sections in pp collisions at $\sqrt{s} = 13$ TeV*, *JHEP* **03** (2016) 159, arXiv: [1510.01707 \[hep-ex\]](#).
- [11] ATLAS Collaboration, *The ATLAS Experiment at the CERN Large Hadron Collider*, *JINST* **3** (2008) S08003.
- [12] ATLAS Collaboration, *ATLAS Insertable B-Layer: Technical Design Report*, ATLAS-TDR-19; CERN-LHCC-2010-013, 2010, URL: <https://cds.cern.ch/record/1291633>, Addendum: ATLAS-TDR-19-ADD-1; CERN-LHCC-2012-009, 2012, URL: <https://cds.cern.ch/record/1451888>.
- [13] B. Abbott et al., *Production and integration of the ATLAS Insertable B-Layer*, *JINST* **13** (2018) T05008, arXiv: [1803.00844 \[physics.ins-det\]](#).
- [14] G. Avoni et al., *The new LUCID-2 detector for luminosity measurement and monitoring in ATLAS*, *JINST* **13** (2018) P07017.
- [15] ATLAS Collaboration, *Performance of the ATLAS trigger system in 2015*, *Eur. Phys. J. C* **77** (2017) 317, arXiv: [1611.09661 \[hep-ex\]](#).
- [16] ATLAS Collaboration, *Software and computing for Run 3 of the ATLAS experiment at the LHC*, (2024), arXiv: [2404.06335 \[hep-ex\]](#).
- [17] ATLAS Collaboration, *ATLAS data quality operations and performance for 2015–2018 data-taking*, *JINST* **15** (2020) P04003, arXiv: [1911.04632 \[physics.ins-det\]](#).
- [18] ATLAS Collaboration, *Luminosity determination in pp collisions at $\sqrt{s} = 13$ TeV using the ATLAS detector at the LHC*, *Eur. Phys. J. C* **83** (2023) 982, arXiv: [2212.09379 \[hep-ex\]](#).
- [19] T. Sjöstrand et al., *An introduction to PYTHIA 8.2*, *Comput. Phys. Commun.* **191** (2015) 159, arXiv: [1410.3012 \[hep-ph\]](#).
- [20] NNPDF Collaboration, R. D. Ball et al., *Parton distributions with LHC data*, *Nucl. Phys. B* **867** (2013) 244, arXiv: [1207.1303 \[hep-ph\]](#).
- [21] ATLAS Collaboration, *ATLAS Pythia 8 tunes to 7 TeV data*, ATL-PHYS-PUB-2014-021, 2014, URL: <https://cds.cern.ch/record/1966419>.
- [22] ATLAS Collaboration, *The ATLAS Simulation Infrastructure*, *Eur. Phys. J. C* **70** (2010) 823, arXiv: [1005.4568 \[physics.ins-det\]](#).
- [23] S. Agostinelli et al., *GEANT4 – a simulation toolkit*, *Nucl. Instrum. Meth. A* **506** (2003) 250.
- [24] T. Sjöstrand, S. Mrenna and P. Skands, *A brief introduction to PYTHIA 8.1*, *Comput. Phys. Commun.* **178** (2008) 852, arXiv: [0710.3820 \[hep-ph\]](#).
- [25] ATLAS Collaboration, *The Pythia 8 A3 tune description of ATLAS minimum bias and inelastic measurements incorporating the Donnachie–Landshoff diffractive model*, ATL-PHYS-PUB-2016-017, 2016, URL: <https://cds.cern.ch/record/2206965>.
- [26] B. A. Kniehl, G. Kramer, I. Schienbein and H. Spiesberger, *Inclusive $D^{*\pm}$ production in pp collisions with massive charm quarks*, *Phys. Rev. D* **71** (2005) 014018, arXiv: [hep-ph/0410289](#).
- [27] B. A. Kniehl, G. Kramer, I. Schienbein and H. Spiesberger, *Open charm hadroproduction and the charm content of the proton*, *Phys. Rev. D* **79** (2009) 094009, arXiv: [0901.4130 \[hep-ph\]](#).

- [28] M. Benzke et al., *Prompt neutrinos from atmospheric charm in the general-mass variable-flavor-number scheme*, *JHEP* **12** (2017) 021, arXiv: [1705.10386 \[hep-ph\]](#).
- [29] B. A. Kniehl and G. Kramer, *D^0 , D^+ , D_s^+ , and Λ_c^+ fragmentation functions from CERN LEP1*, *Phys. Rev. D* **71** (2005) 094013, arXiv: [hep-ph/0504058](#).
- [30] M. Cacciari, M. Greco and P. Nason, *The p_T spectrum in heavy-flavour hadroproduction*, *JHEP* **05** (1998) 007, arXiv: [hep-ph/9803400](#).
- [31] M. Cacciari et al., *Theoretical predictions for charm and bottom production at the LHC*, *JHEP* **10** (2012) 137, arXiv: [1205.6344 \[hep-ph\]](#).
- [32] S. Dulat et al., *New parton distribution functions from a global analysis of quantum chromodynamics*, *Phys. Rev. D* **93** (2016) 033006, arXiv: [1506.07443 \[hep-ph\]](#).
- [33] T. Kneesch, B. A. Kniehl, G. Kramer and I. Schienbein, *Charmed-meson fragmentation functions with finite-mass corrections*, *Nucl. Phys. B* **799** (2008) 34, arXiv: [0712.0481 \[hep-ph\]](#).
- [34] M. Cacciari, S. Frixione and P. Nason, *The p_T spectrum in heavy-flavour photoproduction*, *JHEP* **03** (2001) 006, arXiv: [hep-ph/0102134](#).
- [35] M. Cacciari, M. L. Mangano and P. Nason, *Gluon PDF constraints from the ratio of forward heavy-quark production at the LHC at $\sqrt{s} = 7$ and 13 TeV*, *Eur. Phys. J. C* **75** (2015) 610, arXiv: [1507.06197 \[hep-ph\]](#).
- [36] NNPDF Collaboration, R. D. Ball et al., *Parton distributions for the LHC run II*, *JHEP* **04** (2015) 040, arXiv: [1410.8849 \[hep-ph\]](#).
- [37] L. Gladilin, *Fragmentation fractions of c and b quarks into charmed hadrons at LEP*, *Eur. Phys. J. C* **75** (2015) 19, arXiv: [1404.3888 \[hep-ex\]](#).
- [38] ATLAS Collaboration, *Performance of the ATLAS muon triggers in Run 2*, *JINST* **15** (2020) P09015, arXiv: [2004.13447 \[physics.ins-det\]](#).
- [39] ATLAS Collaboration, *Muon reconstruction and identification efficiency in ATLAS using the full Run 2 pp collision data set at $\sqrt{s} = 13$ TeV*, *Eur. Phys. J. C* **81** (2021) 578, arXiv: [2012.00578 \[hep-ex\]](#).
- [40] ATLAS Collaboration, *Early Inner Detector Tracking Performance in the 2015 Data at $\sqrt{s} = 13$ TeV*, ATL-PHYS-PUB-2015-051, 2015, URL: <https://cds.cern.ch/record/2110140>.
- [41] ATLAS Collaboration, *Vertex Reconstruction Performance of the ATLAS Detector at $\sqrt{s} = 13$ TeV*, ATL-PHYS-PUB-2015-026, 2015, URL: <https://cds.cern.ch/record/2037717>.
- [42] W. Voigt, *On the law of intensity distribution within the lines of a gas spectrum*, vol. 1912,25, Meeting reports, Munich, 1912, URL: <https://publikationen.badw.de/de/003395768>.
- [43] W. Verkerke and D. Kirkby, *The RooFit toolkit for data modeling*, 2003, arXiv: [physics/0306116 \[physics.data-an\]](#).
- [44] ATLAS Collaboration, *Studies of the muon momentum calibration and performance of the ATLAS detector with pp collisions at $\sqrt{s} = 13$ TeV*, *Eur. Phys. J. C* **83** (2023) 686, arXiv: [2212.07338 \[hep-ex\]](#).

- [45] ATLAS Collaboration, *Performance of the ATLAS track reconstruction algorithms in dense environments in LHC Run 2*, *Eur. Phys. J. C* **77** (2017) 673, arXiv: [1704.07983 \[hep-ex\]](#).
- [46] ATLAS Collaboration, *Measurement of upsilon production in 7 TeV pp collisions at ATLAS*, *Phys. Rev. D* **87** (2013) 052004, arXiv: [1211.7255 \[hep-ex\]](#).
- [47] A. D. Bukin, *Fitting function for asymmetric peaks*, (2007), arXiv: [0711.4449 \[physics.data-an\]](#).
- [48] ATLAS Collaboration, *ATLAS Computing Acknowledgements*, ATL-SOFT-PUB-2023-001, 2023, URL: <https://cds.cern.ch/record/2869272>.

The ATLAS Collaboration

G. Aad ¹⁰⁴, E. Aakvaag ¹⁷, B. Abbott ¹²³, S. Abdelhameed ^{119a}, K. Abeling ⁵⁶, N.J. Abicht ⁵⁰, S.H. Abidi ³⁰, M. Aboeela ⁴⁵, A. Aboulhorma ^{36e}, H. Abramowicz ¹⁵⁵, H. Abreu ¹⁵⁴, Y. Abulaiti ¹²⁰, B.S. Acharya ^{70a,70b,1}, A. Ackermann ^{64a}, C. Adam Bourdarios ⁴, L. Adamczyk ^{87a}, S.V. Addepalli ²⁷, M.J. Addison ¹⁰³, J. Adelman ¹¹⁸, A. Adiguzel ^{22c}, T. Adye ¹³⁷, A.A. Affolder ¹³⁹, Y. Afik ⁴⁰, M.N. Agaras ¹³, J. Agarwala ^{74a,74b}, A. Aggarwal ¹⁰², C. Agheorghiesei ^{28c}, F. Ahmadov ^{39,z}, W.S. Ahmed ¹⁰⁶, S. Ahuja ⁹⁷, X. Ai ^{63e}, G. Aielli ^{77a,77b}, A. Aikot ¹⁶⁶, M. Ait Tamlihat ^{36e}, B. Aitbenkikh ^{36a}, M. Akbiyik ¹⁰², T.P.A. Åkesson ¹⁰⁰, A.V. Akimov ³⁸, D. Akiyama ¹⁷¹, N.N. Akolkar ²⁵, S. Aktas ^{22a}, K. Al Houry ⁴², G.L. Alberghi ^{24b}, J. Albert ¹⁶⁸, P. Albicocco ⁵⁴, G.L. Albouy ⁶¹, S. Alderweireldt ⁵³, Z.L. Alegria ¹²⁴, M. Aleksa ³⁷, I.N. Aleksandrov ³⁹, C. Alexa ^{28b}, T. Alexopoulos ¹⁰, F. Alfonsi ^{24b}, M. Algren ⁵⁷, M. Alhroob ¹⁷⁰, B. Ali ¹³⁵, H.M.J. Ali ^{93,t}, S. Ali ³², S.W. Alibocus ⁹⁴, M. Aliev ^{34c}, G. Alimonti ^{72a}, W. Alkahi ⁵⁶, C. Allaire ⁶⁷, B.M.M. Allbrooke ¹⁵⁰, J.S. Allen ¹⁰³, J.F. Allen ⁵³, C.A. Allendes Flores ^{140f}, P.P. Allport ²¹, A. Aloisio ^{73a,73b}, F. Alonso ⁹², C. Alpighiani ¹⁴², Z.M.K. Alsolami ⁹³, M. Alvarez Estevez ¹⁰¹, A. Alvarez Fernandez ¹⁰², M. Alves Cardoso ⁵⁷, M.G. Alvigi ^{73a,73b}, M. Aly ¹⁰³, Y. Amaral Coutinho ^{84b}, A. Ambler ¹⁰⁶, C. Amelung ³⁷, M. Amerl ¹⁰³, C.G. Ames ¹¹¹, D. Amidei ¹⁰⁸, B. Amini ⁵⁵, K.J. Amirie ¹⁵⁸, S.P. Amor Dos Santos ^{133a}, K.R. Amos ¹⁶⁶, D. Amperiadou ¹⁵⁶, S. An ⁸⁵, V. Ananiev ¹²⁸, C. Anastopoulos ¹⁴³, T. Andeen ¹¹, J.K. Anders ³⁷, A.C. Anderson ⁶⁰, S.Y. Andrean ^{48a,48b}, A. Andreazza ^{72a,72b}, S. Angelidakis ⁹, A. Angerami ⁴², A.V. Anisenkov ³⁸, A. Annovi ^{75a}, C. Antel ⁵⁷, E. Antipov ¹⁴⁹, M. Antonelli ⁵⁴, F. Anulli ^{76a}, M. Aoki ⁸⁵, T. Aoki ¹⁵⁷, M.A. Aparo ¹⁵⁰, L. Aperio Bella ⁴⁹, C. Appelt ¹⁹, A. Apyan ²⁷, S.J. Arbiol Val ⁸⁸, C. Arcangeletti ⁵⁴, A.T.H. Arce ⁵², J-F. Arguin ¹¹⁰, S. Argyropoulos ⁵⁵, J.-H. Arling ⁴⁹, O. Arnaez ⁴, H. Arnold ¹⁴⁹, G. Artoni ^{76a,76b}, H. Asada ¹¹³, K. Asai ¹²¹, S. Asai ¹⁵⁷, N.A. Asbah ³⁷, R.A. Ashby Pickering ¹⁷⁰, K. Assamagan ³⁰, R. Astalos ^{29a}, K.S.V. Astrand ¹⁰⁰, S. Atashi ¹⁶², R.J. Atkin ^{34a}, M. Atkinson ¹⁶⁵, H. Atmani ^{36f}, P.A. Atmasiddha ¹³¹, K. Augsten ¹³⁵, S. Auricchio ^{73a,73b}, A.D. Auriol ²¹, V.A. Austrup ¹⁰³, G. Avolio ³⁷, K. Axiotis ⁵⁷, G. Azuelos ^{110,ae}, D. Babal ^{29b}, H. Bachacou ¹³⁸, K. Bachas ^{156,p}, A. Bachi ³⁵, F. Backman ^{48a,48b}, A. Badea ⁴⁰, T.M. Baer ¹⁰⁸, P. Bagnaia ^{76a,76b}, M. Bahmani ¹⁹, D. Bahner ⁵⁵, K. Bai ¹²⁶, J.T. Baines ¹³⁷, L. Baines ⁹⁶, O.K. Baker ¹⁷⁵, E. Bakos ¹⁶, D. Bakshi Gupta ⁸, L.E. Balabram Filho ^{84b}, V. Balakrishnan ¹²³, R. Balasubramanian ⁴, E.M. Baldin ³⁸, P. Balek ^{87a}, E. Ballabene ^{24b,24a}, F. Balli ¹³⁸, L.M. Baltes ^{64a}, W.K. Balunas ³³, J. Balz ¹⁰², I. Bamwidhi ^{119b}, E. Banas ⁸⁸, M. Bandieramonte ¹³², A. Bandyopadhyay ²⁵, S. Bansal ²⁵, L. Barak ¹⁵⁵, M. Barakat ⁴⁹, E.L. Barberio ¹⁰⁷, D. Barberis ^{58b,58a}, M. Barbero ¹⁰⁴, M.Z. Barel ¹¹⁷, T. Barillari ¹¹², M-S. Barisits ³⁷, T. Barklow ¹⁴⁷, P. Baron ¹²⁵, D.A. Baron Moreno ¹⁰³, A. Baroncelli ^{63a}, A.J. Barr ¹²⁹, J.D. Barr ⁹⁸, F. Barreiro ¹⁰¹, J. Barreiro Guimarães da Costa ¹⁴, U. Barron ¹⁵⁵, M.G. Barros Teixeira ^{133a}, S. Barsov ³⁸, F. Bartels ^{64a}, R. Bartoldus ¹⁴⁷, A.E. Barton ⁹³, P. Bartos ^{29a}, A. Basan ¹⁰², M. Baselga ⁵⁰, A. Bassalat ^{67,b}, M.J. Basso ^{159a}, S. Bataju ⁴⁵, R. Bate ¹⁶⁷, R.L. Bates ⁶⁰, S. Batlamous ¹⁰¹, B. Batool ¹⁴⁵, M. Battaglia ¹³⁹, D. Battulga ¹⁹, M. Baucé ^{76a,76b}, M. Bauer ⁸⁰, P. Bauer ²⁵, L.T. Bazzano Hurrell ³¹, J.B. Beacham ⁵², T. Beau ¹³⁰, J.Y. Beaucamp ⁹², P.H. Beauchemin ¹⁶¹, P. Bechtel ²⁵, H.P. Beck ^{20,o}, K. Becker ¹⁷⁰, A.J. Beddall ⁸³, V.A. Bednyakov ³⁹, C.P. Bee ¹⁴⁹, L.J. Beemster ¹⁶, T.A. Beermann ³⁷, M. Begalli ^{84d}, M. Begel ³⁰, A. Behera ¹⁴⁹, J.K. Behr ⁴⁹, J.F. Beirer ³⁷, F. Beisiegel ²⁵, M. Belfkir ^{119b}, G. Bella ¹⁵⁵, L. Bellagamba ^{24b}, A. Bellerive ³⁵, P. Bellos ²¹, K. Beloborodov ³⁸, D. Benčekroun ^{36a}, F. Bendebba ^{36a}, Y. Benhammou ¹⁵⁵,

K.C. Benkendorfer ⁶², L. Beresford ⁴⁹, M. Beretta ⁵⁴, E. Bergeaas Kuutmann ¹⁶⁴, N. Berger ⁴,
 B. Bergmann ¹³⁵, J. Beringer ^{18a}, G. Bernardi ⁵, C. Bernius ¹⁴⁷, F.U. Bernlochner ²⁵,
 F. Bernon ³⁷, A. Berrocal Guardia ¹³, T. Berry ⁹⁷, P. Berta ¹³⁶, A. Berthold ⁵¹, S. Bethke ¹¹²,
 A. Betti ^{76a,76b}, A.J. Bevan ⁹⁶, N.K. Bhalla ⁵⁵, S. Bhatta ¹⁴⁹, D.S. Bhattacharya ¹⁶⁹,
 P. Bhattarai ¹⁴⁷, K.D. Bhide ⁵⁵, V.S. Bhopatkar ¹²⁴, R.M. Bianchi ¹³², G. Bianco ^{24b,24a},
 O. Biebel ¹¹¹, R. Bielski ¹²⁶, M. Biglietti ^{78a}, C.S. Billingsley ⁴⁵, Y. Bimgdi ^{36f}, M. Bindi ⁵⁶,
 A. Bingul ^{22b}, C. Bini ^{76a,76b}, G.A. Bird ³³, M. Birman ¹⁷², M. Biros ¹³⁶, S. Biryukov ¹⁵⁰,
 T. Bisanz ⁵⁰, E. Bisceglie ^{44b,44a}, J.P. Biswal ¹³⁷, D. Biswas ¹⁴⁵, I. Bloch ⁴⁹, A. Blue ⁶⁰,
 U. Blumenschein ⁹⁶, J. Blumenthal ¹⁰², V.S. Bobrovnikov ³⁸, M. Boehler ⁵⁵, B. Boehm ¹⁶⁹,
 D. Bogavac ³⁷, A.G. Bogdanchikov ³⁸, L.S. Boggia ¹³⁰, C. Bohm ^{48a}, V. Boisvert ⁹⁷,
 P. Bokan ³⁷, T. Bold ^{87a}, M. Bomben ⁵, M. Bona ⁹⁶, M. Boonekamp ¹³⁸, C.D. Booth ⁹⁷,
 A.G. Borbély ⁶⁰, I.S. Bordulev ³⁸, G. Borissov ⁹³, D. Bortoletto ¹²⁹, D. Boscherini ^{24b},
 M. Bosman ¹³, J.D. Bossio Sola ³⁷, K. Bouaouda ^{36a}, N. Bouchhar ¹⁶⁶, L. Boudet ⁴,
 J. Boudreau ¹³², E.V. Bouhova-Thacker ⁹³, D. Boumediene ⁴¹, R. Bouquet ^{58b,58a}, A. Boveia ¹²²,
 J. Boyd ³⁷, D. Boye ³⁰, I.R. Boyko ³⁹, L. Bozianu ⁵⁷, J. Bracinek ²¹, N. Brahimi ⁴,
 G. Brandt ¹⁷⁴, O. Brandt ³³, F. Braren ⁴⁹, B. Brau ¹⁰⁵, J.E. Brau ¹²⁶, R. Brenner ¹⁷²,
 L. Brenner ¹¹⁷, R. Brenner ¹⁶⁴, S. Bressler ¹⁷², G. Brianti ^{79a,79b}, D. Britton ⁶⁰, D. Britzger ¹¹²,
 I. Brock ²⁵, R. Brock ¹⁰⁹, G. Brooijmans ⁴², E.M. Brooks ^{159b}, E. Brost ³⁰, L.M. Brown ¹⁶⁸,
 L.E. Bruce ⁶², T.L. Bruckler ¹²⁹, P.A. Bruckman de Renstrom ⁸⁸, B. Brüers ⁴⁹, A. Bruni ^{24b},
 G. Bruni ^{24b}, M. Bruschi ^{24b}, N. Brusino ^{76a,76b}, T. Buanes ¹⁷, Q. Buat ¹⁴², D. Buchin ¹¹²,
 A.G. Buckley ⁶⁰, O. Bulekov ³⁸, B.A. Bullard ¹⁴⁷, S. Burdin ⁹⁴, C.D. Burgard ⁵⁰,
 A.M. Burger ³⁷, B. Burghgrave ⁸, O. Burlayenko ⁵⁵, J. Burleson ¹⁶⁵, J.T.P. Burr ³³,
 J.C. Burzynski ¹⁴⁶, E.L. Busch ⁴², V. Büscher ¹⁰², P.J. Bussey ⁶⁰, J.M. Butler ²⁶, C.M. Buttar ⁶⁰,
 J.M. Butterworth ⁹⁸, W. Buttinger ¹³⁷, C.J. Buxo Vazquez ¹⁰⁹, A.R. Buzykaev ³⁸,
 S. Cabrera Urbán ¹⁶⁶, L. Cadamuro ⁶⁷, D. Caforio ⁵⁹, H. Cai ¹³², Y. Cai ^{14,114c}, Y. Cai ^{114a},
 V.M.M. Cairo ³⁷, O. Cakir ^{3a}, N. Calace ³⁷, P. Calafiura ^{18a}, G. Calderini ¹³⁰, P. Calfayan ⁶⁹,
 G. Callea ⁶⁰, L.P. Caloba ^{84b}, D. Calvet ⁴¹, S. Calvet ⁴¹, M. Calvetti ^{75a,75b}, R. Camacho Toro ¹³⁰,
 S. Camarda ³⁷, D. Camarero Munoz ²⁷, P. Camarri ^{77a,77b}, M.T. Camerlingo ^{73a,73b},
 D. Cameron ³⁷, C. Camincher ¹⁶⁸, M. Campanelli ⁹⁸, A. Camplani ⁴³, V. Canale ^{73a,73b},
 A.C. Canbay ^{3a}, E. Canonero ⁹⁷, J. Cantero ¹⁶⁶, Y. Cao ¹⁶⁵, F. Capocasa ²⁷, M. Capua ^{44b,44a},
 A. Carbone ^{72a,72b}, R. Cardarelli ^{77a}, J.C.J. Cardenas ⁸, G. Carducci ^{44b,44a}, T. Carli ³⁷,
 G. Carlino ^{73a}, J.I. Carlotto ¹³, B.T. Carlson ^{132,q}, E.M. Carlson ^{168,159a}, J. Carmignani ⁹⁴,
 L. Carminati ^{72a,72b}, A. Carnelli ¹³⁸, M. Carnesale ³⁷, S. Caron ¹¹⁶, E. Carquin ^{140f},
 I.B. Carr ¹⁰⁷, S. Carrá ^{72a}, G. Carratta ^{24b,24a}, A.M. Carroll ¹²⁶, M.P. Casado ^{13,i}, M. Caspar ⁴⁹,
 F.L. Castillo ⁴, L. Castillo Garcia ¹³, V. Castillo Gimenez ¹⁶⁶, N.F. Castro ^{133a,133e},
 A. Catinaccio ³⁷, J.R. Catmore ¹²⁸, T. Cavaliere ⁴, V. Cavaliere ³⁰, N. Cavalli ^{24b,24a},
 L.J. Caviedes Betancourt ^{23b}, Y.C. Cekmecelioglu ⁴⁹, E. Celebi ⁸³, S. Cella ³⁷,
 M.S. Centonze ^{71a,71b}, V. Cepaitis ⁵⁷, K. Cerny ¹²⁵, A.S. Cerqueira ^{84a}, A. Cerri ¹⁵⁰,
 L. Cerrito ^{77a,77b}, F. Cerutti ^{18a}, B. Cervato ¹⁴⁵, A. Cervelli ^{24b}, G. Cesarini ⁵⁴, S.A. Cetin ⁸³,
 D. Chakraborty ¹¹⁸, J. Chan ^{18a}, W.Y. Chan ¹⁵⁷, J.D. Chapman ³³, E. Chapon ¹³⁸,
 B. Chargeishvili ^{153b}, D.G. Charlton ²¹, M. Chatterjee ²⁰, C. Chauhan ¹³⁶, Y. Che ^{114a},
 S. Chekanov ⁶, S.V. Chekulaev ^{159a}, G.A. Chelkov ^{39,a}, A. Chen ¹⁰⁸, B. Chen ¹⁵⁵, B. Chen ¹⁶⁸,
 H. Chen ^{114a}, H. Chen ³⁰, J. Chen ^{63c}, J. Chen ¹⁴⁶, M. Chen ¹²⁹, S. Chen ⁸⁹, S.J. Chen ^{114a},
 X. Chen ^{63c}, X. Chen ^{15,ad}, Y. Chen ^{63a}, C.L. Cheng ¹⁷³, H.C. Cheng ^{65a}, S. Cheong ¹⁴⁷,
 A. Cheplakov ³⁹, E. Cheremushkina ⁴⁹, E. Cherepanova ¹¹⁷, R. Cherkaoui El Moursli ^{36e},
 E. Cheu ⁷, K. Cheung ⁶⁶, L. Chevalier ¹³⁸, V. Chiarella ⁵⁴, G. Chiarelli ^{75a}, N. Chiedde ¹⁰⁴,
 G. Chiodini ^{71a}, A.S. Chisholm ²¹, A. Chitan ^{28b}, M. Chitishvili ¹⁶⁶, M.V. Chizhov ^{39,r},

K. Choi ¹¹, Y. Chou ¹⁴², E.Y.S. Chow ¹¹⁶, K.L. Chu ¹⁷², M.C. Chu ^{65a}, X. Chu ^{14,114c},
 Z. Chubinidze ⁵⁴, J. Chudoba ¹³⁴, J.J. Chwastowski ⁸⁸, D. Cieri ¹¹², K.M. Ciesla ^{87a},
 V. Cindro ⁹⁵, A. Ciocio ^{18a}, F. Cirotto ^{73a,73b}, Z.H. Citron ¹⁷², M. Citterio ^{72a}, D.A. Ciubotaru ^{28b},
 A. Clark ⁵⁷, P.J. Clark ⁵³, N. Clarke Hall ⁹⁸, C. Clarry ¹⁵⁸, J.M. Clavijo Columbie ⁴⁹,
 S.E. Clawson ⁴⁹, C. Clement ^{48a,48b}, Y. Coadou ¹⁰⁴, M. Cobal ^{70a,70c}, A. Coccaro ^{58b},
 R.F. Coelho Barrue ^{133a}, R. Coelho Lopes De Sa ¹⁰⁵, S. Coelli ^{72a}, B. Cole ⁴², J. Collot ⁶¹,
 P. Conde Muiño ^{133a,133g}, M.P. Connell ^{34c}, S.H. Connell ^{34c}, E.I. Conroy ¹²⁹, F. Conventi ^{73a,af},
 H.G. Cooke ²¹, A.M. Cooper-Sarkar ¹²⁹, F.A. Corchia ^{24b,24a}, A. Cordeiro Oudot Choi ¹³⁰,
 L.D. Corpe ⁴¹, M. Corradi ^{76a,76b}, F. Corriveau ^{106,y}, A. Cortes-Gonzalez ¹⁹, M.J. Costa ¹⁶⁶,
 F. Costanza ⁴, D. Costanzo ¹⁴³, B.M. Cote ¹²², J. Couthures ⁴, G. Cowan ⁹⁷, K. Cranmer ¹⁷³,
 L. Cremer ⁵⁰, D. Cremonini ^{24b,24a}, S. Crépé-Renaudin ⁶¹, F. Crescioli ¹³⁰, M. Cristinziani ¹⁴⁵,
 M. Cristoforetti ^{79a,79b}, V. Croft ¹¹⁷, J.E. Crosby ¹²⁴, G. Crosetti ^{44b,44a}, A. Cueto ¹⁰¹, H. Cui ⁹⁸,
 Z. Cui ⁷, W.R. Cunningham ⁶⁰, F. Curcio ¹⁶⁶, J.R. Curran ⁵³, P. Czodrowski ³⁷,
 M.J. Da Cunha Sargedas De Sousa ^{58b,58a}, J.V. Da Fonseca Pinto ^{84b}, C. Da Via ¹⁰³,
 W. Dabrowski ^{87a}, T. Dado ³⁷, S. Dahbi ¹⁵², T. Dai ¹⁰⁸, D. Dal Santo ²⁰, C. Dallapiccola ¹⁰⁵,
 M. Dam ⁴³, G. D'amen ³⁰, V. D'Amico ¹¹¹, J. Damp ¹⁰², J.R. Dandoy ³⁵, D. Dannheim ³⁷,
 M. Danninger ¹⁴⁶, V. Dao ¹⁴⁹, G. Darbo ^{58b}, S.J. Das ³⁰, F. Dattola ⁴⁹, S. D'Auria ^{72a,72b},
 A. D'Avanzo ^{73a,73b}, C. David ^{34a}, T. Davidek ¹³⁶, I. Dawson ⁹⁶, H.A. Day-hall ¹³⁵, K. De ⁸,
 R. De Asmundis ^{73a}, N. De Biase ⁴⁹, S. De Castro ^{24b,24a}, N. De Groot ¹¹⁶, P. de Jong ¹¹⁷,
 H. De la Torre ¹¹⁸, A. De Maria ^{114a}, A. De Salvo ^{76a}, U. De Sanctis ^{77a,77b}, F. De Santis ^{71a,71b},
 A. De Santo ¹⁵⁰, J.B. De Vivie De Regie ⁶¹, J. Debevc ⁹⁵, D.V. Dedovich ³⁹, J. Degens ⁹⁴,
 A.M. Deiana ⁴⁵, F. Del Corso ^{24b,24a}, J. Del Peso ¹⁰¹, L. Delagrangé ¹³⁰, F. Deliot ¹³⁸,
 C.M. Delitzsch ⁵⁰, M. Della Pietra ^{73a,73b}, D. Della Volpe ⁵⁷, A. Dell'Acqua ³⁷,
 L. Dell'Asta ^{72a,72b}, M. Delmastro ⁴, P.A. Delsart ⁶¹, S. Demers ¹⁷⁵, M. Demichev ³⁹,
 S.P. Denisov ³⁸, L. D'Eramo ⁴¹, D. Derendarz ⁸⁸, F. Derue ¹³⁰, P. Dervan ⁹⁴, K. Desch ²⁵,
 C. Deutsch ²⁵, F.A. Di Bello ^{58b,58a}, A. Di Ciaccio ^{77a,77b}, L. Di Ciaccio ⁴,
 A. Di Domenico ^{76a,76b}, C. Di Donato ^{73a,73b}, A. Di Girolamo ³⁷, G. Di Gregorio ³⁷,
 A. Di Luca ^{79a,79b}, B. Di Micco ^{78a,78b}, R. Di Nardo ^{78a,78b}, K.F. Di Petrillo ⁴⁰,
 M. Diamantopoulou ³⁵, F.A. Dias ¹¹⁷, T. Dias Do Vale ¹⁴⁶, M.A. Diaz ^{140a,140b},
 F.G. Diaz Capriles ²⁵, A.R. Didenko ³⁹, M. Didenko ¹⁶⁶, E.B. Diehl ¹⁰⁸, S. Díez Cornell ⁴⁹,
 C. Díez Pardos ¹⁴⁵, C. Dimitriadi ¹⁶⁴, A. Dimitrievska ²¹, J. Dingfelder ²⁵, T. Dingley ¹²⁹,
 I-M. Dinu ^{28b}, S.J. Dittmeier ^{64b}, F. Dittus ³⁷, M. Divisek ¹³⁶, B. Dixit ⁹⁴, F. Djama ¹⁰⁴,
 T. Djobava ^{153b}, C. Doglioni ^{103,100}, A. Dohalova ^{29a}, J. Dolejsi ¹³⁶, Z. Dolezal ¹³⁶,
 K. Domijan ^{87a}, K.M. Dona ⁴⁰, M. Donadelli ^{84d}, B. Dong ¹⁰⁹, J. Donini ⁴¹,
 A. D'Onofrio ^{73a,73b}, M. D'Onofrio ⁹⁴, J. Dopke ¹³⁷, A. Doria ^{73a}, N. Dos Santos Fernandes ^{133a},
 P. Dougan ¹⁰³, M.T. Dova ⁹², A.T. Doyle ⁶⁰, M.A. Draguet ¹²⁹, M.P. Drescher ⁵⁶, E. Dreyer ¹⁷²,
 I. Drivas-koulouris ¹⁰, M. Drnevich ¹²⁰, M. Drozdova ⁵⁷, D. Du ^{63a}, T.A. du Pree ¹¹⁷,
 F. Dubinin ³⁸, M. Dubovsky ^{29a}, E. Duchovni ¹⁷², G. Duckeck ¹¹¹, O.A. Ducu ^{28b}, D. Duda ⁵³,
 A. Dudarev ³⁷, E.R. Duden ²⁷, M. D'uffizi ¹⁰³, L. Duflot ⁶⁷, M. Dührssen ³⁷, I. Duminica ^{28g},
 A.E. Dumitriu ^{28b}, M. Dunford ^{64a}, S. Dungs ⁵⁰, K. Dunne ^{48a,48b}, A. Duperrin ¹⁰⁴,
 H. Duran Yildiz ^{3a}, M. Düren ⁵⁹, A. Durglishvili ^{153b}, D. Duvnjak ³⁵, B.L. Dwyer ¹¹⁸,
 G.I. Dyckes ^{18a}, M. Dyndal ^{87a}, B.S. Dziedzic ³⁷, Z.O. Earnshaw ¹⁵⁰, G.H. Eberwein ¹²⁹,
 B. Eckerova ^{29a}, S. Eggebrecht ⁵⁶, E. Egidio Purcino De Souza ^{84e}, L.F. Ehrke ⁵⁷, G. Eigen ¹⁷,
 K. Einsweiler ^{18a}, T. Ekelof ¹⁶⁴, P.A. Ekman ¹⁰⁰, S. El Farkh ^{36b}, Y. El Ghazali ^{63a},
 H. El Jarrari ³⁷, A. El Moussaouy ^{36a}, V. Ellajosyula ¹⁶⁴, M. Ellert ¹⁶⁴, F. Ellinghaus ¹⁷⁴,
 N. Ellis ³⁷, J. Elmsheuser ³⁰, M. Elsayy ^{119a}, M. Elsing ³⁷, D. Emeliyanov ¹³⁷, Y. Enari ⁸⁵,
 I. Ene ^{18a}, S. Epari ¹³, P.A. Erland ⁸⁸, D. Ernani Martins Neto ⁸⁸, M. Errenst ¹⁷⁴, M. Escalier ⁶⁷,

C. Escobar [ID166](#), E. Etzion [ID155](#), G. Evans [ID133a,133b](#), H. Evans [ID69](#), L.S. Evans [ID97](#), A. Ezhilov [ID38](#),
 S. Ezzarqtouni [ID36a](#), F. Fabbri [ID24b,24a](#), L. Fabbri [ID24b,24a](#), G. Facini [ID98](#), V. Fadeyev [ID139](#),
 R.M. Fakhrutdinov [ID38](#), D. Fakoudis [ID102](#), S. Falciano [ID76a](#), L.F. Falda Ulhoa Coelho [ID37](#),
 F. Fallavollita [ID112](#), G. Falsetti [ID44b,44a](#), J. Faltova [ID136](#), C. Fan [ID165](#), K.Y. Fan [ID65b](#), Y. Fan [ID14](#),
 Y. Fang [ID14,114c](#), M. Fanti [ID72a,72b](#), M. Faraj [ID70a,70b](#), Z. Farazpay [ID99](#), A. Farbin [ID8](#), A. Farilla [ID78a](#),
 T. Farooque [ID109](#), S.M. Farrington [ID53](#), F. Fassi [ID36e](#), D. Fassouliotis [ID9](#), M. Faucci Giannelli [ID77a,77b](#),
 W.J. Fawcett [ID33](#), L. Fayard [ID67](#), P. Federic [ID136](#), P. Federicova [ID134](#), O.L. Fedin [ID38,a](#), M. Feickert [ID173](#),
 L. Feligioni [ID104](#), D.E. Fellers [ID126](#), C. Feng [ID63b](#), Z. Feng [ID117](#), M.J. Fenton [ID162](#), L. Ferencz [ID49](#),
 R.A.M. Ferguson [ID93](#), S.I. Fernandez Luengo [ID140f](#), P. Fernandez Martinez [ID68](#), M.J.V. Fernoux [ID104](#),
 J. Ferrando [ID93](#), A. Ferrari [ID164](#), P. Ferrari [ID117,116](#), R. Ferrari [ID74a](#), D. Ferrere [ID57](#), C. Ferretti [ID108](#),
 D. Fiacco [ID76a,76b](#), F. Fiedler [ID102](#), P. Fiedler [ID135](#), S. Filimonov [ID38](#), A. Filipčič [ID95](#), E.K. Filmer [ID1](#),
 F. Filthaut [ID116](#), M.C.N. Fiolhais [ID133a,133c,c](#), L. Fiorini [ID166](#), W.C. Fisher [ID109](#), T. Fitschen [ID103](#),
 P.M. Fitzhugh [ID138](#), I. Fleck [ID145](#), P. Fleischmann [ID108](#), T. Flick [ID174](#), M. Flores [ID34d,ab](#),
 L.R. Flores Castillo [ID65a](#), L. Flores Sanz De Acedo [ID37](#), F.M. Follega [ID79a,79b](#), N. Fomin [ID33](#),
 J.H. Foo [ID158](#), A. Formica [ID138](#), A.C. Forti [ID103](#), E. Fortin [ID37](#), A.W. Fortman [ID18a](#), M.G. Foti [ID18a](#),
 L. Fountas [ID9j](#), D. Fournier [ID67](#), H. Fox [ID93](#), P. Francavilla [ID75a,75b](#), S. Francescato [ID62](#),
 S. Franchellucci [ID57](#), M. Franchini [ID24b,24a](#), S. Franchino [ID64a](#), D. Francis [ID37](#), L. Franco [ID116](#),
 V. Franco Lima [ID37](#), L. Franconi [ID49](#), M. Franklin [ID62](#), G. Frattari [ID27](#), Y.Y. Frid [ID155](#), J. Friend [ID60](#),
 N. Fritzsche [ID37](#), A. Froch [ID55](#), D. Froidevaux [ID37](#), J.A. Frost [ID129](#), Y. Fu [ID63a](#),
 S. Fuenzalida Garrido [ID140f](#), M. Fujimoto [ID104](#), K.Y. Fung [ID65a](#), E. Furtado De Simas Filho [ID84e](#),
 M. Furukawa [ID157](#), J. Fuster [ID166](#), A. Gaa [ID56](#), A. Gabrielli [ID24b,24a](#), A. Gabrielli [ID158](#), P. Gadow [ID37](#),
 G. Gagliardi [ID58b,58a](#), L.G. Gagnon [ID18a](#), S. Gaid [ID163](#), S. Galantzan [ID155](#), J. Gallagher [ID1](#),
 E.J. Gallas [ID129](#), B.J. Gallop [ID137](#), K.K. Gan [ID122](#), S. Ganguly [ID157](#), Y. Gao [ID53](#),
 F.M. Garay Walls [ID140a,140b](#), B. Garcia [ID30](#), C. García [ID166](#), A. Garcia Alonso [ID117](#),
 A.G. Garcia Caffaro [ID175](#), J.E. García Navarro [ID166](#), M. Garcia-Sciveres [ID18a](#), G.L. Gardner [ID131](#),
 R.W. Gardner [ID40](#), N. Garelli [ID161](#), D. Garg [ID81](#), R.B. Garg [ID147](#), J.M. Gargan [ID53](#), C.A. Garner [ID158](#),
 C.M. Garvey [ID34a](#), V.K. Gassmann [ID161](#), G. Gaudio [ID74a](#), V. Gautam [ID13](#), P. Gauzzi [ID76a,76b](#),
 J. Gavranovic [ID95](#), I.L. Gavrilenko [ID38](#), A. Gavrilyuk [ID38](#), C. Gay [ID167](#), G. Gaycken [ID126](#),
 E.N. Gazis [ID10](#), A.A. Geanta [ID28b](#), C.M. Gee [ID139](#), A. Gekow [ID122](#), C. Gemme [ID58b](#), M.H. Genest [ID61](#),
 A.D. Gentry [ID115](#), S. George [ID97](#), W.F. George [ID21](#), T. Geralis [ID47](#), P. Gessinger-Befurt [ID37](#),
 M.E. Geyik [ID174](#), M. Ghani [ID170](#), K. Ghorbanian [ID96](#), A. Ghosal [ID145](#), A. Ghosh [ID162](#), A. Ghosh [ID7](#),
 B. Giacobbe [ID24b](#), S. Giagu [ID76a,76b](#), T. Giani [ID117](#), A. Giannini [ID63a](#), S.M. Gibson [ID97](#), M. Gignac [ID139](#),
 D.T. Gil [ID87b](#), A.K. Gilbert [ID87a](#), B.J. Gilbert [ID42](#), D. Gillberg [ID35](#), G. Gilles [ID117](#), L. Ginabat [ID130](#),
 D.M. Gingrich [ID2,ae](#), M.P. Giordani [ID70a,70c](#), P.F. Giraud [ID138](#), G. Giugliarelli [ID70a,70c](#), D. Giugni [ID72a](#),
 F. Giuli [ID77a,77b](#), I. Gkialas [ID9j](#), L.K. Gladilin [ID38](#), C. Glasman [ID101](#), G.R. Gledhill [ID126](#), G. Glemža [ID49](#),
 M. Glisic [ID126](#), I. Gnesi [ID44b](#), Y. Go [ID30](#), M. Goblirsch-Kolb [ID37](#), B. Gocke [ID50](#), D. Godin [ID110](#),
 B. Gokturk [ID22a](#), S. Goldfarb [ID107](#), T. Golling [ID57](#), M.G.D. Gololo [ID34g](#), D. Golubkov [ID38](#),
 J.P. Gombas [ID109](#), A. Gomes [ID133a,133b](#), G. Gomes Da Silva [ID145](#), A.J. Gomez Delegido [ID166](#),
 R. Gonçalves [ID133a](#), L. Gonella [ID21](#), A. Gongadze [ID153c](#), F. Gonnella [ID21](#), J.L. Gonski [ID147](#),
 R.Y. González Andana [ID53](#), S. González de la Hoz [ID166](#), R. Gonzalez Lopez [ID94](#),
 C. Gonzalez Renteria [ID18a](#), M.V. Gonzalez Rodrigues [ID49](#), R. Gonzalez Suarez [ID164](#),
 S. Gonzalez-Sevilla [ID57](#), L. Goossens [ID37](#), B. Gorini [ID37](#), E. Gorini [ID71a,71b](#), A. Gorišek [ID95](#),
 T.C. Gosart [ID131](#), A.T. Goshaw [ID52](#), M.I. Gostkin [ID39](#), S. Goswami [ID124](#), C.A. Gottardo [ID37](#),
 S.A. Gotz [ID111](#), M. Goughri [ID36b](#), V. Goumarre [ID49](#), A.G. Goussiou [ID142](#), N. Govender [ID34c](#),
 R.P. Grabarczyk [ID129](#), I. Grabowska-Bold [ID87a](#), K. Graham [ID35](#), E. Gramstad [ID128](#),
 S. Grancagnolo [ID71a,71b](#), C.M. Grant [ID1,138](#), P.M. Gravila [ID28f](#), F.G. Gravili [ID71a,71b](#), H.M. Gray [ID18a](#),
 M. Greco [ID71a,71b](#), M.J. Green [ID1](#), C. Grefe [ID25](#), A.S. Grefsrud [ID17](#), I.M. Gregor [ID49](#), K.T. Greif [ID162](#),

P. Grenier ¹⁴⁷, S.G. Grewe ¹¹², A.A. Grillo ¹³⁹, K. Grimm ³², S. Grinstein ^{13,u}, J.-F. Grivaz ⁶⁷,
 E. Gross ¹⁷², J. Grosse-Knetter ⁵⁶, L. Guan ¹⁰⁸, J.G.R. Guerrero Rojas ¹⁶⁶, G. Guerrieri ³⁷,
 R. Gugel ¹⁰², J.A.M. Guhit ¹⁰⁸, A. Guida ¹⁹, E. Guilloton ¹⁷⁰, S. Guindon ³⁷, F. Guo ^{14,114c},
 J. Guo ^{63c}, L. Guo ⁴⁹, Y. Guo ¹⁰⁸, A. Gupta ⁵⁰, R. Gupta ¹³², S. Gurbuz ²⁵, S.S. Gurdasani ⁵⁵,
 G. Gustavino ^{76a,76b}, P. Gutierrez ¹²³, L.F. Gutierrez Zagazeta ¹³¹, M. Gutsche ⁵¹,
 C. Gutschow ⁹⁸, C. Gwenlan ¹²⁹, C.B. Gwilliam ⁹⁴, E.S. Haaland ¹²⁸, A. Haas ¹²⁰,
 M. Habedank ⁶⁰, C. Haber ^{18a}, H.K. Hadavand ⁸, A. Hadeef ⁵¹, S. Hadzic ¹¹², A.I. Hagan ⁹³,
 J.J. Hahn ¹⁴⁵, E.H. Haines ⁹⁸, M. Haleem ¹⁶⁹, J. Haley ¹²⁴, G.D. Hallowell ¹⁰⁴, L. Halser ²⁰,
 K. Hamano ¹⁶⁸, M. Hamer ²⁵, E.J. Hampshire ⁹⁷, J. Han ^{63b}, L. Han ^{114a}, L. Han ^{63a},
 S. Han ^{18a}, Y.F. Han ¹⁵⁸, K. Hanagaki ⁸⁵, M. Hance ¹³⁹, D.A. Hangal ⁴², H. Hanif ¹⁴⁶,
 M.D. Hank ¹³¹, J.B. Hansen ⁴³, P.H. Hansen ⁴³, D. Harada ⁵⁷, T. Harenberg ¹⁷⁴, S. Harkusha ³⁸,
 M.L. Harris ¹⁰⁵, Y.T. Harris ²⁵, J. Harrison ¹³, N.M. Harrison ¹²², P.F. Harrison ¹⁷⁰,
 N.M. Hartman ¹¹², N.M. Hartmann ¹¹¹, R.Z. Hasan ^{97,137}, Y. Hasegawa ¹⁴⁴, F. Haslbeck ¹²⁹,
 S. Hassan ¹⁷, R. Hauser ¹⁰⁹, C.M. Hawkes ²¹, R.J. Hawkins ³⁷, Y. Hayashi ¹⁵⁷, D. Hayden ¹⁰⁹,
 C. Hayes ¹⁰⁸, R.L. Hayes ¹¹⁷, C.P. Hays ¹²⁹, J.M. Hays ⁹⁶, H.S. Hayward ⁹⁴, F. He ^{63a},
 M. He ^{14,114c}, Y. He ⁴⁹, Y. He ⁹⁸, N.B. Heatley ⁹⁶, V. Hedberg ¹⁰⁰, A.L. Heggelund ¹²⁸,
 N.D. Hehir ^{96,*}, C. Heidegger ⁵⁵, K.K. Heidegger ⁵⁵, J. Heilman ³⁵, S. Heim ⁴⁹, T. Heim ^{18a},
 J.G. Heinlein ¹³¹, J.J. Heinrich ¹²⁶, L. Heinrich ^{112,ac}, J. Hejbal ¹³⁴, A. Held ¹⁷³,
 S. Hellesund ¹⁷, C.M. Helling ¹⁶⁷, S. Hellman ^{48a,48b}, R.C.W. Henderson ⁹³, L. Henkelmann ³³,
 A.M. Henriques Correia ³⁷, H. Herde ¹⁰⁰, Y. Hernández Jiménez ¹⁴⁹, L.M. Herrmann ²⁵,
 T. Herrmann ⁵¹, G. Herten ⁵⁵, R. Hertenberger ¹¹¹, L. Hervas ³⁷, M.E. Hespings ¹⁰²,
 N.P. Hessey ^{159a}, J. Hessler ¹¹², M. Hidaoui ^{36b}, N. Hidic ¹³⁶, E. Hill ¹⁵⁸, S.J. Hillier ²¹,
 J.R. Hinds ¹⁰⁹, F. Hinterkeuser ²⁵, M. Hirose ¹²⁷, S. Hirose ¹⁶⁰, D. Hirschbuehl ¹⁷⁴,
 T.G. Hitchings ¹⁰³, B. Hiti ⁹⁵, J. Hobbs ¹⁴⁹, R. Hobincu ^{28e}, N. Hod ¹⁷², M.C. Hodgkinson ¹⁴³,
 B.H. Hodgkinson ¹²⁹, A. Hoecker ³⁷, D.D. Hofer ¹⁰⁸, J. Hofer ¹⁶⁶, T. Holm ²⁵, M. Holzbock ³⁷,
 L.B.A.H. Hommels ³³, B.P. Honan ¹⁰³, J.J. Hong ⁶⁹, J. Hong ^{63c}, T.M. Hong ¹³²,
 B.H. Hooberman ¹⁶⁵, W.H. Hopkins ⁶, M.C. Hoppesch ¹⁶⁵, Y. Horii ¹¹³, M.E. Horstmann ¹¹²,
 S. Hou ¹⁵², A.S. Howard ⁹⁵, J. Howarth ⁶⁰, J. Hoya ⁶, M. Hrabovsky ¹²⁵, A. Hrynevich ⁴⁹,
 T. Hryn'ova ⁴, P.J. Hsu ⁶⁶, S.-C. Hsu ¹⁴², T. Hsu ⁶⁷, M. Hu ^{18a}, Q. Hu ^{63a}, S. Huang ^{65b},
 X. Huang ^{14,114c}, Y. Huang ¹⁴³, Y. Huang ¹⁰², Y. Huang ¹⁴, Z. Huang ¹⁰³, Z. Hubacek ¹³⁵,
 M. Huebner ²⁵, F. Hugging ²⁵, T.B. Huffman ¹²⁹, M. Hufnagel Maranha De Faria ^{84a},
 C.A. Hugli ⁴⁹, M. Huhtinen ³⁷, S.K. Huiberts ¹⁷, R. Hulsken ¹⁰⁶, N. Huseynov ^{12,g},
 J. Huston ¹⁰⁹, J. Huth ⁶², R. Hyneman ¹⁴⁷, G. Iacobucci ⁵⁷, G. Iakovidis ³⁰,
 L. Iconomidou-Fayard ⁶⁷, J.P. Iddon ³⁷, P. Iengo ^{73a,73b}, R. Iguchi ¹⁵⁷, Y. Iiyama ¹⁵⁷,
 T. Iizawa ¹²⁹, Y. Ikegami ⁸⁵, N. Ilic ¹⁵⁸, H. Imam ^{84c}, G. Inacio Goncalves ^{84d},
 T. Ingebretsen Carlson ^{48a,48b}, J.M. Inglis ⁹⁶, G. Introzzi ^{74a,74b}, M. Iodice ^{78a}, V. Ippolito ^{76a,76b},
 R.K. Irwin ⁹⁴, M. Ishino ¹⁵⁷, W. Islam ¹⁷³, C. Issever ¹⁹, S. Istin ^{22a,ai}, H. Ito ¹⁷¹,
 R. Iuppa ^{79a,79b}, A. Ivina ¹⁷², J.M. Izen ⁴⁶, V. Izzo ^{73a}, P. Jacka ¹³⁴, P. Jackson ¹,
 C.S. Jagfeld ¹¹¹, G. Jain ^{159a}, P. Jain ⁴⁹, K. Jakobs ⁵⁵, T. Jakoubek ¹⁷², J. Jamieson ⁶⁰,
 W. Jang ¹⁵⁷, M. Javurkova ¹⁰⁵, P. Jawahar ¹⁰³, L. Jeanty ¹²⁶, J. Jejelava ^{153a,aa}, P. Jenni ^{55,f},
 C.E. Jessiman ³⁵, C. Jia ^{63b}, H. Jia ¹⁶⁷, J. Jia ¹⁴⁹, X. Jia ^{14,114c}, Z. Jia ^{114a}, C. Jiang ⁵³,
 S. Jiggins ⁴⁹, J. Jimenez Pena ¹³, S. Jin ^{114a}, A. Jinaru ^{28b}, O. Jinnouchi ¹⁴¹, P. Johansson ¹⁴³,
 K.A. Johns ⁷, J.W. Johnson ¹³⁹, F.A. Jolly ⁴⁹, D.M. Jones ¹⁵⁰, E. Jones ⁴⁹, K.S. Jones ⁸,
 P. Jones ³³, R.W.L. Jones ⁹³, T.J. Jones ⁹⁴, H.L. Joos ^{56,37}, R. Joshi ¹²², J. Jovicevic ¹⁶,
 X. Ju ^{18a}, J.J. Junggeburth ¹⁰⁵, T. Junkermann ^{64a}, A. Juste Rozas ^{13,u}, M.K. Juzek ⁸⁸,
 S. Kabana ^{140e}, A. Kaczmarzka ⁸⁸, M. Kado ¹¹², H. Kagan ¹²², M. Kagan ¹⁴⁷, A. Kahn ¹³¹,
 C. Kahra ¹⁰², T. Kaji ¹⁵⁷, E. Kajomovitz ¹⁵⁴, N. Kakati ¹⁷², I. Kalaitzidou ⁵⁵, C.W. Kalderon ³⁰,

N.J. Kang ¹³⁹, D. Kar ^{34g}, K. Karava ¹²⁹, M.J. Kareem ^{159b}, E. Karentzos ⁵⁵, O. Karkout ¹¹⁷,
 S.N. Karpov ³⁹, Z.M. Karpova ³⁹, V. Kartvelishvili ⁹³, A.N. Karyukhin ³⁸, E. Kasimi ¹⁵⁶,
 J. Katzy ⁴⁹, S. Kaur ³⁵, K. Kawade ¹⁴⁴, M.P. Kawale ¹²³, C. Kawamoto ⁸⁹, T. Kawamoto ^{63a},
 E.F. Kay ³⁷, F.I. Kaya ¹⁶¹, S. Kazakos ¹⁰⁹, V.F. Kazanin ³⁸, Y. Ke ¹⁴⁹, J.M. Keaveney ^{34a},
 R. Keeler ¹⁶⁸, G.V. Kehris ⁶², J.S. Keller ³⁵, J.J. Kempster ¹⁵⁰, O. Kepka ¹³⁴, B.P. Kerridge ¹³⁷,
 S. Kersten ¹⁷⁴, B.P. Kerševan ⁹⁵, L. Keszeghova ^{29a}, S. Ketabchi Haghghat ¹⁵⁸, R.A. Khan ¹³²,
 A. Khanov ¹²⁴, A.G. Kharlamov ³⁸, T. Kharlamova ³⁸, E.E. Khoda ¹⁴², M. Kholodenko ^{133a},
 T.J. Khoo ¹⁹, G. Khoriali ¹⁶⁹, J. Khubua ^{153b,*}, Y.A.R. Khwaira ¹³⁰, B. Kibirige ^{34g}, D. Kim ⁶,
 D.W. Kim ^{48a,48b}, Y.K. Kim ⁴⁰, N. Kimura ⁹⁸, M.K. Kingston ⁵⁶, A. Kirchhoff ⁵⁶, C. Kirfel ²⁵,
 F. Kirfel ²⁵, J. Kirk ¹³⁷, A.E. Kiryunin ¹¹², S. Kita ¹⁶⁰, C. Kitsaki ¹⁰, O. Kivernyk ²⁵,
 M. Klassen ¹⁶¹, C. Klein ³⁵, L. Klein ¹⁶⁹, M.H. Klein ⁴⁵, S.B. Klein ⁵⁷, U. Klein ⁹⁴,
 A. Klimentov ³⁰, T. Klioutchnikova ³⁷, P. Kluit ¹¹⁷, S. Kluth ¹¹², E. Kneringer ⁸⁰,
 T.M. Knight ¹⁵⁸, A. Knue ⁵⁰, D. Kobylanski ¹⁷², S.F. Koch ¹²⁹, M. Kocian ¹⁴⁷, P. Kodyš ¹³⁶,
 D.M. Koeck ¹²⁶, P.T. Koenig ²⁵, T. Koffas ³⁵, O. Kolay ⁵¹, I. Koletsou ⁴, T. Komarek ⁸⁸,
 K. Köneke ⁵⁵, A.X.Y. Kong ¹, T. Kono ¹²¹, N. Konstantinidis ⁹⁸, P. Kontaxakis ⁵⁷,
 B. Konya ¹⁰⁰, R. Kopeliansky ⁴², S. Koperny ^{87a}, K. Korcyl ⁸⁸, K. Kordas ^{156,e}, A. Korn ⁹⁸,
 S. Korn ⁵⁶, I. Korolkov ¹³, N. Korotkova ³⁸, B. Kortman ¹¹⁷, O. Kortner ¹¹², S. Kortner ¹¹²,
 W.H. Kostecka ¹¹⁸, V.V. Kostyukhin ¹⁴⁵, A. Kotsokechagia ³⁷, A. Kotwal ⁵², A. Koulouris ³⁷,
 A. Kourkoumeli-Charalampidi ^{74a,74b}, C. Kourkoumelis ⁹, E. Kourlitis ^{112,ac}, O. Kovanda ¹²⁶,
 R. Kowalewski ¹⁶⁸, W. Kozanecki ¹²⁶, A.S. Kozhin ³⁸, V.A. Kramarenko ³⁸, G. Kramberger ⁹⁵,
 P. Kramer ¹⁰², M.W. Krasny ¹³⁰, A. Krasznahorkay ³⁷, A.C. Kraus ¹¹⁸, J.W. Kraus ¹⁷⁴,
 J.A. Kremer ⁴⁹, T. Kresse ⁵¹, L. Kretschmann ¹⁷⁴, J. Kretschmar ⁹⁴, K. Kreul ¹⁹,
 P. Krieger ¹⁵⁸, M. Krivos ¹³⁶, K. Krizka ²¹, K. Kroeninger ⁵⁰, H. Kroha ¹¹², J. Kroll ¹³⁴,
 J. Kroll ¹³¹, K.S. Krowpman ¹⁰⁹, U. Kruchonak ³⁹, H. Krüger ²⁵, N. Krumnack ⁸², M.C. Kruse ⁵²,
 O. Kuchinskaia ³⁸, S. Kuday ^{3a}, S. Kuehn ³⁷, R. Kuesters ⁵⁵, T. Kuhl ⁴⁹, V. Kukhtin ³⁹,
 Y. Kulchitsky ^{38,a}, S. Kuleshov ^{140d,140b}, M. Kumar ^{34g}, N. Kumari ⁴⁹, P. Kumari ^{159b},
 A. Kupco ¹³⁴, T. Kupfer ⁵⁰, A. Kupich ³⁸, O. Kuprash ⁵⁵, H. Kurashige ⁸⁶, L.L. Kurchaninov ^{159a},
 O. Kurdysh ⁶⁷, Y.A. Kurochkin ³⁸, A. Kurova ³⁸, M. Kuze ¹⁴¹, A.K. Kvam ¹⁰⁵, J. Kvitá ¹²⁵,
 T. Kwan ¹⁰⁶, N.G. Kyriacou ¹⁰⁸, L.A.O. Laatu ¹⁰⁴, C. Lacasta ¹⁶⁶, F. Lacava ^{76a,76b},
 H. Lacker ¹⁹, D. Lacour ¹³⁰, N.N. Lad ⁹⁸, E. Ladygin ³⁹, A. Lafarge ⁴¹, B. Laforge ¹³⁰,
 T. Lagouri ¹⁷⁵, F.Z. Lahbabi ^{36a}, S. Lai ⁵⁶, J.E. Lambert ¹⁶⁸, S. Lammers ⁶⁹, W. Lampl ⁷,
 C. Lampoudis ^{156,e}, G. Lamprinoudis ¹⁰², A.N. Lancaster ¹¹⁸, E. Lançon ³⁰, U. Landgraf ⁵⁵,
 M.P.J. Landon ⁹⁶, V.S. Lang ⁵⁵, O.K.B. Langrekken ¹²⁸, A.J. Lankford ¹⁶², F. Lanni ³⁷,
 K. Lantzsck ²⁵, A. Lanza ^{74a}, M. Lanzac Berrocal ¹⁶⁶, J.F. Laporte ¹³⁸, T. Lari ^{72a},
 F. Lasagni Manghi ^{24b}, M. Lassnig ³⁷, V. Latonova ¹³⁴, A. Laurier ¹⁵⁴, S.D. Lawlor ¹⁴³,
 Z. Lawrence ¹⁰³, R. Lazaridou ¹⁷⁰, M. Lazzaroni ^{72a,72b}, B. Le ¹⁰³, H.D.M. Le ¹⁰⁹,
 E.M. Le Boulicaut ¹⁷⁵, L.T. Le Pottier ^{18a}, B. Leban ^{24b,24a}, A. Lebedev ⁸², M. LeBlanc ¹⁰³,
 F. Ledroit-Guillon ⁶¹, S.C. Lee ¹⁵², S. Lee ^{48a,48b}, T.F. Lee ⁹⁴, L.L. Leeuw ^{34c}, H.P. Lefebvre ⁹⁷,
 M. Lefebvre ¹⁶⁸, C. Leggett ^{18a}, G. Lehmann Miotto ³⁷, M. Leigh ⁵⁷, W.A. Leight ¹⁰⁵,
 W. Leinonen ¹¹⁶, A. Leisos ^{156,s}, M.A.L. Leite ^{84c}, C.E. Leitgeb ¹⁹, R. Leitner ¹³⁶,
 K.J.C. Leney ⁴⁵, T. Lenz ²⁵, S. Leone ^{75a}, C. Leonidopoulos ⁵³, A. Leopold ¹⁴⁸, R. Les ¹⁰⁹,
 C.G. Lester ³³, M. Levchenko ³⁸, J. Levêque ⁴, L.J. Levinson ¹⁷², G. Levrini ^{24b,24a},
 M.P. Lewicki ⁸⁸, C. Lewis ¹⁴², D.J. Lewis ⁴, L. Lewitt ¹⁴³, A. Li ³⁰, B. Li ^{63b}, C. Li ^{63a},
 C-Q. Li ¹¹², H. Li ^{63a}, H. Li ^{63b}, H. Li ^{114a}, H. Li ¹⁵, H. Li ^{63b}, J. Li ^{63c}, K. Li ¹⁴, L. Li ^{63c},
 M. Li ^{14,114c}, S. Li ^{14,114c}, S. Li ^{63d,63c,d}, T. Li ⁵, X. Li ¹⁰⁶, Z. Li ¹⁵⁷, Z. Li ^{14,114c}, Z. Li ^{63a},
 S. Liang ^{14,114c}, Z. Liang ¹⁴, M. Liberatore ¹³⁸, B. Liberti ^{77a}, K. Lie ^{65c}, J. Lieber Marin ^{84e},
 H. Lien ⁶⁹, H. Lin ¹⁰⁸, K. Lin ¹⁰⁹, R.E. Lindley ⁷, J.H. Lindon ², J. Ling ⁶², E. Lipeles ¹³¹,

A. Lipniacka ¹⁷, A. Lister ¹⁶⁷, J.D. Little ⁶⁹, B. Liu ¹⁴, B.X. Liu ^{114b}, D. Liu ^{63d,63c},
 E.H.L. Liu ²¹, J.B. Liu ^{63a}, J.K.K. Liu ³³, K. Liu ^{63d}, K. Liu ^{63d,63c}, M. Liu ^{63a}, M.Y. Liu ^{63a},
 P. Liu ¹⁴, Q. Liu ^{63d,142,63c}, X. Liu ^{63a}, X. Liu ^{63b}, Y. Liu ^{114b,114c}, Y.L. Liu ^{63b}, Y.W. Liu ^{63a},
 S.L. Lloyd ⁹⁶, E.M. Lobodzinska ⁴⁹, P. Loch ⁷, E. Lodhi ¹⁵⁸, T. Lohse ¹⁹, K. Lohwasser ¹⁴³,
 E. Loiacono ⁴⁹, M. Lokajicek ^{134,*}, J.D. Lomas ²¹, J.D. Long ⁴², I. Longarini ¹⁶², R. Longo ¹⁶⁵,
 I. Lopez Paz ⁶⁸, A. Lopez Solis ⁴⁹, N.A. Lopez-canelas ⁷, N. Lorenzo Martinez ⁴, A.M. Lory ¹¹¹,
 M. Losada ^{119a}, G. Löschcke Centeno ¹⁵⁰, O. Loseva ³⁸, X. Lou ^{48a,48b}, X. Lou ^{14,114c},
 A. Lounis ⁶⁷, P.A. Love ⁹³, G. Lu ^{14,114c}, M. Lu ⁶⁷, S. Lu ¹³¹, Y.J. Lu ⁶⁶, H.J. Lubatti ¹⁴²,
 C. Luci ^{76a,76b}, F.L. Lucio Alves ^{114a}, F. Luehring ⁶⁹, O. Lukianchuk ⁶⁷, B.S. Lunday ¹³¹,
 O. Lundberg ¹⁴⁸, B. Lund-Jensen ^{148,*}, N.A. Luongo ⁶, M.S. Lutz ³⁷, A.B. Lux ²⁶, D. Lynn ³⁰,
 R. Lysak ¹³⁴, E. Lytken ¹⁰⁰, V. Lyubushkin ³⁹, T. Lyubushkina ³⁹, M.M. Lyukova ¹⁴⁹,
 M.Firdaus M. Soberi ⁵³, H. Ma ³⁰, K. Ma ^{63a}, L.L. Ma ^{63b}, W. Ma ^{63a}, Y. Ma ¹²⁴,
 J.C. MacDonald ¹⁰², P.C. Machado De Abreu Farias ^{84e}, R. Madar ⁴¹, T. Madula ⁹⁸, J. Maeda ⁸⁶,
 T. Maeno ³⁰, H. Maguire ¹⁴³, V. Maiboroda ¹³⁸, A. Maio ^{133a,133b,133d}, K. Maj ^{87a},
 O. Majersky ⁴⁹, S. Majewski ¹²⁶, N. Makovec ⁶⁷, V. Maksimovic ¹⁶, B. Malaescu ¹³⁰,
 Pa. Malecki ⁸⁸, V.P. Maleev ³⁸, F. Malek ^{61,n}, M. Mali ⁹⁵, D. Malito ⁹⁷, U. Mallik ^{81,*},
 S. Maltezos ¹⁰, S. Malyukov ³⁹, J. Mamuzic ¹³, G. Mancini ⁵⁴, M.N. Mancini ²⁷, G. Manco ^{74a,74b},
 J.P. Mandalia ⁹⁶, S.S. Mandarray ¹⁵⁰, I. Mandić ⁹⁵, L. Manhaes de Andrade Filho ^{84a},
 I.M. Maniatis ¹⁷², J. Manjarres Ramos ⁹¹, D.C. Mankad ¹⁷², A. Mann ¹¹¹, S. Manzoni ³⁷,
 L. Mao ^{63c}, X. Mapekula ^{34c}, A. Marantis ^{156,s}, G. Marchiori ⁵, M. Marcisovsky ¹³⁴,
 C. Marcon ^{72a}, M. Marinescu ²¹, S. Marium ⁴⁹, M. Marjanovic ¹²³, A. Markhoos ⁵⁵,
 M. Markovitch ⁶⁷, E.J. Marshall ⁹³, Z. Marshall ^{18a}, S. Marti-Garcia ¹⁶⁶, J. Martin ⁹⁸,
 T.A. Martin ¹³⁷, V.J. Martin ⁵³, B. Martin dit Latour ¹⁷, L. Martinelli ^{76a,76b}, M. Martinez ^{13,u},
 P. Martinez Agullo ¹⁶⁶, V.I. Martinez Outschoorn ¹⁰⁵, P. Martinez Suarez ¹³, S. Martin-Haugh ¹³⁷,
 G. Martinovicova ¹³⁶, V.S. Martoiu ^{28b}, A.C. Martyniuk ⁹⁸, A. Marzin ³⁷, D. Mascione ^{79a,79b},
 L. Masetti ¹⁰², J. Masik ¹⁰³, A.L. Maslennikov ³⁸, S.L. Mason ⁴², P. Massarotti ^{73a,73b},
 P. Mastrandrea ^{75a,75b}, A. Mastroberardino ^{44b,44a}, T. Masubuchi ¹²⁷, T.T. Mathew ¹²⁶,
 T. Mathisen ¹⁶⁴, J. Matousek ¹³⁶, D.M. Mattern ⁵⁰, J. Maurer ^{28b}, T. Maurin ⁶⁰, A.J. Maury ⁶⁷,
 B. Maček ⁹⁵, D.A. Maximov ³⁸, A.E. May ¹⁰³, R. Mazini ¹⁵², I. Maznas ¹¹⁸, M. Mazza ¹⁰⁹,
 S.M. Mazza ¹³⁹, E. Mazzeo ^{72a,72b}, C. Mc Ginn ³⁰, J.P. Mc Gowan ¹⁶⁸, S.P. Mc Kee ¹⁰⁸,
 C.A. Mc Lean ⁶, C.C. McCracken ¹⁶⁷, E.F. McDonald ¹⁰⁷, A.E. McDougall ¹¹⁷,
 J.A. Mcfayden ¹⁵⁰, R.P. McGovern ¹³¹, R.P. Mckenzie ^{34g}, T.C. Mclachlan ⁴⁹, D.J. Mclaughlin ⁹⁸,
 S.J. McMahan ¹³⁷, C.M. Mcpartland ⁹⁴, R.A. McPherson ^{168,y}, S. Mehlhase ¹¹¹, A. Mehta ⁹⁴,
 D. Melini ¹⁶⁶, B.R. Mellado Garcia ^{34g}, A.H. Melo ⁵⁶, F. Meloni ⁴⁹,
 A.M. Mendes Jacques Da Costa ¹⁰³, H.Y. Meng ¹⁵⁸, L. Meng ⁹³, S. Menke ¹¹², M. Mentink ³⁷,
 E. Meoni ^{44b,44a}, G. Mercado ¹¹⁸, S. Merianos ¹⁵⁶, C. Merlassino ^{70a,70c}, L. Merola ^{73a,73b},
 C. Meroni ^{72a,72b}, J. Metcalfe ⁶, A.S. Mete ⁶, E. Meuser ¹⁰², C. Meyer ⁶⁹, J-P. Meyer ¹³⁸,
 R.P. Middleton ¹³⁷, L. Mijović ⁵³, G. Mikenberg ¹⁷², M. Mikestikova ¹³⁴, M. Mikuž ⁹⁵,
 H. Mildner ¹⁰², A. Milic ³⁷, D.W. Miller ⁴⁰, E.H. Miller ¹⁴⁷, L.S. Miller ³⁵, A. Milov ¹⁷²,
 D.A. Milstead ^{48a,48b}, T. Min ^{114a}, A.A. Minaenko ³⁸, I.A. Minashvili ^{153b}, L. Mince ⁶⁰,
 A.I. Mincer ¹²⁰, B. Mindur ^{87a}, M. Mineev ³⁹, Y. Mino ⁸⁹, L.M. Mir ¹³, M. Miralles Lopez ⁶⁰,
 M. Mironova ^{18a}, M.C. Missio ¹¹⁶, A. Mitra ¹⁷⁰, V.A. Mitsou ¹⁶⁶, Y. Mitsumori ¹¹³, O. Miu ¹⁵⁸,
 P.S. Miyagawa ⁹⁶, T. Mkrtychyan ^{64a}, M. Mlinarevic ⁹⁸, T. Mlinarevic ⁹⁸, M. Mlynarikova ³⁷,
 S. Mobius ²⁰, P. Mogg ¹¹¹, M.H. Mohamed Farook ¹¹⁵, A.F. Mohammed ^{14,114c}, S. Mohapatra ⁴²,
 G. Mokgatitswane ^{34g}, L. Moleri ¹⁷², B. Mondal ¹⁴⁵, S. Mondal ¹³⁵, K. Mönig ⁴⁹,
 E. Monnier ¹⁰⁴, L. Monsonis Romero ¹⁶⁶, J. Montejo Berlingen ¹³, A. Montella ^{48a,48b},
 M. Montella ¹²², F. Montekali ^{78a,78b}, F. Monticelli ⁹², S. Monzani ^{70a,70c}, A. Morancho Tarda ⁴³,

N. Morange ⁶⁷, A.L. Moreira De Carvalho ⁴⁹, M. Moreno Llácer ¹⁶⁶, C. Moreno Martinez ⁵⁷,
 J.M. Moreno Perez ^{23b}, P. Morettini ^{58b}, S. Morgenstern ³⁷, M. Morii ⁶², M. Morinaga ¹⁵⁷,
 M. Moritsu ⁹⁰, F. Morodei ^{76a,76b}, P. Moschovakos ³⁷, B. Moser ¹²⁹, M. Mosidze ^{153b},
 T. Moskalets ⁴⁵, P. Moskvitina ¹¹⁶, J. Moss ^{32,k}, P. Moszkowicz ^{87a}, A. Moussa ^{36d},
 E.J.W. Moyse ¹⁰⁵, O. Mtintsilana ^{34g}, S. Muanza ¹⁰⁴, J. Mueller ¹³², D. Muenstermann ⁹³,
 R. Müller ³⁷, G.A. Mullier ¹⁶⁴, A.J. Mullin ³³, J.J. Mullin ¹³¹, A.E. Mulski ⁶², D.P. Mungo ¹⁵⁸,
 D. Munoz Perez ¹⁶⁶, F.J. Munoz Sanchez ¹⁰³, M. Murin ¹⁰³, W.J. Murray ^{170,137}, M. Muškinja ⁹⁵,
 C. Mwewa ³⁰, A.G. Myagkov ^{38,a}, A.J. Myers ⁸, G. Myers ¹⁰⁸, M. Myska ¹³⁵, B.P. Nachman ^{18a},
 O. Nackenhorst ⁵⁰, K. Nagai ¹²⁹, K. Nagano ⁸⁵, R. Nagasaka ¹⁵⁷, J.L. Nagle ^{30,ag}, E. Nagy ¹⁰⁴,
 A.M. Nairz ³⁷, Y. Nakahama ⁸⁵, K. Nakamura ⁸⁵, K. Nakkalil ⁵, H. Nanjo ¹²⁷,
 E.A. Narayanan ⁴⁵, I. Naryshkin ³⁸, L. Nasella ^{72a,72b}, M. Naseri ³⁵, S. Nasri ^{119b}, C. Nass ²⁵,
 G. Navarro ^{23a}, J. Navarro-Gonzalez ¹⁶⁶, R. Nayak ¹⁵⁵, A. Nayaz ¹⁹, P.Y. Nechaeva ³⁸,
 S. Nechaeva ^{24b,24a}, F. Nechansky ¹³⁴, L. Nedic ¹²⁹, T.J. Neep ²¹, A. Negri ^{74a,74b},
 M. Negrini ^{24b}, C. Nellist ¹¹⁷, C. Nelson ¹⁰⁶, K. Nelson ¹⁰⁸, S. Nemecek ¹³⁴, M. Nessi ^{37,h},
 M.S. Neubauer ¹⁶⁵, F. Neuhaus ¹⁰², J. Neundorf ⁴⁹, J. Newell ⁹⁴, P.R. Newman ²¹, C.W. Ng ¹³²,
 Y.W.Y. Ng ⁴⁹, B. Ngair ^{119a}, H.D.N. Nguyen ¹¹⁰, R.B. Nickerson ¹²⁹, R. Nicolaidou ¹³⁸,
 J. Nielsen ¹³⁹, M. Niemeyer ⁵⁶, J. Niermann ⁵⁶, N. Nikiforou ³⁷, V. Nikolaenko ^{38,a},
 I. Nikolic-Audit ¹³⁰, K. Nikolopoulos ²¹, P. Nilsson ³⁰, I. Ninca ⁴⁹, G. Ninio ¹⁵⁵, A. Nisati ^{76a},
 N. Nishu ², R. Nisius ¹¹², J-E. Nitschke ⁵¹, E.K. Nkadimeng ^{34g}, T. Nobe ¹⁵⁷,
 T. Nommensen ¹⁵¹, M.B. Norfolk ¹⁴³, B.J. Norman ³⁵, M. Noury ^{36a}, J. Novak ⁹⁵, T. Novak ⁹⁵,
 L. Novotny ¹³⁵, R. Novotny ¹¹⁵, L. Nozka ¹²⁵, K. Ntekas ¹⁶², N.M.J. Nunes De Moura Junior ^{84b},
 J. Ocariz ¹³⁰, A. Ochi ⁸⁶, I. Ochoa ^{133a}, S. Oerdek ^{49,v}, J.T. Offermann ⁴⁰, A. Ogrodnik ¹³⁶,
 A. Oh ¹⁰³, C.C. Ohm ¹⁴⁸, H. Oide ⁸⁵, R. Oishi ¹⁵⁷, M.L. Ojeda ³⁷, Y. Okumura ¹⁵⁷,
 L.F. Oleiro Seabra ^{133a}, I. Oleksiyuk ⁵⁷, S.A. Olivares Pino ^{140d}, G. Oliveira Correa ¹³,
 D. Oliveira Damazio ³⁰, J.L. Oliver ¹⁶², Ö.O. Öncel ⁵⁵, A.P. O'Neill ²⁰, A. Onofre ^{133a,133e},
 P.U.E. Onyisi ¹¹, M.J. Oreglia ⁴⁰, G.E. Orellana ⁹², D. Orestano ^{78a,78b}, N. Orlando ¹³,
 R.S. Orr ¹⁵⁸, L.M. Osojnak ¹³¹, R. Ospanov ^{63a}, Y. Osumi ¹¹³, G. Otero y Garzon ³¹, H. Otono ⁹⁰,
 P.S. Ott ^{64a}, G.J. Ottino ^{18a}, M. Ouchrif ^{36d}, F. Ould-Saada ¹²⁸, T. Ovsianikova ¹⁴²,
 M. Owen ⁶⁰, R.E. Owen ¹³⁷, V.E. Ozcan ^{22a}, F. Ozturk ⁸⁸, N. Ozturk ⁸, S. Ozturk ⁸³,
 H.A. Pacey ¹²⁹, A. Pacheco Pages ¹³, C. Padilla Aranda ¹³, G. Padovano ^{76a,76b},
 S. Pagan Griso ^{18a}, G. Palacino ⁶⁹, A. Palazzo ^{71a,71b}, J. Pampel ²⁵, J. Pan ¹⁷⁵, T. Pan ^{65a},
 D.K. Panchal ¹¹, C.E. Pandini ¹¹⁷, J.G. Panduro Vazquez ¹³⁷, H.D. Pandya ¹, H. Pang ¹⁵,
 P. Pani ⁴⁹, G. Panizzo ^{70a,70c}, L. Panwar ¹³⁰, L. Paolozzi ⁵⁷, S. Parajuli ¹⁶⁵, A. Paramonov ⁶,
 C. Paraskevopoulos ⁵⁴, D. Paredes Hernandez ^{65b}, A. Pareti ^{74a,74b}, K.R. Park ⁴², T.H. Park ¹⁵⁸,
 M.A. Parker ³³, F. Parodi ^{58b,58a}, E.W. Parrish ¹¹⁸, V.A. Parrish ⁵³, J.A. Parsons ⁴²,
 U. Parzefall ⁵⁵, B. Pascual Dias ¹¹⁰, L. Pascual Dominguez ¹⁰¹, E. Pasqualucci ^{76a},
 S. Passaggio ^{58b}, F. Pastore ⁹⁷, P. Patel ⁸⁸, U.M. Patel ⁵², J.R. Pater ¹⁰³, T. Pauly ³⁷,
 F. Pauwels ¹³⁶, C.I. Pazos ¹⁶¹, M. Pedersen ¹²⁸, R. Pedro ^{133a}, S.V. Peleganchuk ³⁸, O. Penc ³⁷,
 E.A. Pender ⁵³, S. Peng ¹⁵, G.D. Penn ¹⁷⁵, K.E. Penski ¹¹¹, M. Penzin ³⁸, B.S. Peralva ^{84d},
 A.P. Pereira Peixoto ¹⁴², L. Pereira Sanchez ¹⁴⁷, D.V. Perepelitsa ^{30,ag}, G. Perera ¹⁰⁵,
 E. Perez Codina ^{159a}, M. Perganti ¹⁰, H. Pernegger ³⁷, S. Perrella ^{76a,76b}, O. Perrin ⁴¹,
 K. Peters ⁴⁹, R.F.Y. Peters ¹⁰³, B.A. Petersen ³⁷, T.C. Petersen ⁴³, E. Petit ¹⁰⁴, V. Petousis ¹³⁵,
 C. Petridou ^{156,e}, T. Petru ¹³⁶, A. Petrukhin ¹⁴⁵, M. Pettee ^{18a}, A. Petukhov ³⁸, K. Petukhova ³⁷,
 R. Pezoa ^{140f}, L. Pezzotti ³⁷, G. Pezzullo ¹⁷⁵, A.J. Pflieger ³⁷, T.M. Pham ¹⁷³, T. Pham ¹⁰⁷,
 P.W. Phillips ¹³⁷, G. Piacquadio ¹⁴⁹, E. Pianori ^{18a}, F. Piazza ¹²⁶, R. Piegai ³¹, D. Pietreanu ^{28b},
 A.D. Pilkington ¹⁰³, M. Pinamonti ^{70a,70c}, J.L. Pinfeld ², B.C. Pinheiro Pereira ^{133a},
 J. Pinol Bel ¹³, A.E. Pinto Pinoargote ^{138,138}, L. Pintucci ^{70a,70c}, K.M. Piper ¹⁵⁰, A. Pirttikoski ⁵⁷,

D.A. Pizzi [ID³⁵](#), L. Pizzimento [ID^{65b}](#), A. Pizzini [ID¹¹⁷](#), M.-A. Pleier [ID³⁰](#), V. Pleskot [ID¹³⁶](#), E. Plotnikova [ID³⁹](#),
 G. Poddar [ID⁹⁶](#), R. Poettgen [ID¹⁰⁰](#), L. Poggioli [ID¹³⁰](#), I. Pokharel [ID⁵⁶](#), S. Polacek [ID¹³⁶](#), G. Polesello [ID^{74a}](#),
 A. Poley [ID^{146,159a}](#), A. Polini [ID^{24b}](#), C.S. Pollard [ID¹⁷⁰](#), Z.B. Pollock [ID¹²²](#), E. Pompa Pacchi [ID^{76a,76b}](#),
 N.I. Pond [ID⁹⁸](#), D. Ponomarenko [ID⁶⁹](#), L. Pontecorvo [ID³⁷](#), S. Popa [ID^{28a}](#), G.A. Popeneciu [ID^{28d}](#),
 A. Poreba [ID³⁷](#), D.M. Portillo Quintero [ID^{159a}](#), S. Pospisil [ID¹³⁵](#), M.A. Postill [ID¹⁴³](#), P. Postolache [ID^{28c}](#),
 K. Potamianos [ID¹⁷⁰](#), P.A. Potepa [ID^{87a}](#), I.N. Potrap [ID³⁹](#), C.J. Potter [ID³³](#), H. Potti [ID¹⁵¹](#), J. Poveda [ID¹⁶⁶](#),
 M.E. Pozo Astigarraga [ID³⁷](#), A. Prades Ibanez [ID^{77a,77b}](#), J. Pretel [ID¹⁶⁸](#), D. Price [ID¹⁰³](#), M. Primavera [ID^{71a}](#),
 L. Primomo [ID^{70a,70c}](#), M.A. Principe Martin [ID¹⁰¹](#), R. Privara [ID¹²⁵](#), T. Procter [ID⁶⁰](#), M.L. Proffitt [ID¹⁴²](#),
 N. Proklova [ID¹³¹](#), K. Prokofiev [ID^{65c}](#), G. Proto [ID¹¹²](#), J. Proudfoot [ID⁶](#), M. Przybycien [ID^{87a}](#),
 W.W. Przygoda [ID^{87b}](#), A. Psallidas [ID⁴⁷](#), J.E. Puddefoot [ID¹⁴³](#), D. Pudzha [ID⁵⁵](#), D. Pyatiizbyantseva [ID³⁸](#),
 J. Qian [ID¹⁰⁸](#), D. Qichen [ID¹⁰³](#), Y. Qin [ID¹³](#), T. Qiu [ID⁵³](#), A. Quadt [ID⁵⁶](#), M. Queitsch-Maitland [ID¹⁰³](#),
 G. Quetant [ID⁵⁷](#), R.P. Quinn [ID¹⁶⁷](#), G. Rabanal Bolanos [ID⁶²](#), D. Rafanoharana [ID⁵⁵](#), F. Raffaeli [ID^{77a,77b}](#),
 F. Ragusa [ID^{72a,72b}](#), J.L. Rainbolt [ID⁴⁰](#), J.A. Raine [ID⁵⁷](#), S. Rajagopalan [ID³⁰](#), E. Ramakoti [ID³⁸](#),
 L. Rambelli [ID^{58b,58a}](#), I.A. Ramirez-Berend [ID³⁵](#), K. Ran [ID^{49,114c}](#), D.S. Rankin [ID¹³¹](#), N.P. Rapheeha [ID^{34g}](#),
 H. Rasheed [ID^{28b}](#), V. Raskina [ID¹³⁰](#), D.F. Rassloff [ID^{64a}](#), A. Rastogi [ID^{18a}](#), S. Rave [ID¹⁰²](#), S. Ravera [ID^{58b,58a}](#),
 B. Ravina [ID⁵⁶](#), I. Ravinovich [ID¹⁷²](#), M. Raymond [ID³⁷](#), A.L. Read [ID¹²⁸](#), N.P. Readioff [ID¹⁴³](#),
 D.M. Rebuzzi [ID^{74a,74b}](#), G. Redlinger [ID³⁰](#), A.S. Reed [ID¹¹²](#), K. Reeves [ID²⁷](#), J.A. Reidelsturz [ID¹⁷⁴](#),
 D. Reikher [ID¹²⁶](#), A. Rej [ID⁵⁰](#), C. Rembser [ID³⁷](#), M. Renda [ID^{28b}](#), F. Renner [ID⁴⁹](#), A.G. Rennie [ID¹⁶²](#),
 A.L. Rescia [ID⁴⁹](#), S. Resconi [ID^{72a}](#), M. Ressegotti [ID^{58b,58a}](#), S. Rettie [ID³⁷](#), J.G. Reyes Rivera [ID¹⁰⁹](#),
 E. Reynolds [ID^{18a}](#), O.L. Rezanova [ID³⁸](#), P. Reznicek [ID¹³⁶](#), H. Riani [ID^{36d}](#), N. Ribaric [ID⁵²](#), E. Ricci [ID^{79a,79b}](#),
 R. Richter [ID¹¹²](#), S. Richter [ID^{48a,48b}](#), E. Richter-Was [ID^{87b}](#), M. Ridel [ID¹³⁰](#), S. Ridouani [ID^{36d}](#), P. Rieck [ID¹²⁰](#),
 P. Riedler [ID³⁷](#), E.M. Riefel [ID^{48a,48b}](#), J.O. Rieger [ID¹¹⁷](#), M. Rijssenbeek [ID¹⁴⁹](#), M. Rimoldi [ID³⁷](#),
 L. Rinaldi [ID^{24b,24a}](#), P. Rincke [ID^{56,164}](#), T.T. Rinn [ID³⁰](#), M.P. Rinnagel [ID¹¹¹](#), G. Ripellino [ID¹⁶⁴](#), I. Riu [ID¹³](#),
 J.C. Rivera Vergara [ID¹⁶⁸](#), F. Rizatdinova [ID¹²⁴](#), E. Rizvi [ID⁹⁶](#), B.R. Roberts [ID^{18a}](#), S.S. Roberts [ID¹³⁹](#),
 S.H. Robertson [ID^{106,y}](#), D. Robinson [ID³³](#), M. Robles Manzano [ID¹⁰²](#), A. Robson [ID⁶⁰](#), A. Rocchi [ID^{77a,77b}](#),
 C. Roda [ID^{75a,75b}](#), S. Rodriguez Bosca [ID³⁷](#), Y. Rodriguez Garcia [ID^{23a}](#), A. Rodriguez Rodriguez [ID⁵⁵](#),
 A.M. Rodríguez Vera [ID¹¹⁸](#), S. Roe [ID³⁷](#), J.T. Roemer [ID³⁷](#), A.R. Roepke-Gier [ID¹³⁹](#), O. Røhne [ID¹²⁸](#),
 R.A. Rojas [ID¹⁰⁵](#), C.P.A. Roland [ID¹³⁰](#), J. Roloff [ID³⁰](#), A. Romaniouk [ID⁸⁰](#), E. Romano [ID^{74a,74b}](#),
 M. Romano [ID^{24b}](#), A.C. Romero Hernandez [ID¹⁶⁵](#), N. Rompotis [ID⁹⁴](#), L. Roos [ID¹³⁰](#), S. Rosati [ID^{76a}](#),
 B.J. Rosser [ID⁴⁰](#), E. Rossi [ID¹²⁹](#), E. Rossi [ID^{73a,73b}](#), L.P. Rossi [ID⁶²](#), L. Rossini [ID⁵⁵](#), R. Rosten [ID¹²²](#),
 M. Rotaru [ID^{28b}](#), B. Rottler [ID⁵⁵](#), C. Rougier [ID⁹¹](#), D. Rousseau [ID⁶⁷](#), D. Rousso [ID⁴⁹](#), A. Roy [ID¹⁶⁵](#),
 S. Roy-Garand [ID¹⁵⁸](#), A. Rozanov [ID¹⁰⁴](#), Z.M.A. Rozario [ID⁶⁰](#), Y. Rozen [ID¹⁵⁴](#), A. Rubio Jimenez [ID¹⁶⁶](#),
 A.J. Ruby [ID⁹⁴](#), V.H. Ruelas Rivera [ID¹⁹](#), T.A. Ruggeri [ID¹](#), A. Ruggiero [ID¹²⁹](#), A. Ruiz-Martinez [ID¹⁶⁶](#),
 A. Rummler [ID³⁷](#), Z. Rurikova [ID⁵⁵](#), N.A. Rusakovich [ID³⁹](#), H.L. Russell [ID¹⁶⁸](#), G. Russo [ID^{76a,76b}](#),
 J.P. Rutherford [ID⁷](#), S. Rutherford Colmenares [ID³³](#), M. Rybar [ID¹³⁶](#), E.B. Rye [ID¹²⁸](#), A. Ryzhov [ID⁴⁵](#),
 J.A. Sabater Iglesias [ID⁵⁷](#), H.F.W. Sadrozinski [ID¹³⁹](#), F. Safai Tehrani [ID^{76a}](#), B. Safarzadeh Samani [ID¹³⁷](#),
 S. Saha [ID¹](#), M. Sahinsoy [ID⁸³](#), A. Saibel [ID¹⁶⁶](#), M. Saimpert [ID¹³⁸](#), M. Saito [ID¹⁵⁷](#), T. Saito [ID¹⁵⁷](#),
 A. Sala [ID^{72a,72b}](#), D. Salamani [ID³⁷](#), A. Salnikov [ID¹⁴⁷](#), J. Salt [ID¹⁶⁶](#), A. Salvador Salas [ID¹⁵⁵](#),
 D. Salvatore [ID^{44b,44a}](#), F. Salvatore [ID¹⁵⁰](#), A. Salzburger [ID³⁷](#), D. Sammel [ID⁵⁵](#), E. Sampson [ID⁹³](#),
 D. Sampsonidis [ID^{156,e}](#), D. Sampsonidou [ID¹²⁶](#), J. Sánchez [ID¹⁶⁶](#), V. Sanchez Sebastian [ID¹⁶⁶](#),
 H. Sandaker [ID¹²⁸](#), C.O. Sander [ID⁴⁹](#), J.A. Sandesara [ID¹⁰⁵](#), M. Sandhoff [ID¹⁷⁴](#), C. Sandoval [ID^{23b}](#),
 L. Sanfilippo [ID^{64a}](#), D.P.C. Sankey [ID¹³⁷](#), T. Sano [ID⁸⁹](#), A. Sansoni [ID⁵⁴](#), L. Santi [ID^{37,76b}](#), C. Santoni [ID⁴¹](#),
 H. Santos [ID^{133a,133b}](#), A. Santra [ID¹⁷²](#), E. Sanzani [ID^{24b,24a}](#), K.A. Saoucha [ID¹⁶³](#), J.G. Saraiva [ID^{133a,133d}](#),
 J. Sardain [ID⁷](#), O. Sasaki [ID⁸⁵](#), K. Sato [ID¹⁶⁰](#), C. Sauer [ID^{64b}](#), E. Sauvan [ID⁴](#), P. Savard [ID^{158,ae}](#), R. Sawada [ID¹⁵⁷](#),
 C. Sawyer [ID¹³⁷](#), L. Sawyer [ID⁹⁹](#), C. Sbarra [ID^{24b}](#), A. Sbrizzi [ID^{24b,24a}](#), T. Scanlon [ID⁹⁸](#),
 J. Schaarschmidt [ID¹⁴²](#), U. Schäfer [ID¹⁰²](#), A.C. Schaffer [ID^{67,45}](#), D. Schaile [ID¹¹¹](#), R.D. Schamberger [ID¹⁴⁹](#),
 C. Scharf [ID¹⁹](#), M.M. Schefer [ID²⁰](#), V.A. Schegelsky [ID³⁸](#), D. Scheirich [ID¹³⁶](#), M. Schernau [ID¹⁶²](#),

C. Scheulen [ID⁵⁶](#), C. Schiavi [ID^{58b,58a}](#), M. Schioppa [ID^{44b,44a}](#), B. Schlag [ID¹⁴⁷](#), S. Schlenker [ID³⁷](#),
 J. Schmeing [ID¹⁷⁴](#), M.A. Schmidt [ID¹⁷⁴](#), K. Schmieden [ID¹⁰²](#), C. Schmitt [ID¹⁰²](#), N. Schmitt [ID¹⁰²](#),
 S. Schmitt [ID⁴⁹](#), L. Schoeffel [ID¹³⁸](#), A. Schoening [ID^{64b}](#), P.G. Scholer [ID³⁵](#), E. Schopf [ID¹²⁹](#), M. Schott [ID²⁵](#),
 J. Schovancova [ID³⁷](#), S. Schramm [ID⁵⁷](#), T. Schroer [ID⁵⁷](#), H-C. Schultz-Coulon [ID^{64a}](#), M. Schumacher [ID⁵⁵](#),
 B.A. Schumm [ID¹³⁹](#), Ph. Schune [ID¹³⁸](#), A.J. Schuy [ID¹⁴²](#), H.R. Schwartz [ID¹³⁹](#), A. Schwartzman [ID¹⁴⁷](#),
 T.A. Schwarz [ID¹⁰⁸](#), Ph. Schwemling [ID¹³⁸](#), R. Schwienhorst [ID¹⁰⁹](#), F.G. Sciacca [ID²⁰](#), A. Sciandra [ID³⁰](#),
 G. Sciolla [ID²⁷](#), F. Scuri [ID^{75a}](#), C.D. Sebastiani [ID⁹⁴](#), K. Sedlaczek [ID¹¹⁸](#), S.C. Seidel [ID¹¹⁵](#), A. Seiden [ID¹³⁹](#),
 B.D. Seidlitz [ID⁴²](#), C. Seitz [ID⁴⁹](#), J.M. Seixas [ID^{84b}](#), G. Sekhniaidze [ID^{73a}](#), L. Selem [ID⁶¹](#),
 N. Semprini-Cesari [ID^{24b,24a}](#), D. Sengupta [ID⁵⁷](#), V. Senthilkumar [ID¹⁶⁶](#), L. Serin [ID⁶⁷](#), M. Sessa [ID^{77a,77b}](#),
 H. Severini [ID¹²³](#), F. Sforza [ID^{58b,58a}](#), A. Sfyrla [ID⁵⁷](#), Q. Sha [ID¹⁴](#), E. Shabalina [ID⁵⁶](#), A.H. Shah [ID³³](#),
 R. Shaheen [ID¹⁴⁸](#), J.D. Shahinian [ID¹³¹](#), D. Shaked Renous [ID¹⁷²](#), L.Y. Shan [ID¹⁴](#), M. Shapiro [ID^{18a}](#),
 A. Sharma [ID³⁷](#), A.S. Sharma [ID¹⁶⁷](#), P. Sharma [ID⁸¹](#), P.B. Shatalov [ID³⁸](#), K. Shaw [ID¹⁵⁰](#), S.M. Shaw [ID¹⁰³](#),
 Q. Shen [ID^{63c}](#), D.J. Sheppard [ID¹⁴⁶](#), P. Sherwood [ID⁹⁸](#), L. Shi [ID⁹⁸](#), X. Shi [ID¹⁴](#), S. Shimizu [ID⁸⁵](#),
 C.O. Shimmin [ID¹⁷⁵](#), J.D. Shinner [ID⁹⁷](#), I.P.J. Shipsey [ID^{129,*}](#), S. Shirabe [ID⁹⁰](#), M. Shiyakova [ID^{39,w}](#),
 M.J. Shochet [ID⁴⁰](#), D.R. Shope [ID¹²⁸](#), B. Shrestha [ID¹²³](#), S. Shrestha [ID^{122,ah}](#), I. Shreyber [ID³⁸](#),
 M.J. Shroff [ID¹⁶⁸](#), P. Sicho [ID¹³⁴](#), A.M. Sickles [ID¹⁶⁵](#), E. Sideras Haddad [ID^{34g}](#), A.C. Sidley [ID¹¹⁷](#),
 A. Sidoti [ID^{24b}](#), F. Siegert [ID⁵¹](#), Dj. Sijacki [ID¹⁶](#), F. Sili [ID⁹²](#), J.M. Silva [ID⁵³](#), I. Silva Ferreira [ID^{84b}](#),
 M.V. Silva Oliveira [ID³⁰](#), S.B. Silverstein [ID^{48a}](#), S. Simion [ID⁶⁷](#), R. Simoniello [ID³⁷](#), E.L. Simpson [ID¹⁰³](#),
 H. Simpson [ID¹⁵⁰](#), L.R. Simpson [ID¹⁰⁸](#), S. Simsek [ID⁸³](#), S. Sindhu [ID⁵⁶](#), P. Sinervo [ID¹⁵⁸](#), S. Singh [ID¹⁵⁸](#),
 S. Sinha [ID⁴⁹](#), S. Sinha [ID¹⁰³](#), M. Sioli [ID^{24b,24a}](#), I. Siral [ID³⁷](#), E. Sitnikova [ID⁴⁹](#), J. Sjölin [ID^{48a,48b}](#),
 A. Skaf [ID⁵⁶](#), E. Skorda [ID²¹](#), P. Skubic [ID¹²³](#), M. Slawinska [ID⁸⁸](#), V. Smakhtin [ID¹⁷²](#), B.H. Smart [ID¹³⁷](#),
 S.Yu. Smirnov [ID³⁸](#), Y. Smirnov [ID³⁸](#), L.N. Smirnova [ID^{38,a}](#), O. Smirnova [ID¹⁰⁰](#), A.C. Smith [ID⁴²](#),
 D.R. Smith [ID¹⁶²](#), E.A. Smith [ID⁴⁰](#), J.L. Smith [ID¹⁰³](#), R. Smith [ID¹⁴⁷](#), M. Smizanska [ID⁹³](#), K. Smolek [ID¹³⁵](#),
 A.A. Snesarev [ID³⁸](#), H.L. Snoek [ID¹¹⁷](#), S. Snyder [ID³⁰](#), R. Sobie [ID^{168,y}](#), A. Soffer [ID¹⁵⁵](#),
 C.A. Solans Sanchez [ID³⁷](#), E.Yu. Soldatov [ID³⁸](#), U. Soldevila [ID¹⁶⁶](#), A.A. Solodkov [ID³⁸](#), S. Solomon [ID²⁷](#),
 A. Soloshenko [ID³⁹](#), K. Solovieva [ID⁵⁵](#), O.V. Solovyanov [ID⁴¹](#), P. Sommer [ID⁵¹](#), A. Sonay [ID¹³](#),
 W.Y. Song [ID^{159b}](#), A. Sopczak [ID¹³⁵](#), A.L. Soppio [ID⁵³](#), F. Sopkova [ID^{29b}](#), J.D. Sorenson [ID¹¹⁵](#),
 I.R. Sotarriva Alvarez [ID¹⁴¹](#), V. Sothilingam [ID^{64a}](#), O.J. Soto Sandoval [ID^{140c,140b}](#), S. Sottocornola [ID⁶⁹](#),
 R. Soualah [ID¹⁶³](#), Z. Soumami [ID^{36e}](#), D. South [ID⁴⁹](#), N. Soybelman [ID¹⁷²](#), S. Spagnolo [ID^{71a,71b}](#),
 M. Spalla [ID¹¹²](#), D. Sperlich [ID⁵⁵](#), G. Spigo [ID³⁷](#), B. Spisso [ID^{73a,73b}](#), D.P. Spiteri [ID⁶⁰](#), M. Spousta [ID¹³⁶](#),
 E.J. Staats [ID³⁵](#), R. Stamen [ID^{64a}](#), A. Stampeki [ID²¹](#), E. Stanecka [ID⁸⁸](#), W. Stanek-Maslouska [ID⁴⁹](#),
 M.V. Stange [ID⁵¹](#), B. Stanislaus [ID^{18a}](#), M.M. Stanitzki [ID⁴⁹](#), B. Stapf [ID⁴⁹](#), E.A. Starchenko [ID³⁸](#),
 G.H. Stark [ID¹³⁹](#), J. Stark [ID⁹¹](#), P. Staroba [ID¹³⁴](#), P. Starovoitov [ID^{64a}](#), S. Stärz [ID¹⁰⁶](#), R. Staszewski [ID⁸⁸](#),
 G. Stavropoulos [ID⁴⁷](#), A. Stefl [ID³⁷](#), P. Steinberg [ID³⁰](#), B. Stelzer [ID^{146,159a}](#), H.J. Stelzer [ID¹³²](#),
 O. Stelzer-Chilton [ID^{159a}](#), H. Stenzel [ID⁵⁹](#), T.J. Stevenson [ID¹⁵⁰](#), G.A. Stewart [ID³⁷](#), J.R. Stewart [ID¹²⁴](#),
 M.C. Stockton [ID³⁷](#), G. Stoicea [ID^{28b}](#), M. Stolarski [ID^{133a}](#), S. Stonjek [ID¹¹²](#), A. Straessner [ID⁵¹](#),
 J. Strandberg [ID¹⁴⁸](#), S. Strandberg [ID^{48a,48b}](#), M. Stratmann [ID¹⁷⁴](#), M. Strauss [ID¹²³](#), T. Strebler [ID¹⁰⁴](#),
 P. Strizenec [ID^{29b}](#), R. Ströhmer [ID¹⁶⁹](#), D.M. Strom [ID¹²⁶](#), R. Stroynowski [ID⁴⁵](#), A. Strubig [ID^{48a,48b}](#),
 S.A. Stucci [ID³⁰](#), B. Stugu [ID¹⁷](#), J. Stupak [ID¹²³](#), N.A. Styles [ID⁴⁹](#), D. Su [ID¹⁴⁷](#), S. Su [ID^{63a}](#), W. Su [ID^{63d}](#),
 X. Su [ID^{63a}](#), D. Suchy [ID^{29a}](#), K. Sugizaki [ID¹⁵⁷](#), V.V. Sulin [ID³⁸](#), M.J. Sullivan [ID⁹⁴](#), D.M.S. Sultan [ID¹²⁹](#),
 L. Sultaniyeva [ID³⁸](#), S. Sultansoy [ID^{3b}](#), T. Sumida [ID⁸⁹](#), S. Sun [ID¹⁷³](#), O. Sunneborn Gudnadottir [ID¹⁶⁴](#),
 N. Sur [ID¹⁰⁴](#), M.R. Sutton [ID¹⁵⁰](#), H. Suzuki [ID¹⁶⁰](#), M. Svatos [ID¹³⁴](#), M. Swiatlowski [ID^{159a}](#), T. Swirski [ID¹⁶⁹](#),
 I. Sykora [ID^{29a}](#), M. Sykora [ID¹³⁶](#), T. Sykora [ID¹³⁶](#), D. Ta [ID¹⁰²](#), K. Tackmann [ID^{49,v}](#), A. Taffard [ID¹⁶²](#),
 R. Tafirout [ID^{159a}](#), J.S. Tafoya Vargas [ID⁶⁷](#), Y. Takubo [ID⁸⁵](#), M. Talby [ID¹⁰⁴](#), A.A. Talyshev [ID³⁸](#),
 K.C. Tam [ID^{65b}](#), N.M. Tamir [ID¹⁵⁵](#), A. Tanaka [ID¹⁵⁷](#), J. Tanaka [ID¹⁵⁷](#), R. Tanaka [ID⁶⁷](#), M. Tanasini [ID¹⁴⁹](#),
 Z. Tao [ID¹⁶⁷](#), S. Tapia Araya [ID^{140f}](#), S. Tapprogge [ID¹⁰²](#), A. Tarek Abouelfadl Mohamed [ID¹⁰⁹](#),
 S. Tarem [ID¹⁵⁴](#), K. Tariq [ID¹⁴](#), G. Tarna [ID^{28b}](#), G.F. Tartarelli [ID^{72a}](#), M.J. Tartarin [ID⁹¹](#), P. Tas [ID¹³⁶](#),

M. Tasevsky ¹³⁴, E. Tassi ^{44b,44a}, A.C. Tate ¹⁶⁵, G. Tateno ¹⁵⁷, Y. Tayalati ^{36e,x}, G.N. Taylor ¹⁰⁷,
W. Taylor ^{159b}, R. Teixeira De Lima ¹⁴⁷, P. Teixeira-Dias ⁹⁷, J.J. Teoh ¹⁵⁸, K. Terashi ¹⁵⁷,
J. Terron ¹⁰¹, S. Terzo ¹³, M. Testa ⁵⁴, R.J. Teuscher ^{158,y}, A. Thaler ⁸⁰, O. Theiner ⁵⁷,
T. Thevenaux-Pelzer ¹⁰⁴, O. Thielmann ¹⁷⁴, D.W. Thomas ⁹⁷, J.P. Thomas ²¹, E.A. Thompson ^{18a},
P.D. Thompson ²¹, E. Thomson ¹³¹, R.E. Thornberry ⁴⁵, C. Tian ^{63a}, Y. Tian ⁵⁷,
V. Tikhomirov ^{38,a}, Yu.A. Tikhonov ³⁸, S. Timoshenko ³⁸, D. Timoshyn ¹³⁶, E.X.L. Ting ¹,
P. Tipton ¹⁷⁵, A. Tishelman-Charny ³⁰, S.H. Tlou ^{34g}, K. Todome ¹⁴¹, S. Todorova-Nova ¹³⁶,
S. Todt ⁵¹, L. Toffolin ^{70a,70c}, M. Togawa ⁸⁵, J. Tojo ⁹⁰, S. Tokár ^{29a}, K. Tokushuku ⁸⁵,
O. Toldaiev ⁶⁹, M. Tomoto ^{85,113}, L. Tompkins ^{147,m}, K.W. Topolnicki ^{87b}, E. Torrence ¹²⁶,
H. Torres ⁹¹, E. Torró Pastor ¹⁶⁶, M. Toscani ³¹, C. Toscirci ⁴⁰, M. Tost ¹¹, D.R. Tovey ¹⁴³,
I.S. Trandafir ^{28b}, T. Trefzger ¹⁶⁹, A. Tricoli ³⁰, I.M. Trigger ^{159a}, S. Trincaz-Duvoid ¹³⁰,
D.A. Trischuk ²⁷, B. Trocmé ⁶¹, A. Tropina ³⁹, L. Truong ^{34c}, M. Trzebinski ⁸⁸, A. Trzupiek ⁸⁸,
F. Tsai ¹⁴⁹, M. Tsai ¹⁰⁸, A. Tsiamis ¹⁵⁶, P.V. Tsiarehshka ³⁸, S. Tsigaridas ^{159a}, A. Tsirigotis ^{156,s},
V. Tsiskaridze ¹⁵⁸, E.G. Tskhadadze ^{153a}, M. Tsopoulou ¹⁵⁶, Y. Tsujikawa ⁸⁹, I.I. Tsukerman ³⁸,
V. Tsulaia ^{18a}, S. Tsuno ⁸⁵, K. Tsuri ¹²¹, D. Tsybychev ¹⁴⁹, Y. Tu ^{65b}, A. Tudorache ^{28b},
V. Tudorache ^{28b}, A.N. Tuna ⁶², S. Turchikhin ^{58b,58a}, I. Turk Cakir ^{3a}, R. Turra ^{72a},
T. Turtuvshin ³⁹, P.M. Tuts ⁴², S. Tzamarias ^{156,e}, E. Tzovara ¹⁰², F. Ukegawa ¹⁶⁰,
P.A. Ulloa Poblete ^{140c,140b}, E.N. Umaka ³⁰, G. Unal ³⁷, A. Undrus ³⁰, G. Unel ¹⁶², J. Urban ^{29b},
P. Urrejola ^{140a}, G. Usai ⁸, R. Ushioda ¹⁴¹, M. Usman ¹¹⁰, F. Ustuner ⁵³, Z. Uysal ⁸³,
V. Vacek ¹³⁵, B. Vachon ¹⁰⁶, T. Vafeiadis ³⁷, A. Vaitkus ⁹⁸, C. Valderanis ¹¹¹,
E. Valdes Santurio ^{48a,48b}, M. Valente ^{159a}, S. Valentinetti ^{24b,24a}, A. Valero ¹⁶⁶,
E. Valiente Moreno ¹⁶⁶, A. Vallier ⁹¹, J.A. Valls Ferrer ¹⁶⁶, D.R. Van Arneman ¹¹⁷,
T.R. Van Daalen ¹⁴², A. Van Der Graaf ⁵⁰, P. Van Gemmeren ⁶, M. Van Rijnbach ³⁷,
S. Van Stroud ⁹⁸, I. Van Vulpen ¹¹⁷, P. Vana ¹³⁶, M. Vanadia ^{77a,77b}, U.M. Vande Voorde ¹⁴⁸,
W. Vandelli ³⁷, E.R. Vandewall ¹²⁴, D. Vannicola ¹⁵⁵, L. Vannoli ⁵⁴, R. Vari ^{76a}, E.W. Varnes ⁷,
C. Varni ^{18b}, T. Varol ¹⁵², D. Varouchas ⁶⁷, L. Varriale ¹⁶⁶, K.E. Varvell ¹⁵¹, M.E. Vasile ^{28b},
L. Vaslin ⁸⁵, G.A. Vasquez ¹⁶⁸, A. Vasyukov ³⁹, L.M. Vaughan ¹²⁴, R. Vavricka ¹⁰²,
T. Vazquez Schroeder ³⁷, J. Veatch ³², V. Vecchio ¹⁰³, M.J. Veen ¹⁰⁵, I. Veliscek ³⁰,
L.M. Veloce ¹⁵⁸, F. Veloso ^{133a,133c}, S. Veneziano ^{76a}, A. Ventura ^{71a,71b}, S. Ventura Gonzalez ¹³⁸,
A. Verbytskyi ¹¹², M. Verducci ^{75a,75b}, C. Vergis ⁹⁶, M. Verissimo De Araujo ^{84b},
W. Verkerke ¹¹⁷, J.C. Vermeulen ¹¹⁷, C. Vernieri ¹⁴⁷, M. Vessella ¹⁰⁵, M.C. Vetterli ^{146,ae},
A. Vgenopoulos ¹⁰², N. Viaux Maira ^{140f}, T. Vickey ¹⁴³, O.E. Vickey Boeriu ¹⁴³,
G.H.A. Viehhauser ¹²⁹, L. Vigani ^{64b}, M. Vigl ¹¹², M. Villa ^{24b,24a}, M. Villaplana Perez ¹⁶⁶,
E.M. Villhauer ⁵³, E. Vilucchi ⁵⁴, M.G. Vincter ³⁵, A. Visibile ¹¹⁷, C. Vittori ³⁷, I. Vivarelli ^{24b,24a},
E. Voevodina ¹¹², F. Vogel ¹¹¹, J.C. Voigt ⁵¹, P. Vokac ¹³⁵, Yu. Volkotrub ^{87b}, E. Von Toerne ²⁵,
B. Vormwald ³⁷, V. Vorobel ¹³⁶, K. Vorobev ³⁸, M. Vos ¹⁶⁶, K. Voss ¹⁴⁵, M. Vozak ¹¹⁷,
L. Vozdecky ¹²³, N. Vranjes ¹⁶, M. Vranjes Milosavljevic ¹⁶, M. Vreeswijk ¹¹⁷, N.K. Vu ^{63d,63c},
R. Vuillermet ³⁷, O. Vujinovic ¹⁰², I. Vukotic ⁴⁰, I.K. Vyas ³⁵, S. Wada ¹⁶⁰, C. Wagner ¹⁴⁷,
J.M. Wagner ^{18a}, W. Wagner ¹⁷⁴, S. Wahdan ¹⁷⁴, H. Wahlberg ⁹², J. Walder ¹³⁷, R. Walker ¹¹¹,
W. Walkowiak ¹⁴⁵, A. Wall ¹³¹, E.J. Wallin ¹⁰⁰, T. Wamorkar ⁶, A.Z. Wang ¹³⁹, C. Wang ¹⁰²,
C. Wang ¹¹, H. Wang ^{18a}, J. Wang ^{65c}, P. Wang ⁹⁸, R. Wang ⁶², R. Wang ⁶, S.M. Wang ¹⁵²,
S. Wang ^{63b}, S. Wang ¹⁴, T. Wang ^{63a}, W.T. Wang ⁸¹, W. Wang ¹⁴, X. Wang ^{114a}, X. Wang ¹⁶⁵,
X. Wang ^{63c}, Y. Wang ^{63d}, Y. Wang ^{114a}, Y. Wang ^{63a}, Z. Wang ¹⁰⁸, Z. Wang ^{63d,52,63c},
Z. Wang ¹⁰⁸, A. Warburton ¹⁰⁶, R.J. Ward ²¹, N. Warrack ⁶⁰, S. Waterhouse ⁹⁷, A.T. Watson ²¹,
H. Watson ⁵³, M.F. Watson ²¹, E. Watton ^{60,137}, G. Watts ¹⁴², B.M. Waugh ⁹⁸, J.M. Webb ⁵⁵,
C. Weber ³⁰, H.A. Weber ¹⁹, M.S. Weber ²⁰, S.M. Weber ^{64a}, C. Wei ^{63a}, Y. Wei ⁵⁵,
A.R. Weidberg ¹²⁹, E.J. Weik ¹²⁰, J. Weingarten ⁵⁰, C. Weiser ⁵⁵, C.J. Wells ⁴⁹, T. Wenaus ³⁰,

B. Wendland ^{id50}, T. Wengler ^{id37}, N.S. Wenke¹¹², N. Wermes ^{id25}, M. Wessels ^{id64a}, A.M. Wharton ^{id93}, A.S. White ^{id62}, A. White ^{id8}, M.J. White ^{id1}, D. Whiteson ^{id162}, L. Wickremasinghe ^{id127}, W. Wiedenmann ^{id173}, M. Wielers ^{id137}, C. Wiglesworth ^{id43}, D.J. Wilbern¹²³, H.G. Wilkens ^{id37}, J.J.H. Wilkinson ^{id33}, D.M. Williams ^{id42}, H.H. Williams¹³¹, S. Williams ^{id33}, S. Willocq ^{id105}, B.J. Wilson ^{id103}, P.J. Windischhofer ^{id40}, F.I. Winkel ^{id31}, F. Winklmeier ^{id126}, B.T. Winter ^{id55}, J.K. Winter ^{id103}, M. Wittgen¹⁴⁷, M. Wobisch ^{id99}, T. Wojtkowski⁶¹, Z. Wolffs ^{id117}, J. Wollrath¹⁶², M.W. Wolter ^{id88}, H. Wolters ^{id133a,133c}, M.C. Wong¹³⁹, E.L. Woodward ^{id42}, S.D. Worm ^{id49}, B.K. Wosiek ^{id88}, K.W. Woźniak ^{id88}, S. Wozniowski ^{id56}, K. Wraight ^{id60}, C. Wu ^{id21}, M. Wu ^{id114b}, M. Wu ^{id116}, S.L. Wu ^{id173}, X. Wu ^{id57}, Y. Wu ^{id63a}, Z. Wu ^{id4}, J. Wuerzinger ^{id112,ac}, T.R. Wyatt ^{id103}, B.M. Wynne ^{id53}, S. Xella ^{id43}, L. Xia ^{id114a}, M. Xia ^{id15}, M. Xie ^{id63a}, S. Xin ^{id14,114c}, A. Xiong ^{id126}, J. Xiong ^{id18a}, D. Xu ^{id14}, H. Xu ^{id63a}, L. Xu ^{id63a}, R. Xu ^{id131}, T. Xu ^{id108}, Y. Xu ^{id15}, Z. Xu ^{id53}, Z. Xu^{114a}, B. Yabsley ^{id151}, S. Yacoub ^{id34a}, Y. Yamaguchi ^{id85}, E. Yamashita ^{id157}, H. Yamauchi ^{id160}, T. Yamazaki ^{id18a}, Y. Yamazaki ^{id86}, S. Yan ^{id60}, Z. Yan ^{id105}, H.J. Yang ^{id63c,63d}, H.T. Yang ^{id63a}, S. Yang ^{id63a}, T. Yang ^{id65c}, X. Yang ^{id37}, X. Yang ^{id14}, Y. Yang ^{id45}, Y. Yang^{63a}, Z. Yang ^{id63a}, W-M. Yao ^{id18a}, H. Ye ^{id114a}, H. Ye ^{id56}, J. Ye ^{id14}, S. Ye ^{id30}, X. Ye ^{id63a}, Y. Yeh ^{id98}, I. Yeletsikh ^{id39}, B. Yeo ^{id18b}, M.R. Yexley ^{id98}, T.P. Yildirim ^{id129}, P. Yin ^{id42}, K. Yorita ^{id171}, S. Younas ^{id28b}, C.J.S. Young ^{id37}, C. Young ^{id147}, C. Yu ^{id14,114c}, Y. Yu ^{id63a}, J. Yuan ^{id14,114c}, M. Yuan ^{id108}, R. Yuan ^{id63d,63c}, L. Yue ^{id98}, M. Zaazoua ^{id63a}, B. Zabinski ^{id88}, E. Zaid⁵³, Z.K. Zak ^{id88}, T. Zakareishvili ^{id166}, S. Zambito ^{id57}, J.A. Zamora Saa ^{id140d,140b}, J. Zang ^{id157}, D. Zanzi ^{id55}, O. Zaplatilek ^{id135}, C. Zeitnitz ^{id174}, H. Zeng ^{id14}, J.C. Zeng ^{id165}, D.T. Zenger Jr ^{id27}, O. Zenin ^{id38}, T. Ženiš ^{id29a}, S. Zenz ^{id96}, S. Zerradi ^{id36a}, D. Zerwas ^{id67}, M. Zhai ^{id14,114c}, D.F. Zhang ^{id143}, J. Zhang ^{id63b}, J. Zhang ^{id6}, K. Zhang ^{id14,114c}, L. Zhang ^{id63a}, L. Zhang ^{id114a}, P. Zhang ^{id14,114c}, R. Zhang ^{id173}, S. Zhang ^{id108}, S. Zhang ^{id91}, T. Zhang ^{id157}, X. Zhang ^{id63c}, X. Zhang ^{id63b}, Y. Zhang ^{id63c}, Y. Zhang ^{id98}, Y. Zhang ^{id114a}, Z. Zhang ^{id18a}, Z. Zhang ^{id63b}, Z. Zhang ^{id67}, H. Zhao ^{id142}, T. Zhao ^{id63b}, Y. Zhao ^{id139}, Z. Zhao ^{id63a}, Z. Zhao ^{id63a}, A. Zhemchugov ^{id39}, J. Zheng ^{id114a}, K. Zheng ^{id165}, X. Zheng ^{id63a}, Z. Zheng ^{id147}, D. Zhong ^{id165}, B. Zhou ^{id108}, H. Zhou ^{id7}, N. Zhou ^{id63c}, Y. Zhou ^{id15}, Y. Zhou ^{id114a}, Y. Zhou⁷, C.G. Zhu ^{id63b}, J. Zhu ^{id108}, X. Zhu^{63d}, Y. Zhu ^{id63c}, Y. Zhu ^{id63a}, X. Zhuang ^{id14}, K. Zhukov ^{id69}, N.I. Zimine ^{id39}, J. Zinsser ^{id64b}, M. Ziolkowski ^{id145}, L. Živković ^{id16}, A. Zoccoli ^{id24b,24a}, K. Zoch ^{id62}, T.G. Zorbas ^{id143}, O. Zormpa ^{id47}, W. Zou ^{id42}, L. Zwalinski ^{id37}.

¹Department of Physics, University of Adelaide, Adelaide; Australia.

²Department of Physics, University of Alberta, Edmonton AB; Canada.

³(^a)Department of Physics, Ankara University, Ankara;(b)Division of Physics, TOBB University of Economics and Technology, Ankara; Türkiye.

⁴LAPP, Université Savoie Mont Blanc, CNRS/IN2P3, Annecy; France.

⁵APC, Université Paris Cité, CNRS/IN2P3, Paris; France.

⁶High Energy Physics Division, Argonne National Laboratory, Argonne IL; United States of America.

⁷Department of Physics, University of Arizona, Tucson AZ; United States of America.

⁸Department of Physics, University of Texas at Arlington, Arlington TX; United States of America.

⁹Physics Department, National and Kapodistrian University of Athens, Athens; Greece.

¹⁰Physics Department, National Technical University of Athens, Zografou; Greece.

¹¹Department of Physics, University of Texas at Austin, Austin TX; United States of America.

¹²Institute of Physics, Azerbaijan Academy of Sciences, Baku; Azerbaijan.

¹³Institut de Física d'Altes Energies (IFAE), Barcelona Institute of Science and Technology, Barcelona; Spain.

¹⁴Institute of High Energy Physics, Chinese Academy of Sciences, Beijing; China.

- ¹⁵Physics Department, Tsinghua University, Beijing; China.
- ¹⁶Institute of Physics, University of Belgrade, Belgrade; Serbia.
- ¹⁷Department for Physics and Technology, University of Bergen, Bergen; Norway.
- ¹⁸(^a)Physics Division, Lawrence Berkeley National Laboratory, Berkeley CA; (^b)University of California, Berkeley CA; United States of America.
- ¹⁹Institut für Physik, Humboldt Universität zu Berlin, Berlin; Germany.
- ²⁰Albert Einstein Center for Fundamental Physics and Laboratory for High Energy Physics, University of Bern, Bern; Switzerland.
- ²¹School of Physics and Astronomy, University of Birmingham, Birmingham; United Kingdom.
- ²²(^a)Department of Physics, Bogazici University, Istanbul; (^b)Department of Physics Engineering, Gaziantep University, Gaziantep; (^c)Department of Physics, Istanbul University, Istanbul; Türkiye.
- ²³(^a)Facultad de Ciencias y Centro de Investigaciones, Universidad Antonio Nariño, Bogotá; (^b)Departamento de Física, Universidad Nacional de Colombia, Bogotá; Colombia.
- ²⁴(^a)Dipartimento di Fisica e Astronomia A. Righi, Università di Bologna, Bologna; (^b)INFN Sezione di Bologna; Italy.
- ²⁵Physikalisches Institut, Universität Bonn, Bonn; Germany.
- ²⁶Department of Physics, Boston University, Boston MA; United States of America.
- ²⁷Department of Physics, Brandeis University, Waltham MA; United States of America.
- ²⁸(^a)Transilvania University of Brasov, Brasov; (^b)Horia Hulubei National Institute of Physics and Nuclear Engineering, Bucharest; (^c)Department of Physics, Alexandru Ioan Cuza University of Iasi, Iasi; (^d)National Institute for Research and Development of Isotopic and Molecular Technologies, Physics Department, Cluj-Napoca; (^e)National University of Science and Technology Politehnica, Bucharest; (^f)West University in Timisoara, Timisoara; (^g)Faculty of Physics, University of Bucharest, Bucharest; Romania.
- ²⁹(^a)Faculty of Mathematics, Physics and Informatics, Comenius University, Bratislava; (^b)Department of Subnuclear Physics, Institute of Experimental Physics of the Slovak Academy of Sciences, Kosice; Slovak Republic.
- ³⁰Physics Department, Brookhaven National Laboratory, Upton NY; United States of America.
- ³¹Universidad de Buenos Aires, Facultad de Ciencias Exactas y Naturales, Departamento de Física, y CONICET, Instituto de Física de Buenos Aires (IFIBA), Buenos Aires; Argentina.
- ³²California State University, CA; United States of America.
- ³³Cavendish Laboratory, University of Cambridge, Cambridge; United Kingdom.
- ³⁴(^a)Department of Physics, University of Cape Town, Cape Town; (^b)iThemba Labs, Western Cape; (^c)Department of Mechanical Engineering Science, University of Johannesburg, Johannesburg; (^d)National Institute of Physics, University of the Philippines Diliman (Philippines); (^e)University of South Africa, Department of Physics, Pretoria; (^f)University of Zululand, KwaDlangezwa; (^g)School of Physics, University of the Witwatersrand, Johannesburg; South Africa.
- ³⁵Department of Physics, Carleton University, Ottawa ON; Canada.
- ³⁶(^a)Faculté des Sciences Ain Chock, Université Hassan II de Casablanca; (^b)Faculté des Sciences, Université Ibn-Tofail, Kénitra; (^c)Faculté des Sciences Semlalia, Université Cadi Ayyad, LPHEA-Marrakech; (^d)LPMR, Faculté des Sciences, Université Mohamed Premier, Oujda; (^e)Faculté des sciences, Université Mohammed V, Rabat; (^f)Institute of Applied Physics, Mohammed VI Polytechnic University, Ben Guerir; Morocco.
- ³⁷CERN, Geneva; Switzerland.
- ³⁸Affiliated with an institute covered by a cooperation agreement with CERN.
- ³⁹Affiliated with an international laboratory covered by a cooperation agreement with CERN.
- ⁴⁰Enrico Fermi Institute, University of Chicago, Chicago IL; United States of America.
- ⁴¹LPC, Université Clermont Auvergne, CNRS/IN2P3, Clermont-Ferrand; France.

- ⁴²Nevis Laboratory, Columbia University, Irvington NY; United States of America.
- ⁴³Niels Bohr Institute, University of Copenhagen, Copenhagen; Denmark.
- ⁴⁴(^a)Dipartimento di Fisica, Università della Calabria, Rende;(^b)INFN Gruppo Collegato di Cosenza, Laboratori Nazionali di Frascati; Italy.
- ⁴⁵Physics Department, Southern Methodist University, Dallas TX; United States of America.
- ⁴⁶Physics Department, University of Texas at Dallas, Richardson TX; United States of America.
- ⁴⁷National Centre for Scientific Research "Demokritos", Agia Paraskevi; Greece.
- ⁴⁸(^a)Department of Physics, Stockholm University;(^b)Oskar Klein Centre, Stockholm; Sweden.
- ⁴⁹Deutsches Elektronen-Synchrotron DESY, Hamburg and Zeuthen; Germany.
- ⁵⁰Fakultät Physik , Technische Universität Dortmund, Dortmund; Germany.
- ⁵¹Institut für Kern- und Teilchenphysik, Technische Universität Dresden, Dresden; Germany.
- ⁵²Department of Physics, Duke University, Durham NC; United States of America.
- ⁵³SUPA - School of Physics and Astronomy, University of Edinburgh, Edinburgh; United Kingdom.
- ⁵⁴INFN e Laboratori Nazionali di Frascati, Frascati; Italy.
- ⁵⁵Physikalisches Institut, Albert-Ludwigs-Universität Freiburg, Freiburg; Germany.
- ⁵⁶II. Physikalisches Institut, Georg-August-Universität Göttingen, Göttingen; Germany.
- ⁵⁷Département de Physique Nucléaire et Corpusculaire, Université de Genève, Genève; Switzerland.
- ⁵⁸(^a)Dipartimento di Fisica, Università di Genova, Genova;(^b)INFN Sezione di Genova; Italy.
- ⁵⁹II. Physikalisches Institut, Justus-Liebig-Universität Giessen, Giessen; Germany.
- ⁶⁰SUPA - School of Physics and Astronomy, University of Glasgow, Glasgow; United Kingdom.
- ⁶¹LPSC, Université Grenoble Alpes, CNRS/IN2P3, Grenoble INP, Grenoble; France.
- ⁶²Laboratory for Particle Physics and Cosmology, Harvard University, Cambridge MA; United States of America.
- ⁶³(^a)Department of Modern Physics and State Key Laboratory of Particle Detection and Electronics, University of Science and Technology of China, Hefei;(^b)Institute of Frontier and Interdisciplinary Science and Key Laboratory of Particle Physics and Particle Irradiation (MOE), Shandong University, Qingdao;(^c)School of Physics and Astronomy, Shanghai Jiao Tong University, Key Laboratory for Particle Astrophysics and Cosmology (MOE), SKLPPC, Shanghai;(^d)Tsung-Dao Lee Institute, Shanghai;(^e)School of Physics, Zhengzhou University; China.
- ⁶⁴(^a)Kirchhoff-Institut für Physik, Ruprecht-Karls-Universität Heidelberg, Heidelberg;(^b)Physikalisches Institut, Ruprecht-Karls-Universität Heidelberg, Heidelberg; Germany.
- ⁶⁵(^a)Department of Physics, Chinese University of Hong Kong, Shatin, N.T., Hong Kong;(^b)Department of Physics, University of Hong Kong, Hong Kong;(^c)Department of Physics and Institute for Advanced Study, Hong Kong University of Science and Technology, Clear Water Bay, Kowloon, Hong Kong; China.
- ⁶⁶Department of Physics, National Tsing Hua University, Hsinchu; Taiwan.
- ⁶⁷IJCLab, Université Paris-Saclay, CNRS/IN2P3, 91405, Orsay; France.
- ⁶⁸Centro Nacional de Microelectrónica (IMB-CNM-CSIC), Barcelona; Spain.
- ⁶⁹Department of Physics, Indiana University, Bloomington IN; United States of America.
- ⁷⁰(^a)INFN Gruppo Collegato di Udine, Sezione di Trieste, Udine;(^b)ICTP, Trieste;(^c)Dipartimento Politecnico di Ingegneria e Architettura, Università di Udine, Udine; Italy.
- ⁷¹(^a)INFN Sezione di Lecce;(^b)Dipartimento di Matematica e Fisica, Università del Salento, Lecce; Italy.
- ⁷²(^a)INFN Sezione di Milano;(^b)Dipartimento di Fisica, Università di Milano, Milano; Italy.
- ⁷³(^a)INFN Sezione di Napoli;(^b)Dipartimento di Fisica, Università di Napoli, Napoli; Italy.
- ⁷⁴(^a)INFN Sezione di Pavia;(^b)Dipartimento di Fisica, Università di Pavia, Pavia; Italy.
- ⁷⁵(^a)INFN Sezione di Pisa;(^b)Dipartimento di Fisica E. Fermi, Università di Pisa, Pisa; Italy.
- ⁷⁶(^a)INFN Sezione di Roma;(^b)Dipartimento di Fisica, Sapienza Università di Roma, Roma; Italy.
- ⁷⁷(^a)INFN Sezione di Roma Tor Vergata;(^b)Dipartimento di Fisica, Università di Roma Tor Vergata,

Roma; Italy.

^{78(a)}INFN Sezione di Roma Tre; ^(b)Dipartimento di Matematica e Fisica, Università Roma Tre, Roma; Italy.

^{79(a)}INFN-TIFPA; ^(b)Università degli Studi di Trento, Trento; Italy.

⁸⁰Universität Innsbruck, Department of Astro and Particle Physics, Innsbruck; Austria.

⁸¹University of Iowa, Iowa City IA; United States of America.

⁸²Department of Physics and Astronomy, Iowa State University, Ames IA; United States of America.

⁸³Istinye University, Sariyer, Istanbul; Türkiye.

^{84(a)}Departamento de Engenharia Elétrica, Universidade Federal de Juiz de Fora (UFJF), Juiz de Fora; ^(b)Universidade Federal do Rio De Janeiro COPPE/EE/IF, Rio de Janeiro; ^(c)Instituto de Física, Universidade de São Paulo, São Paulo; ^(d)Rio de Janeiro State University, Rio de Janeiro; ^(e)Federal University of Bahia, Bahia; Brazil.

⁸⁵KEK, High Energy Accelerator Research Organization, Tsukuba; Japan.

⁸⁶Graduate School of Science, Kobe University, Kobe; Japan.

^{87(a)}AGH University of Krakow, Faculty of Physics and Applied Computer Science, Krakow; ^(b)Marian Smoluchowski Institute of Physics, Jagiellonian University, Krakow; Poland.

⁸⁸Institute of Nuclear Physics Polish Academy of Sciences, Krakow; Poland.

⁸⁹Faculty of Science, Kyoto University, Kyoto; Japan.

⁹⁰Research Center for Advanced Particle Physics and Department of Physics, Kyushu University, Fukuoka ; Japan.

⁹¹L2IT, Université de Toulouse, CNRS/IN2P3, UPS, Toulouse; France.

⁹²Instituto de Física La Plata, Universidad Nacional de La Plata and CONICET, La Plata; Argentina.

⁹³Physics Department, Lancaster University, Lancaster; United Kingdom.

⁹⁴Oliver Lodge Laboratory, University of Liverpool, Liverpool; United Kingdom.

⁹⁵Department of Experimental Particle Physics, Jožef Stefan Institute and Department of Physics, University of Ljubljana, Ljubljana; Slovenia.

⁹⁶School of Physics and Astronomy, Queen Mary University of London, London; United Kingdom.

⁹⁷Department of Physics, Royal Holloway University of London, Egham; United Kingdom.

⁹⁸Department of Physics and Astronomy, University College London, London; United Kingdom.

⁹⁹Louisiana Tech University, Ruston LA; United States of America.

¹⁰⁰Fysiska institutionen, Lunds universitet, Lund; Sweden.

¹⁰¹Departamento de Física Teórica C-15 and CIAFF, Universidad Autónoma de Madrid, Madrid; Spain.

¹⁰²Institut für Physik, Universität Mainz, Mainz; Germany.

¹⁰³School of Physics and Astronomy, University of Manchester, Manchester; United Kingdom.

¹⁰⁴CPPM, Aix-Marseille Université, CNRS/IN2P3, Marseille; France.

¹⁰⁵Department of Physics, University of Massachusetts, Amherst MA; United States of America.

¹⁰⁶Department of Physics, McGill University, Montreal QC; Canada.

¹⁰⁷School of Physics, University of Melbourne, Victoria; Australia.

¹⁰⁸Department of Physics, University of Michigan, Ann Arbor MI; United States of America.

¹⁰⁹Department of Physics and Astronomy, Michigan State University, East Lansing MI; United States of America.

¹¹⁰Group of Particle Physics, University of Montreal, Montreal QC; Canada.

¹¹¹Fakultät für Physik, Ludwig-Maximilians-Universität München, München; Germany.

¹¹²Max-Planck-Institut für Physik (Werner-Heisenberg-Institut), München; Germany.

¹¹³Graduate School of Science and Kobayashi-Maskawa Institute, Nagoya University, Nagoya; Japan.

^{114(a)}Department of Physics, Nanjing University, Nanjing; ^(b)School of Science, Shenzhen Campus of Sun Yat-sen University; ^(c)University of Chinese Academy of Science (UCAS), Beijing; China.

- ¹¹⁵Department of Physics and Astronomy, University of New Mexico, Albuquerque NM; United States of America.
- ¹¹⁶Institute for Mathematics, Astrophysics and Particle Physics, Radboud University/Nikhef, Nijmegen; Netherlands.
- ¹¹⁷Nikhef National Institute for Subatomic Physics and University of Amsterdam, Amsterdam; Netherlands.
- ¹¹⁸Department of Physics, Northern Illinois University, DeKalb IL; United States of America.
- ¹¹⁹^(a)New York University Abu Dhabi, Abu Dhabi;^(b)United Arab Emirates University, Al Ain; United Arab Emirates.
- ¹²⁰Department of Physics, New York University, New York NY; United States of America.
- ¹²¹Ochanomizu University, Otsuka, Bunkyo-ku, Tokyo; Japan.
- ¹²²Ohio State University, Columbus OH; United States of America.
- ¹²³Homer L. Dodge Department of Physics and Astronomy, University of Oklahoma, Norman OK; United States of America.
- ¹²⁴Department of Physics, Oklahoma State University, Stillwater OK; United States of America.
- ¹²⁵Palacký University, Joint Laboratory of Optics, Olomouc; Czech Republic.
- ¹²⁶Institute for Fundamental Science, University of Oregon, Eugene, OR; United States of America.
- ¹²⁷Graduate School of Science, Osaka University, Osaka; Japan.
- ¹²⁸Department of Physics, University of Oslo, Oslo; Norway.
- ¹²⁹Department of Physics, Oxford University, Oxford; United Kingdom.
- ¹³⁰LPNHE, Sorbonne Université, Université Paris Cité, CNRS/IN2P3, Paris; France.
- ¹³¹Department of Physics, University of Pennsylvania, Philadelphia PA; United States of America.
- ¹³²Department of Physics and Astronomy, University of Pittsburgh, Pittsburgh PA; United States of America.
- ¹³³^(a)Laboratório de Instrumentação e Física Experimental de Partículas - LIP, Lisboa;^(b)Departamento de Física, Faculdade de Ciências, Universidade de Lisboa, Lisboa;^(c)Departamento de Física, Universidade de Coimbra, Coimbra;^(d)Centro de Física Nuclear da Universidade de Lisboa, Lisboa;^(e)Departamento de Física, Universidade do Minho, Braga;^(f)Departamento de Física Teórica y del Cosmos, Universidad de Granada, Granada (Spain);^(g)Departamento de Física, Instituto Superior Técnico, Universidade de Lisboa, Lisboa; Portugal.
- ¹³⁴Institute of Physics of the Czech Academy of Sciences, Prague; Czech Republic.
- ¹³⁵Czech Technical University in Prague, Prague; Czech Republic.
- ¹³⁶Charles University, Faculty of Mathematics and Physics, Prague; Czech Republic.
- ¹³⁷Particle Physics Department, Rutherford Appleton Laboratory, Didcot; United Kingdom.
- ¹³⁸IRFU, CEA, Université Paris-Saclay, Gif-sur-Yvette; France.
- ¹³⁹Santa Cruz Institute for Particle Physics, University of California Santa Cruz, Santa Cruz CA; United States of America.
- ¹⁴⁰^(a)Departamento de Física, Pontificia Universidad Católica de Chile, Santiago;^(b)Millennium Institute for Subatomic physics at high energy frontier (SAPHIR), Santiago;^(c)Instituto de Investigación Multidisciplinario en Ciencia y Tecnología, y Departamento de Física, Universidad de La Serena;^(d)Universidad Andres Bello, Department of Physics, Santiago;^(e)Instituto de Alta Investigación, Universidad de Tarapacá, Arica;^(f)Departamento de Física, Universidad Técnica Federico Santa María, Valparaíso; Chile.
- ¹⁴¹Department of Physics, Institute of Science, Tokyo; Japan.
- ¹⁴²Department of Physics, University of Washington, Seattle WA; United States of America.
- ¹⁴³Department of Physics and Astronomy, University of Sheffield, Sheffield; United Kingdom.
- ¹⁴⁴Department of Physics, Shinshu University, Nagano; Japan.

- ¹⁴⁵Department Physik, Universität Siegen, Siegen; Germany.
- ¹⁴⁶Department of Physics, Simon Fraser University, Burnaby BC; Canada.
- ¹⁴⁷SLAC National Accelerator Laboratory, Stanford CA; United States of America.
- ¹⁴⁸Department of Physics, Royal Institute of Technology, Stockholm; Sweden.
- ¹⁴⁹Departments of Physics and Astronomy, Stony Brook University, Stony Brook NY; United States of America.
- ¹⁵⁰Department of Physics and Astronomy, University of Sussex, Brighton; United Kingdom.
- ¹⁵¹School of Physics, University of Sydney, Sydney; Australia.
- ¹⁵²Institute of Physics, Academia Sinica, Taipei; Taiwan.
- ¹⁵³^(a)E. Andronikashvili Institute of Physics, Iv. Javakhishvili Tbilisi State University, Tbilisi;^(b)High Energy Physics Institute, Tbilisi State University, Tbilisi;^(c)University of Georgia, Tbilisi; Georgia.
- ¹⁵⁴Department of Physics, Technion, Israel Institute of Technology, Haifa; Israel.
- ¹⁵⁵Raymond and Beverly Sackler School of Physics and Astronomy, Tel Aviv University, Tel Aviv; Israel.
- ¹⁵⁶Department of Physics, Aristotle University of Thessaloniki, Thessaloniki; Greece.
- ¹⁵⁷International Center for Elementary Particle Physics and Department of Physics, University of Tokyo, Tokyo; Japan.
- ¹⁵⁸Department of Physics, University of Toronto, Toronto ON; Canada.
- ¹⁵⁹^(a)TRIUMF, Vancouver BC;^(b)Department of Physics and Astronomy, York University, Toronto ON; Canada.
- ¹⁶⁰Division of Physics and Tomonaga Center for the History of the Universe, Faculty of Pure and Applied Sciences, University of Tsukuba, Tsukuba; Japan.
- ¹⁶¹Department of Physics and Astronomy, Tufts University, Medford MA; United States of America.
- ¹⁶²Department of Physics and Astronomy, University of California Irvine, Irvine CA; United States of America.
- ¹⁶³University of Sharjah, Sharjah; United Arab Emirates.
- ¹⁶⁴Department of Physics and Astronomy, University of Uppsala, Uppsala; Sweden.
- ¹⁶⁵Department of Physics, University of Illinois, Urbana IL; United States of America.
- ¹⁶⁶Instituto de Física Corpuscular (IFIC), Centro Mixto Universidad de Valencia - CSIC, Valencia; Spain.
- ¹⁶⁷Department of Physics, University of British Columbia, Vancouver BC; Canada.
- ¹⁶⁸Department of Physics and Astronomy, University of Victoria, Victoria BC; Canada.
- ¹⁶⁹Fakultät für Physik und Astronomie, Julius-Maximilians-Universität Würzburg, Würzburg; Germany.
- ¹⁷⁰Department of Physics, University of Warwick, Coventry; United Kingdom.
- ¹⁷¹Waseda University, Tokyo; Japan.
- ¹⁷²Department of Particle Physics and Astrophysics, Weizmann Institute of Science, Rehovot; Israel.
- ¹⁷³Department of Physics, University of Wisconsin, Madison WI; United States of America.
- ¹⁷⁴Fakultät für Mathematik und Naturwissenschaften, Fachgruppe Physik, Bergische Universität Wuppertal, Wuppertal; Germany.
- ¹⁷⁵Department of Physics, Yale University, New Haven CT; United States of America.
- ^a Also Affiliated with an institute covered by a cooperation agreement with CERN.
- ^b Also at An-Najah National University, Nablus; Palestine.
- ^c Also at Borough of Manhattan Community College, City University of New York, New York NY; United States of America.
- ^d Also at Center for High Energy Physics, Peking University; China.
- ^e Also at Center for Interdisciplinary Research and Innovation (CIRI-AUTH), Thessaloniki; Greece.
- ^f Also at CERN, Geneva; Switzerland.
- ^g Also at CMD-AC UNEC Research Center, Azerbaijan State University of Economics (UNEC); Azerbaijan.

- h* Also at Département de Physique Nucléaire et Corpusculaire, Université de Genève, Genève; Switzerland.
- i* Also at Departament de Física de la Universitat Autònoma de Barcelona, Barcelona; Spain.
- j* Also at Department of Financial and Management Engineering, University of the Aegean, Chios; Greece.
- k* Also at Department of Physics, California State University, Sacramento; United States of America.
- l* Also at Department of Physics, King's College London, London; United Kingdom.
- m* Also at Department of Physics, Stanford University, Stanford CA; United States of America.
- n* Also at Department of Physics, Stellenbosch University; South Africa.
- o* Also at Department of Physics, University of Fribourg, Fribourg; Switzerland.
- p* Also at Department of Physics, University of Thessaly; Greece.
- q* Also at Department of Physics, Westmont College, Santa Barbara; United States of America.
- r* Also at Faculty of Physics, Sofia University, 'St. Kliment Ohridski', Sofia; Bulgaria.
- s* Also at Hellenic Open University, Patras; Greece.
- t* Also at Imam Mohammad Ibn Saud Islamic University; Saudi Arabia.
- u* Also at Institutio Catalana de Recerca i Estudis Avancats, ICREA, Barcelona; Spain.
- v* Also at Institut für Experimentalphysik, Universität Hamburg, Hamburg; Germany.
- w* Also at Institute for Nuclear Research and Nuclear Energy (INRNE) of the Bulgarian Academy of Sciences, Sofia; Bulgaria.
- x* Also at Institute of Applied Physics, Mohammed VI Polytechnic University, Ben Guerir; Morocco.
- y* Also at Institute of Particle Physics (IPP); Canada.
- z* Also at Institute of Physics, Azerbaijan Academy of Sciences, Baku; Azerbaijan.
- aa* Also at Institute of Theoretical Physics, Ilia State University, Tbilisi; Georgia.
- ab* Also at National Institute of Physics, University of the Philippines Diliman (Philippines); Philippines.
- ac* Also at Technical University of Munich, Munich; Germany.
- ad* Also at The Collaborative Innovation Center of Quantum Matter (CICQM), Beijing; China.
- ae* Also at TRIUMF, Vancouver BC; Canada.
- af* Also at Università di Napoli Parthenope, Napoli; Italy.
- ag* Also at University of Colorado Boulder, Department of Physics, Colorado; United States of America.
- ah* Also at Washington College, Chestertown, MD; United States of America.
- ai* Also at Yeditepe University, Physics Department, Istanbul; Türkiye.
- * Deceased